Novel Scaffolds for Spinal Cord Repair

Krämer, Marina

Award date:
2013

Awarding institution:
University of Bath

NOVEL SCAFFOLDS FOR SPINAL CORD REPAIR

Marina Krämer

A thesis submitted for the degree of Doctor of Philosophy

University of Bath
Department of Chemical Engineering

September 2011

TABLE OF CONTENTS

TABLE OF FIGURES

TABLE OF TABLES

ACKNOWLEDGEMENTS

On the academic side of things, I would like to thank Prof Julian Chaudhuri, Dr Marianne Ellis and Dr Paul De Bank for giving me the opportunity to work in the tissue engineering group at the University of Bath and provide me with support and guidance throughout the duration of the project. In particular I would like to thank Paul who was always very helpful during the various challenges that have arisen during the project. I would also like to thank the members of the tissue engineering group, especially Dr Chris Gribbon for answering all my questions (scientific and non-scientific), Fernando Acosta for finding all the equipment I needed and Giulia Meneghello for providing a listening ear and good entertainment. I finally thank the University of Bath for funding my project.

Many, many thanks go out to my friends who I met in Bath, their support was necessary to get through the last three years.

My biggest thanks go to my parents for being there, supporting me in everything I did, encouraging me and having an open ear when things were great and not so great. Without them I wouldn't be the person I am today.

ABSTRACT

Injuries to the central nervous system (CNS) have traumatic consequences such as irreparable disability due to the inability of the CNS to regenerate injured nerve fibres. The aim of the work presented here was to develop a scaffold which potentially provides guidance to axons in the injured spinal cord thus facilitating signal transduction. A poly-(lactic-co-glycolic acid) (PLGA, PLA:PGA ratio of 75:25) flat sheet membrane scaffold was created using phase inversion with N-methyl pyrrolidinone (NMP) as the solvent and water as the non-solvent for immersion precipitation. PLGA flat sheet membranes were exposed to surface treatments including aminolysis, peptide immobilisation and ozonation in order to achieve higher cell attachment of PC12 cells, a cell line which was cloned from a solid pheochromocytoma tumour of white rats, and used as a tool for measurement of regeneration. Cell attachment studies revealed no significant difference in cell attachment between modified and not-modified PLGA flat sheet membranes. However, the absence of foetal calf serum (FCS) resulted in fivefold higher cell attachment compared to medium supplemented with 10% FCS. A second scaffold was produced by electrospinning 10% (w/w) PLGA in a chloroform:methanol ($CHCl_3$:MeOH) mixture in ratio of 3:1 resulting in a nanofibrous scaffold. Optimum settings for electrospinning were found to be 3 ml/h feeding rate, 15kV applied voltage and 11cm collector-to-needle distance. Random and aligned PLGA nanofibres were produced, with a fibre diameter of 530±140nm. PC12 cells attached and differentiated to the nanofibrous scaffold. When exposed to NGF these cells stopped dividing and extended neurites. On random fibres, neurite orientation was random, whereas on aligned fibres 63% of neurites grew with the fibre orientation ±15°. After 7 days of exposure to NGF, cells had 1-4 neurites on random fibres, reaching a maximum length of 188µm, whereas on aligned fibres, cells had 1-2 neurites, reaching a maximum length of 400µm. PLGA nanofibres were also investigated as a delivery vehicle for bioactive molecules. For this, poly-L-lysine (PLL) was incorporated into electrospun PLGA nanofibres via emulsion electrospinning. PLGA-PLL nanofibres were significantly larger than PLGA nanofibres having a diameter of 830±190nm. In order to visualise the incorporation of PLL, FITC-PLL was electrospun und the resulting nanofibres fluoresced greed. Attachment of PC12s to PLGA-PLL nanofibres was not significantly different compared to PLGA nanofibres. Aligned PLGA-PLL nanofibres were shown to promote neurite outgrowth of PC12s with resulting neurites of up to twice the length compared to aligned PLGA nanofibres. The results suggest that PLGA nanofibres strongly influences neurite organisation, which is potentially useful for future therapeutic approaches. The work in this thesis has shown that electrospun PLGA nanofibre mats have the potential to be used as scaffolds for spinal cord repair addressing topographical guidance and delivery of bioactive molecules to the site of injury.

LIST OF ABBREVIATIONS

2D	Two dimensional
3D	Three dimensional
AFM	Atomic force microscopy
ALS	Amyotrophic lateral screrosis
BBB	Blood brain barrier
BDNF	Bran derived neurotrophic factor
BSCB	Blood-spinal cord barrier
CFDA SE	Carboxy-fluorescein diacetate, succinimidyl ester, also called CFSE
$CHCl_3$	Chloroform
CNS	Central nervous system
CSPGs	chondroitin sulphate proteoglycans
DCM	Dichloremethane
dH_2O	Distilled hydrogen oxide/water
DMF	Dimethylformamide
DRGs	dorsal root ganglia
ECM	Extracellular matrix
EDA	Ethylene diamine
EDC	1-Ethyl-3-(3-dimethyl-aminopropyl)carbodiimide, hydrochloride
FCS	Foetal calf serum
FDA	US Food and Drug Administration
FDA	Fluorescein diacetate
GAG	Glycosaminoglycan
GDA	glutaraldehyde
GDNF	Glial cell derived neurtrophic factor
HTLV-1	Human T-lymphotropic virus type1
IKVAV epitope	Isoleucin-lysine-valine-alanine-valine epitope
MAG	myelin-associated glycoprotein
MeOH	Methanol

MES	2-(*N*-morpholino)ethanesulfonic acid
MP	Methylprednisolone
MTT	3-(4,5-Dimethylthiazol-2-yl)-2,5-diphenyltetrazolium bromide
N2A	Neuro 2A
NaOH	Sodim hydroxide
NT3, 4/5	Neurotrophin-3, 4/5
NGF	Nerve growth factor
NHS	*N*-Hydroxysuccinimide
NMP	1-Methyl-2-pyrrolidinone
NPCs	Neural progenitor cells
NSCs	Neural stem cells
Omgp	Oligodendrocyte myelin glycoprotein
OPCs	Oligodendrocyte precursor cells
PA	Polyacrylamide
PBS	Phosphate buffered saline
PCL	Polycaprolactone
PCLEEP	Poly(caprolactone and ethyl ethylene phosphate)
PDMS	Polydimethylsiloxane
PDS	Poly(dioxanone)
PEG	Poly(ethylene glycol)
PES	Poly(ethersulfone)
PGA	Poly(glucolic acid)
PI	Propidium iodide
PLA	Poly(lactic acid)
PLGA	Poly(lactic-co-glycolic acid)
PLL	Poly-L-lysine
PNS	Peripheral nervous system
PVF	Poly(vinylidene fluoride)
RGD	Arginine-glycine-aspartic acid
rpm	Revolutions per minute

SC	Spinal cord
SCI(s)	Spinal cord injury (-ies)
SCR	Spinal cord repair
SEM	Scanning electron microscopy
THF	Tetrahydrofuran
W/O	water-in-oil
XPS/ESCA	X-ray photoelectron spectroscopy/Electron spectroscopy for chemical analysis
YIGSR epitope	Tyrosine-isoleucine-glycine-serine-arginine epitope

1. INTRODUCTION

Nerve injury, particularly to the central nervous system, can have traumatic consequences such as permanent disability due to loss of motor function. Many scaffold designs have been utilized in order to promote the growth of neurons across areas of nerve injury, bridging the gap created by trauma and offering a permissive environment for neuronal extension. Poly-(lactic-co-glycolic acid) (PLGA) has been widely used as a scaffold materials for tissue engineering applications, as it is biodegradable, biocompatible and FDA approved (Lu et al., 2000). However, cell adhesion and growth can be hampered due to the lack of natural adhesion sites on the polymer. Here, PLGA flat sheet membranes and electrospun nanofibres are evaluated in terms of cytocompatibility using PC12 cells.

This introduction chapter gives an overview of the structure of this thesis, briefly describing the outline of each subsequent chapter.

Chapter 2 presents the current status of tissue engineering for spinal cord repair. It describes the physiology of the spinal cord, etiology of spinal cord injury (SCI), physiological changes following a SCI and current treatments available. The chapter continues by describing the tissue engineering approach and discussing biomaterials, scaffolds, fabrication methods and their potential for spinal cord repair. The chapter concludes by describing further points that require investigation and finishes with the aims and objections of this project.

All materials and methods that were used for the production of the results are described in detail in chapter 3. The chapter is split in three parts: 1. Experimental methods, 2. Analytical methods and 3. Statistical analysis.

Chapter 4 describes the work undertaken with PLGA flat sheet membranes. The aim of this chapter is to investigate the potential of PLGA flat sheet membranes for cell culture studies. It investigates the surface properties, including surface topography and hydrophilicity. Furthermore, surface modification, which was undertaken in order to increase cytocompatibility of PLGA, is presented including aminolysis, peptide modification and ozone treatment. This is concluded with the analysis of

cell attachment data using the PC12 cell line. Effects of foetal calf serum (FCS) on PC12 cell attachment to PLGA is also described and discussed.

Chapter 5 describes the process of electrospinning, which uses a specific set up to produce nano- and micro-scale fibres. The finding of the optimal settings for electrospinning PLGA are described including parameters such as applied voltage, distance between needle tip and collector, solvent, concentration of polymer solution, viscosity of polymer solution and feeding rate. The resulting nanofibres are analysed according to bead formation, fibre diameter and fibre alignment.

In chapter 6, PC12 cells are seeded onto the scaffold described in chapter 5. The behaviour of cells is analysed according to cell attachment, cell proliferation and cell differentiation. As this scaffold is created to support axonal outgrowth, focus is paid to the differentiation of PC12s and specifically to neurite outgrowth including number of neurites per cell, length of neurites and directional outgrowth of neurites. Differentiation is analysed on random and aligned PLGA nanofibres.

In chapter 7, new fibres are created by incorporation of poly-L-lysine (PLL) into the electrospun PLGA fibres by means of emulsion electrospinning. In this emulsion, a water phase containing PLL is mixed with the PLGA solution and then electrospun. Morphology and hydrophilicity of electrospun PLGA-PLL nanofibres are analysed. These fibres are further analysed according to their ability to support attachment, proliferation and differentiation of PC12 cells, investigating number of neurites per cell, length of neurites and directional outgrowth of neurites in comparison to PLGA nanofibres.

Chapter 8 briefly summarises the results and provides a general discussion considering type of scaffold, the process of electrospinning, biocompatibility of polymers as well as cell culture studies.

A general conclusion is presented in chapter 9 connecting the aims of the project with results and discussion. The second half of chapter 9 examines future work,

describing potential short, medium and long term studies as well as general considerations for spinal cord repair.

2. THE CURRENT STATUS OF TISSUE ENGINEERING FOR REPAIR OF SPINAL CORD INJURIES

2.1 Physiology and function of the spinal cord

With the brain, the spinal cord is one the most complex organs in the human body. It is an elongation of the central nervous system (CNS) connecting the brain with the muscles and sensory nerves. The spinal cord is divided into segments, marking where the spinal nerves emerge from the cord to specific regions of the body (Fig 2.1). Cervical spinal nerves (C1 to C8) control the signals to the back of the head, the neck and shoulders, the arms and hands and the diaphragm. Thoracic spinal nerves (T1 to T12) control signals to the chest muscles, some muscles of the back and parts of the abdomen. Lumbar spinal nerves (L1 to L5) control signals to the lower parts of the abdomen and the back, the buttocks, parts of external genital organs and parts of the leg. The lowest sacral spinal nerves (S1 to S5) control signals to most of the external genital organs, the area around the anus, thighs and the lower parts of the legs and the feet (Gondim 2009).

The spinal cord has a core containing nerve cells, surrounded by long tracts of nerve fibres which consist of axons extending up and down the spinal cord. The interior of the spinal cord is made up of neurons, glial cells (support cells) and blood vessels. The neurons and their dendrites are to be found in the H-shaped region called grey matter. The grey matter contains the cell bodies of motor neurons, smaller interneurons and sensory neurons. The grey matter is surrounded by white matter, where myelin-covered axons are to be found. The circumference of the spinal cord varies depending on its location, as it is larger in the cervical and lumbar regions because these areas supply the arms and upper body and the legs and lower body, requiring the most intense muscular control and receive the most sensory signals (Kano et al., 2006).

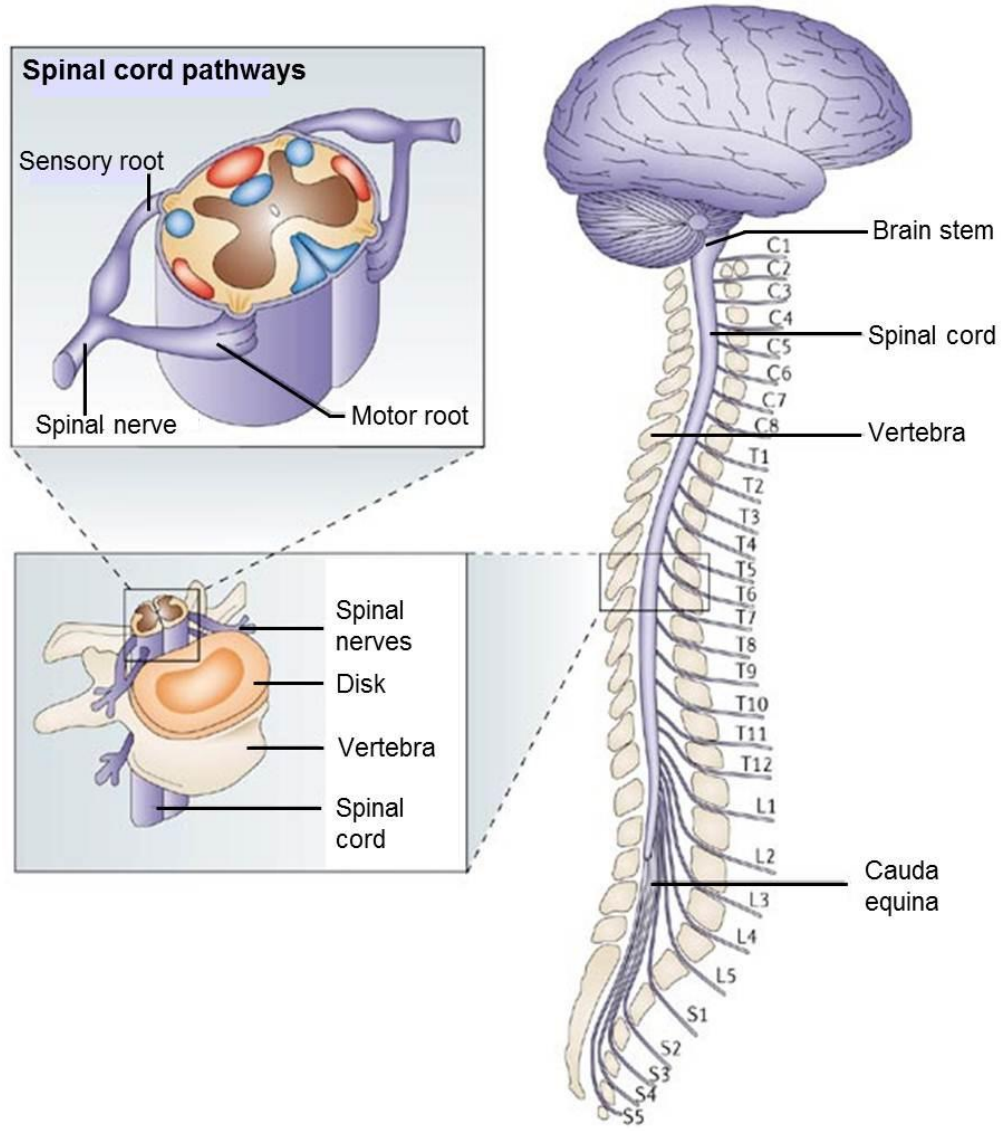

Figure 2.1 Physiology of the spinal cord. The spinal cord is divided into four levels which control different parts of the human body. The outer edge of the spinal cord is the white matter which contains the axons. The grey matter contains the cell bodies of the neurons. Cell bodies of motor neurons are in the motor root; the sensory root contains the primary sensory pathways that transmit sensory information from skin and muscle to the brain. The cell bodies of the sensory neurons are in the sensory root ganglion. Reprinted with permission of Macmillan Publishers Ltd: Nature Reviews Neuroscience (Bradbury and McMahon, 2006), ©.

2.2 Spinal cord injury

2.2.1 Ethiology of spinal cord injury

Spinal cord injuries (SCIs) have a multitude of forms, most of which lead to long term disability, financial and emotional burden, and permanent reduction in the quality of life. In the United States around 11,000 new SCIs are registered each year

and over 250,000 people live with a spinal cord injury (The National SCI Statistical Center 2009). Most SCIs are due to vehicle crashes, accounting for 41.3% of cases, followed by injuries caused by falls (27.3%), violence (15%) and sport (7.9%) (The National SCI Statistical Centre 2009). SCI can also be caused by medical conditions, such as multiple sclerosis, a disorder that destroys the myelin insulation on nerves in the cervical spinal cord. Other medical causes include polio and postpolio syndrome, vitamin B-12 deficiency, amyotrophic lateral sclerosis (ALS; Lou Gehrig's disease), human T-lymphotropic virus type 1 (HTLV-1) as well as causes of myelopathy. As most patients are in their mid-twenties, the cost of long-term care and rehabilitation amount up to an estimated US$ 14.7 billion a year (Sekhon and Fehlings, 2001), plus the immeasurable cost of psychological pressure every patient is exposed to.

2.2.2 Response to injury

SCI triggers a cascade of events starting seconds after the injury and proceeding for months and years. SCIs have an impact on three main body systems: the nervous system, the immune system and the vascular system. These systems respond to the injury and interact with each other. The consequences of a SCI depend on the level at which the cord is damaged and the type of injury sustained including contusion, laceration and solid cord injuries (Table 2.1). Although the events following a SCI are necessary to restore the blood-brain barrier and minimise secondary tissue damage, they result in an environment which is not supportive of tissue regeneration.

Table 2.1 Types of spinal cord injuries (Liverman 2005)

Type of Injury	Total Injuries (%)	Description
Contusion	25 to 40	Bruising, but not severing, of the spinal cord, due to falls and vehicle crashes
Laceration	25	Severing or tearing of the spinal cord and introduction of connective tissue into the spinal cord, typically from gunshot or knife wounds
Solid cord injury	17	Axon injury and demyelination, due to falls and vehicle crashes

Damage to the spinal cord results in tissue loss, and consequently in formation of large cavities at the site of injury (Quencer and Bunge, 1996). The long-term disability from SCI results not only from the injury itself, but also from complications that accumulate later on. Up to 30% of patients with SCI are hospitalized every year with complications (McKinley et al., 1999), such as pain, infections (lung, skin, and urinary tract), severe spasticity, heterotropic ossification, osteoporosis, bone fractures and autonomic dysreflexia (McDonald and Sadowsky, 2002, Sjolund, 2002).

SCI triggers a three phase response: the acute (seconds to minutes after the injury, the secondary (minutes to weeks after the injury), and the chronic response (months to years after the injury) (Table 2.2). Directly after the injury the cord starts swelling preventing venous blood flow, causing a secondary venous infarct in the central part of the cord initiating damage to the neighbouring tissues. During the secondary process, cells die by toxic necrosis as well as apoptosis, resulting in enlargement of the initial injury site. Cells continue to die during the weeks following the injury resulting in cavity formation (Crowe et al., 1997).

Table 2.2 Three major phases after spinal cord injury (Liverman 2005).

Acute	Secondary	Chronic
Systemic hypotension and spinal shock	Continued cell death	Continued apoptosis radiating from site of injury
Haemorrhage	Continued oedema	Alteration of ion channels and receptors
Cell death from direct insult of ischemia (disruption of blood supply)	Continued shifts electrolytes Calcium entry into cells	Formation of fluid-filled cavity Syringomyelia (cavity formation)
Oedema (swelling)	Free-radical production	Scarring of spinal cord by glial cells
Vasospasm (reduction in blood flow)	Lipid peroxidation	Demyelination
Shifts in electrolytes	Neutrophil and lymphocyte invasion and release of cytokines	Regenerative processes, including sprouting by neurons
Accumulation of neurotransmitters	Apoptosis (programmed cell death)	Altered neurocircuits

2.2.3 Repair at injury site

After the sustained injury, the spinal cord is partly able to heal itself, starting at about 24 hours after the injury and continuing for years (Tator, 1998). Unfortunately, mature nerve cells lack the ability to divide once injured. The recovery is due to plasticity of the remaining neurons, which is inhibited by molecules in their extracellular vicinity. Adhesion molecules are not up regulated in the distal spine as they are in the peripheral nervous system (PNS) limiting the recruitment of macrophages, which are responsible for removal of inhibitory myelin and promoting regrowth of neuronal cells (Avellino et al., 1995). Finally, as a general reaction to any type of assault to the CNS, astrocytes proliferate, become dismorphic and form the glial scar that inhibits regeneration (McKeon et al., 1991, Schmidt and Leach, 2003). The glial scar consists of highly interwoven astrocytes which are connected through gap junctions that, together with the inhibitory ECM, form a physical as well as a molecular barrier for nerve regeneration (Fawcett and Asher, 1999) (Fig 2.2). It is still not elucidated what triggers the initial inhibition versus growth-promoting glial environment. To date, only β-amyloid, which was discovered in connection with Alzheimer disease, has been named as a potential trigger for creating astrocytes that are functionally inhibitory (Canning et al., 1993).

The role of the glial scar is to contain the injury site and promote healing. Some evidence has shown similarities between the glial scar and the dermal wound healing processes (Velardo et al., 2004). Although the glial scar is successful in containing further physical damage, it prevents neuroregeneration as cells present in the glial scar secrete neuro-developmental inhibitor molecules, preventing full recovery. In addition to reactive astrocytes, scar formation involves macrophages, microglia and oligodendrocytes precursor cells (OPCs) (Chen et al., 2002).

Apart from astrocytes, OPCs play a major role in inhibition of axonal extension in the injured CNS. They are stem- or stem-like cells that make up 5-8% of the glial cell population in the CNS and are present in white and grey matter areas (Levine et al., 2001) and can differentiate into either astrocytes or oligodendrocytes (Wolswijk and Noble, 1989). Large numbers of OPCs are recruited to any traumatic site of

injury in the CNS thus participating in the glial response to injury. Additionally, OPCs can express proteoglycans, such as NG2, phosphacan, versican and neurocan which participating in rendering the damaged CNS (Fawcett and Asher, 1999).

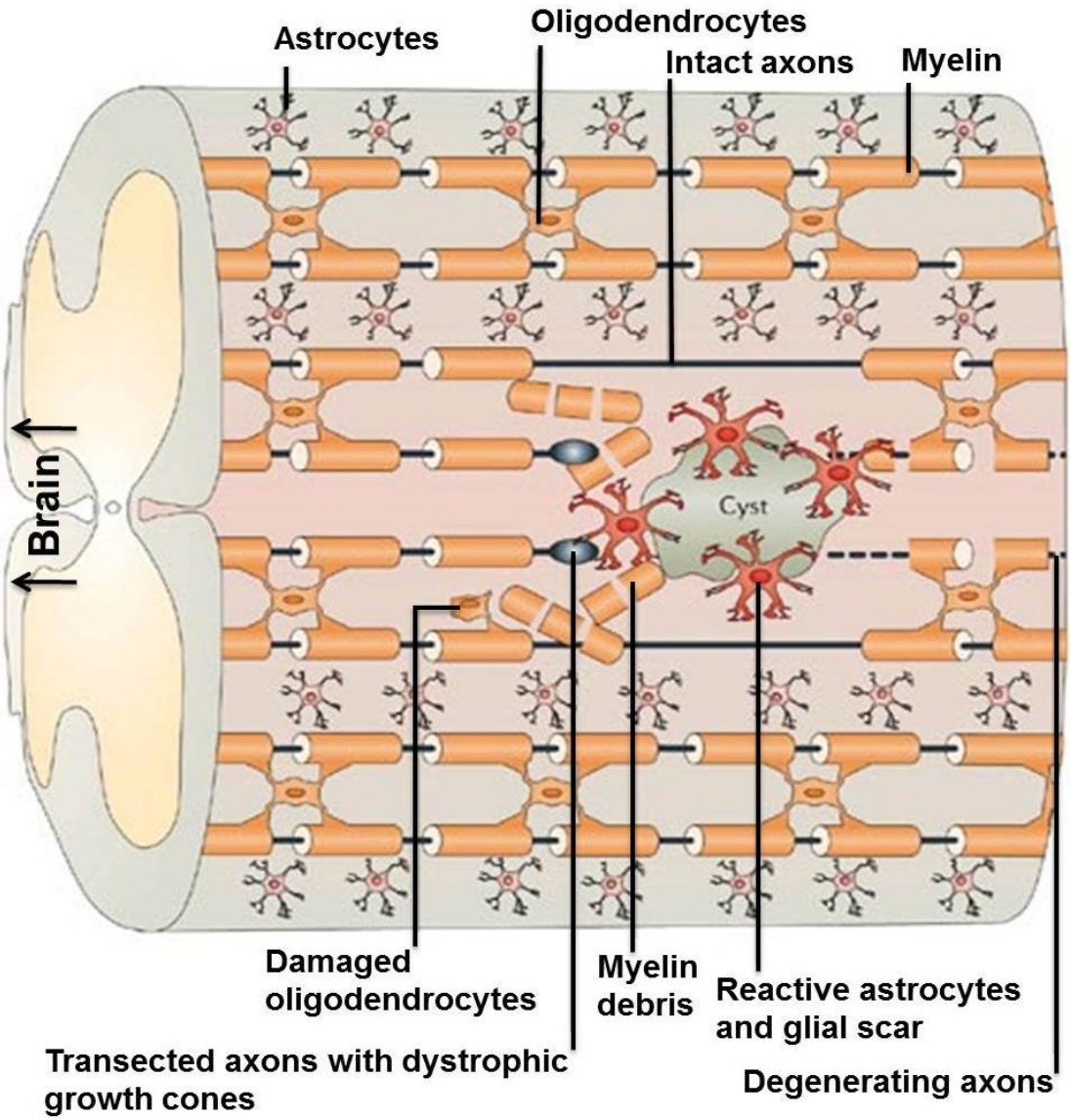

Figure 2.2 Schematic representation of the spinal cord injury site. Many cells die immediately after the injury, as well as later on. Cysts usually form after contusion injury. After penetrating injury, cell from the PNS infiltrate the site of injury to form connective tissue incorporating reactive astrocytes, progenitor cells and microglia. Ascending and descending axons are interrupted and do not regenerate over long distances. Scarring is associated with increased release of chondroitin sulphate proteoglycans (CSPGs) and limit further regeneration resulting in a very hostile environment for axon repair. Reprinted with permission of Macmillan Publishers Ltd: Nature Reviews Neuroscience (Yiu and He, 2006), © (2006).

Fibroblasts of meningeal origin are the main non-neural cells that are recruited to the site of CNS injury when the blood brain barrier is opened. Together with

astrocytes and oligodendrocytes, they must be added to the list of cells expressing inhibitory molecules in the glial scar. Fibroblasts are the main expression source for the semaphorin family, including Sema3B, Sema3C, Sema3E and Sema3F, as well as NG2, tenascin C (Ajemian et al., 1994) and the V0 form of veriscan (Hirschberg and Schwartz, 1995, Pasterkamp et al., 1999). Semaphorins are secreted membrane proteins that play a role during the development of the nervous system where they act as inhibitory short-range molecules preventing axons from growing towards inappropriate targets (Vanderhaeghen and Cheng, 2010, Bolsover et al., 2008).

Extracellular matrix (ECM) molecules such as CSPGs, also known as lecticans or hyaluronan-binding proteins, including aggrecan, versican neurocan and brevican, play the most influential role in the inhibitory process (Grimpe and Silver, 2002). Other CSPG families include small proteoglycans (biglycan, fibromodulin, decorin and lumican) and cell-surface proteoglycans (syndecan-1 and syndecan-4) (Bovolenta and Fernaud-Espinosa, 2000). They comprise large molecular complexes with a protein core to which large, highly sulphated glyscosaminoglycan (GAG) chains are attached (Bradbury et al., 2002). It has been suggested that CSPGs bind laminin and thereby prevent laminin's neurite promoting activity (Bolsover et al., 2008).

Other important neurite outgrowth inhibitory factors are the Nogo family (Nogo-A, B and C) of oligodendrocyte membrane proteins (Schwab, 2004), myelin-associated glycoprotein (MAG) (DeBellard et al., 1996) and oligodendrocyte myelin glycoprotein (OMgp) (Domeniconi and Filbin, 2005). These three proteins signal through a common receptor, the Nogo receptor (NgR). NgR forms a complex with the neurotropin receptor p75 and with LINGO-1 (Wong et al., 2002), which then activates the GTPase RhoA, that recruits the Rho kinase which in turn mediates cytoskeleton remodelling and inhibits neurite outgrowth (Alabed et al., 2006). Additionally, Nogo-A is specifically involved in growth cone collapse and inhibition of neurite outgrowth (Oertle et al., 2003).

MAG is a member of the immunoglobulin superfamily that is expressed in the PNS Schwann cells and CNS oligodendrocytes (McKerracher et al., 1994). It has an inhibitory role on neurite outgrowth after injury, whereas it enhances neurite outgrowth in prenatal dorsal root ganglia (DRGs), embryonic retinal ganglion or spinal neurons (Mukhopadhyay et al., 1994).

The third Nogo receptor ligand, OMgp, has only been characterised *in vitro*, where it was shown to induce growth cone collapse and inhibition of neurite outgrowth (Kottis et al., 2002).

The major promoter molecules within the CNS are laminins, which are a family of large glycoprotein components of the ECM with a strong neurite promoting ability *in vitro*, in the PNS and in the CNS. Laminins play an important role in axonal growth and guidance during development as well as cell attachment and proliferation (Liesi, 1985, Timpl et al., 1979). It is controversial where laminin is expressed as reports contradict each other. For example, laminin is associated with Schwann cells and astrocytes and is detected in extracellular locations (Menet et al., 2001), but it has also been located within neurons (Zhou, 1990), whereas others failed to find laminin in CNS neurons (Thomson et al., 2006).

2.2.5 Current treatment for spinal cord injury

There is still no successful treatment available for chronic SCIs. This is due to several reasons. First, there has been no evidence favouring one process to be responsible for all the pathophysiological consequences following a spinal cord injury, making it difficult to understand the mechanism of the injury. Second, most interventions reported to date focus on one aspect of the injury process, destined to fail when tested or combined with other interventions or even interfere with each other (Thuret et al, 2006). Hence, it is critical to understand the full extent of the mechanism and identify combined therapies, which are more likely to be effective than one approach only.

Furthermore, no therapy is available for the long term consequences such as permanent locomotion impairment, pain, and bladder, sexual and other autonomic

dysfunctions. Currently, the treatment for an acute SCI includes protecting the neurons, preserving residual axons and white matter and preventing further damage by administration of high doses of methylprednisolone (MP, Medrol), an anti-inflammatory agent (Hall and Springer, 2004). Additionally, the spine is immobilized and stabilised, with e.g. a body harness or a rigid neck collar, to accomplish traction and bring the spine into proper alignment during healing. Surgical intervention is necessary to remove fragments of bones, foreign objects, herniated discs or fractured vertebrae that might be compressing the spine. Preventing future pain and deformity are other aims of surgery. The optimum timepoint of surgery is still controversial (Mirza et al., 1999). Although early surgery results in neurological recovery in animals, timing in humans is still unclear (Fehlings and Tator, 1999). Early surgery has been shown to reduce complications, length of stay and hospital costs, but more comprehensive studies are necessary to clearly demonstrate the most beneficial time point for neurological outcome (Kishan et al., 2005).

Once the patient is stabilized, ongoing care takes place concentrating on consequences of immobilization, such as deconditioning, decubitus ulcers, urinary infections, blood clots and muscle contractures. Stays in hospital range from days to months depending on the extent of the paralysis and progress made during therapy. Rehabilitation focuses on regaining leg and arm strength, redeveloping fine motor skills and learning new techniques (e.g. using the wheelchairs, computer devices and functional electrical stimulation systems) which help accomplish day-to-day tasks. Partial recovery usually occurs between one week and six months after the injury. Impairment present after 12 to 24 months is likely to be permanent. Although the capacity of the CNS to regenerate axons and re-establish a functional network after injury is very limited (Schwab and Bartholdi, 1996), studies in animal models have shown that only 5-10% of undamaged descending axonal tracts are needed to maintain a reasonable locomotion (Eidelberg et al., 1977). This gives rise to great hope for therapeutic interventions aiming to spare or re-establish these connections. But without a clear pathway for axon outgrowth, regeneration of the

spinal cord is impossible. The combination of cell therapy and biomaterials may provide a permissive environment that promotes and accelerates spontaneous cellular regeneration. Tissue engineering combines biomaterials with cellular therapies and results in neural guidance conduits which mimic natural neural tissue thus potentially accelerating the healing process.

2.3 Tissue engineering and combined therapies

Tissue engineering has arisen in order to address the extreme shortage of tissues and organs for transplantation and repair. It is an interdisciplinary research area which encompasses different areas of science, ranging from basic biology (physiology, cell biology, and embryology), engineering fundamentals (material science, fluid dynamics, and chemical kinetics), mathematical modelling, clinical aspects (medicine, pathology, and immunology) and relevant biotechnologies (cell culture, cell separation, and gene transfer).

The first symposium under the name of tissue engineering was held in 1988, where a working definition was proposed as follows: “The application of the principles and methods of engineering and life sciences toward the fundamental understanding of structure-function relationships in normal mammalian tissue and the development of biological substitutes to restore, maintain, or improve tissue function.” (Skalak and Fox 1988). Tissue engineering was developed to overcome problems of transplantation (rejection, side effects caused by autoimmune drugs and scarcity of donors), autografting (donor site morbidity) and permanent transplants (long-term side effects, can last for maximum 15 years) (Ries, 2003).

The principle of tissue engineering is to culture cells on a biodegradable scaffold creating an environment as close as possible to the environment present *in vivo* followed by implantation into the body of the patient, where the implant promotes tissue regeneration and degrades with time (Fig. 2.3) (Wald et al., 1993).

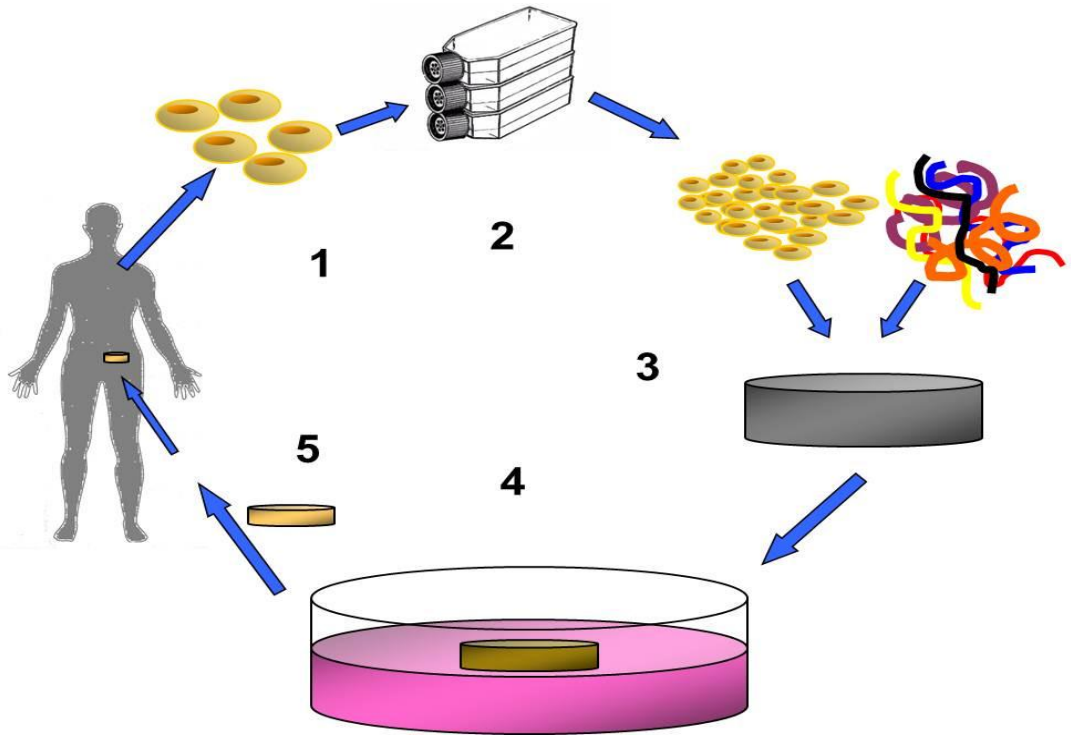

Figure 2.3 Tissue engineering approach. 1. Isolating stem cells, 2. Differentiating stem cells into desired cell type and expanding cell number in culture, 3. Cell seeding on scaffold with growth factors and cytokines, 4. Incubation in culture, 5. Re-implanting tissue into damaged site (George 2006).

To engineer a tissue, three components are required: cells that give rise to the required tissue, scaffolds supporting cell adhesion and proliferation and the creation of an appropriate environment for the cells to grow in and create tissue structures. The same approach as outlined for general tissue engineering can be applied to the specific environment of CNS. The success of the reparative strategy depends on modulating the factors interfering with:

1. Initiation and maintenance of axonal growth and elongation
2. Directed regeneration of axons to reconnect with their target neurons
3. Reconstitution of original circuitry, which leads to functional restoration
4. Protection and replacement of original cellular environment
5. Overcoming the inhibitory signals and limiting the scar formation

2.4 Tissue engineering approaches for nerve regeneration

A nerve regeneration approach cannot be provided by a single solution, such as cellular or chemical therapies. Instead it is more likely to be successful using a multidisciplinary approach, including administration of cells, medication and delivery of a physical scaffold.

A scaffold for nerve regeneration has to fulfil several parameters, such as ease of process into the desired geometry, sterility, tear resistance and ease of handling. Plus, guidance channels must be pliable, but maintain their form and resist collapse during implantation and over time course for regeneration (Schmidt and Leach, 2003). Degradable scaffolds are preferred to non-degradable, as non-degradable scaffolds are more likely to provoke a chronic inflammatory response and might compress the nerve over time (Schmidt and Leach, 2003, Hudson et al., 1999). Furthermore, removal of non-degradable scaffolds from the site of injury is not possible as the scaffolds contain the patient's nerves thus biodegradable materials are preferred. The ideal scaffolding must provide support for the regenerating axons on which they grow, making it necessary to control the degradation rate of biodegradable materials. At the current state of research it is not clear how quickly axons extend in the CNS in order to reconnect with the distal part of the spinal cord, which complicates the design of an ideal biodegradable scaffold.

The desired physical properties of an ideal scaffold were reviewed by Hudson (Fig 2.4) (Hudson et al., 1999). A scaffold is there to bridge the site of injury, fill the cavity preventing further scar formation and to release growth promoting factors. As well as releasing growth-promoting factors, other therapeutic agents can be introduced into the scaffold, which are released while the scaffold degrades, making the scaffold a drug delivery vehicle. These therapeutic agents can be antibodies to inhibitory proteins, digestive enzymes of the glial scar and intracellular signalling molecules, which were all shown to have a positive effect on regeneration in the CNS (Schmidt and Leach, 2003, Piotrowicz and Shoichet, 2006, McKerracher, 2001). This combination of a scaffold (with designed parameters, such as porosity, topography), supporting cells (for example Schwann cells) and growth factors

released from the scaffold is a tissue engineering approach as described in figure 2.4.

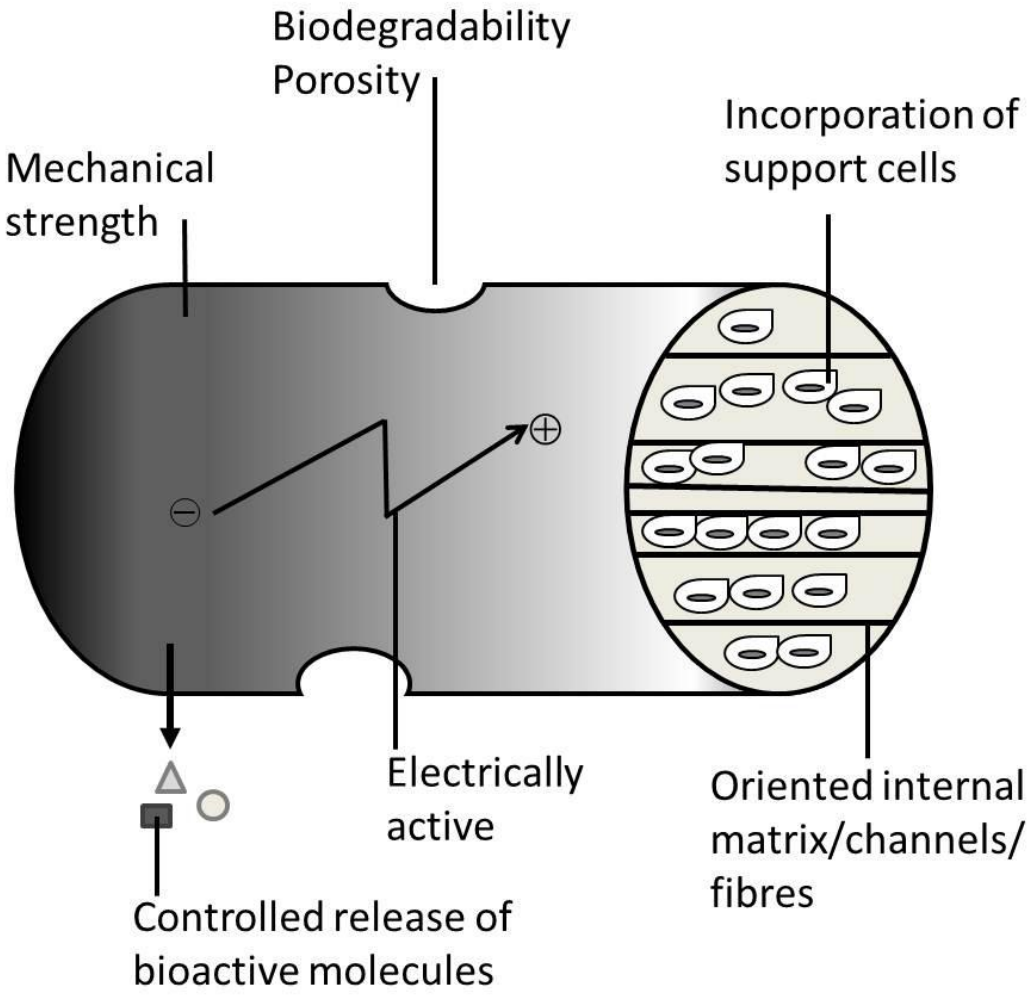

Figure 2.4 Properties of an ideal guidance channel. The desired physical properties of a nerve conduit include: a biodegradable and porous channel wall, the ability to deliver bioactive factors such as growth factors, the incorporation of support cells, a matrix supporting cell migration, intraluminal channels mimicking the structure of nerve fascicles and electrical activity (Schmidt and Leach, 2003, Hudson et al., 1999).

2.5 Scaffolds for neural tissue engineering

Scaffolds play a very important role in tissue engineering and are defined as porous biomaterials designed to perform some or all of the following: (1) promote cell-biomaterial interactions, as most mammalian cell types are anchorage-dependent and die if an adhesive substrate is not provided; (2) provide sufficient transport of gases, nutrients and regulatory factors to provide cell survival, proliferation and

differentiation; (3) biodegrade at an appropriate rate for the tissue of interest, promoting tissue regeneration; and (4) be non-inflammatory and have a low level of toxicity. Scaffolds can be fabricated from natural and synthetic polymers, ceramics and even metals (Atala et al., 2008).

Natural polymers are of great interest because of their biocompatibility, relative abundance, commercial availability and ease of processing. Natural polymers include proteins (collagen, laminin, fibronectin, fibrin, gluten, silk, elastin, hyaluronic acid) (Schense et al., 2000), (Dubey et al., 1999) and carbohydrates (chitosan or chitin, cellulose, starch and alginate) (Nomura et al., 2006), (Stokols and Tuszynski, 2006). On the negative side, natural polymers are usually expensive, suffer from cross-contamination from unknown viruses due to isolation from plant, animal or human tissue, and show batch-to-batch variations (Shorgen 1999).

Synthetic polymers are more easily controlled by physicochemical properties than natural polymers, can be processed with various techniques and can be produced consistently in large amounts and with reduced immunogenicity. Synthetic polymers are largely divided into two groups such as (1) biodegradable and (2) non - biodegradable. Non-biodegradable polymers include for example poly (hydroxyethylmethacryalte) (PHEMA), polyvinylalcohol and poly(N-isopropylacrylamide). Examples of biodegradable polymers are polycaprolactone (PCL), polyurethanes and the family of poly(α-hydroxy) esters such as poly(lactic acid) (PLA), poly(glycolic acid) (PGA) and their copolymer poly(lactic-co-glycolic acid) (PLGA). Biodegradable polymers are preferred to non-biodegradable as they provide temporarily mechanical and biochemical support resulting in the formation of natural tissue with limited chronic foreign body reaction, making second surgery for implant removal not necessary.

2.5.1 Guidance therapies

Various polymers have been tested for SCI repair strategies. Advanced approaches have been developed in order create complex guidance channels and combine multiple stimuli into one single therapy. When creating guidance channels most

research has focused on fabricating intricate internal structures that mimic the nerve architecture more accurately. These involve the inclusion of fibres or channels into the structure of the scaffold. These guidance scaffolds were fabricated in a number of ways, including magnetic polymer fibre alignment, injection molding, phase separation, solid free-form fabrication, ink-jet polymer printing, electrospinning or, more recently, self-assembling techniques.

Injection molding, magnetic alignment and phase separation

Nerve guidance conduits have usually been generated as hollow tubes or as porous rods as they are easily manufactured. One scaffold was produced using an injection molding technique, where a polymer mixture is forced into a heated cask, mixed and fed into a mold where it cools down, solidifies in the shape of the mold and becomes a scaffold onto which cells are seeded. In this approach PLA (Hadlock et al., 1998) and PLGA (Moore et al., 2006) guidance channels were produced containing chambers to mimic the fascicular organization of the nerve and were shown to support *in vivo* nerve regeneration (Hadlock et al., 1998) (Fig 2.5). PLGA was also manipulated by injection molding followed by a thermally induced phase transition process which resulted in scaffolds with longitudinally aligned internal channels ranging from a single channel of 1.35 mm diameter to 100 channels of 0.08 mm diameter (Fig 2.5) (Sundback et al., 2003). Although this approach is promising it was only tested in the PNS (rat sciatic nerve) and its design is relatively basic compared to the complex structure of the spinal cord thus making further *in vivo* research neccessary.

Several investigations concentrated on spun fibres of e.g. collagen or other biodegradable materials that are placed within the lumen of the guidance scaffold. For example, a PGA-collagen tube filled with laminin-coated collagen fibres (4mm inner diameter, 50μm wall thickness, and 90mm in length) was implanted into dogs to bridge an 80mm gap (Matsumoto et al., 2000). Functional recovery was recorded, with the gap being wider than any other previously reported (up to 50mm). The disadvantage of this method lies within its tedious preparation and the absence of control over fibre and chamber alignment because of the non-

automated fabrication method. Thus, more effort was invested into other methods which facilitate the control over internal aligned structure, are less tedious and allow controlled scale-up.

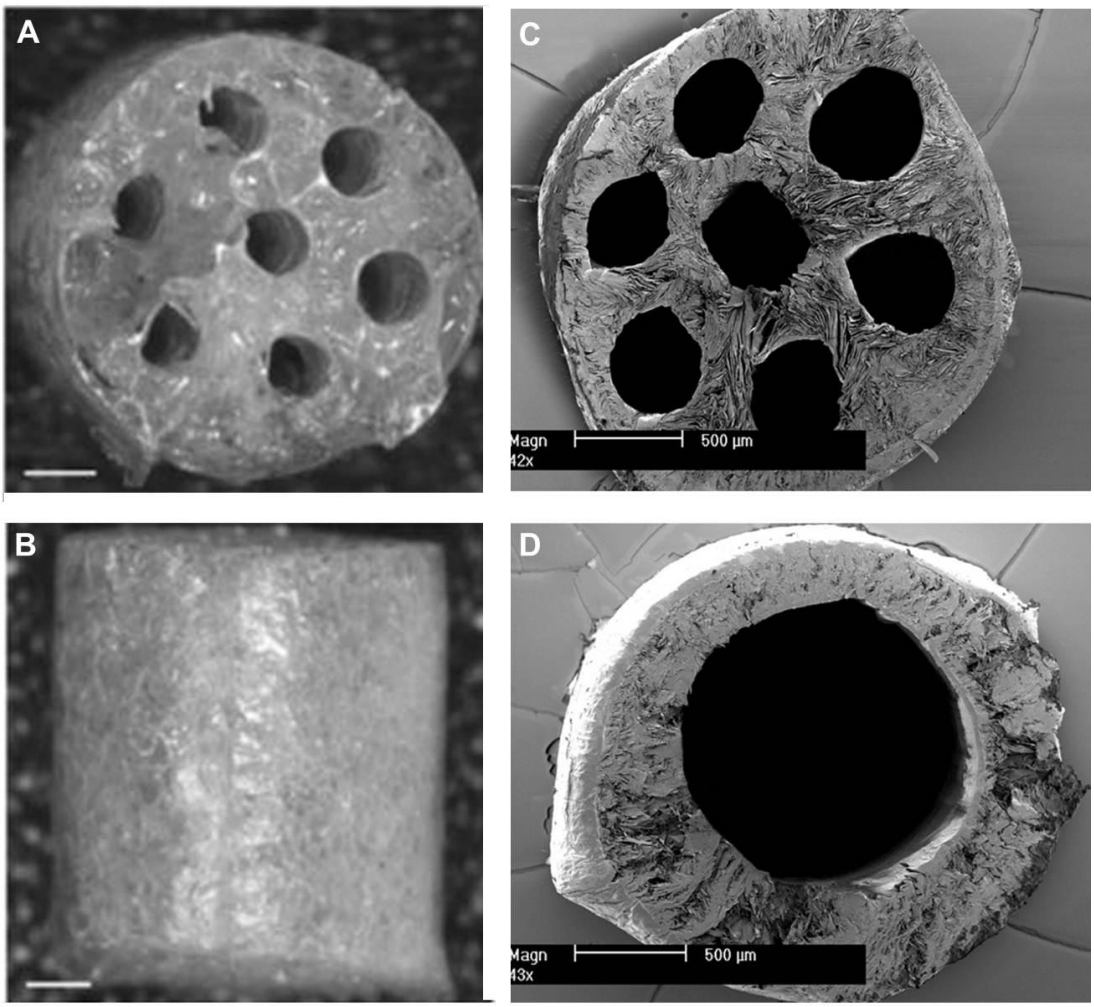

Figure 2.5 Tubular scaffolds scaffold for nerve regeneration. PLGA scaffold created from parallel wire molds (A+B). Scanning electron micrographs of transverse cross sections of 7-channel and single channel PLGA conduits (C+D) (Sundback et al., 2003). Scale bar 500µm. Reprinted from Moore et al., (2006) and Sundback et al., (2003) with permission from Elsevier, ©.

A different approach has used magnetic fields as means of creating matrix alignment of protein polymers. Aligned collagen and fibrin scaffolds have been shown to promote directional neurite outgrowth *in vitro* and *in vivo* compared to random scaffolds (Ceballos et al., 1999, Dubey et al., 2001).

For a rat spinal cord hemisection model a PLGA scaffold was produced using the gas-foaming technique (Fig 2.6). The work focused on tissue studies showing cell

infiltration and alignment within the channels (De Laporte et al., 2009). Using a solid-liquid phase separation technique and a salt-leaching process a conceptually novel PLGA scaffold with inner-oriented pores was created for spinal cord repair and seeded with neural stem cells (Teng et al., 2002) (Fig. 2.6). When implanted into an adult rat hemisection CNS model reduction of secondary injury processes and glial scarring was observed, as well as weight-bearing hindlimb stepping, which was not detected in control animals.

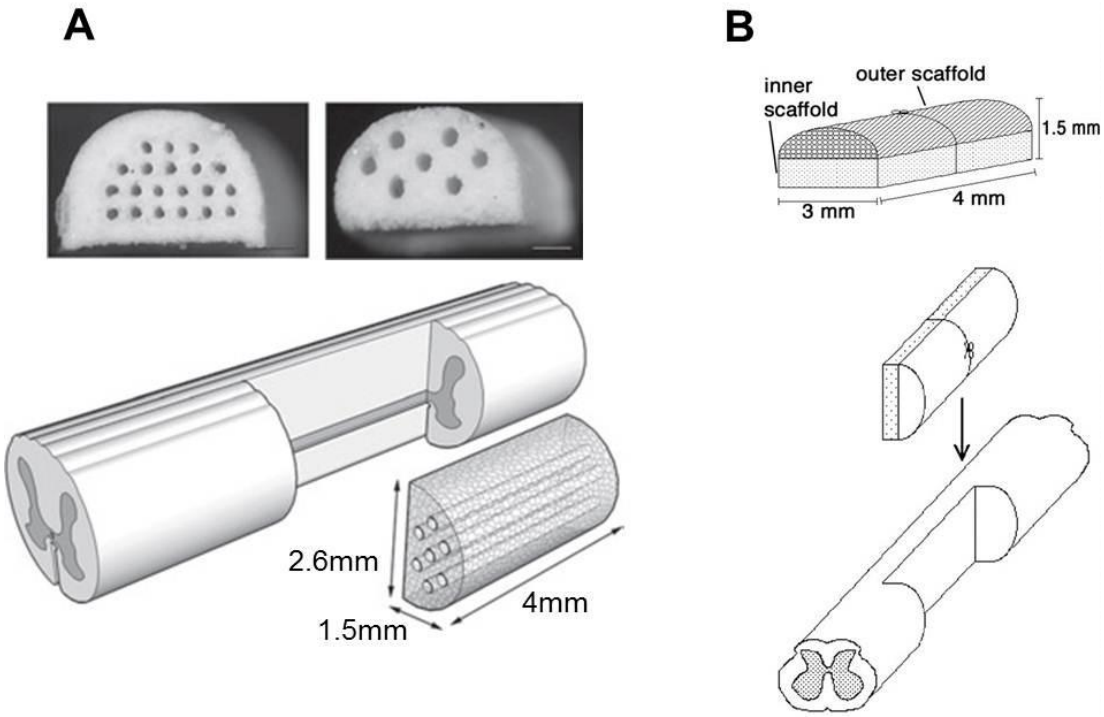

Figure 2.6 Schematic of scaffold designs. (A) PLGA multiple channel bridges with 20 channels of 150µm diameter and 7 channels of 250µm diameter fabricated using gas foaming technique, scale bars = 500µm. Schematic of bridge implantation in spinal cord hemisection. Reprinted from De Laport et al., © (2009) with permission from Elsevier. (B) Schematic of the PLGA-PLL scaffold design showing the inner (fabricated using salt leaching process, seeded with NSCs) and outer (fabricated using the solid–liquid phase separation technique). Reprinted from Teng et al., © (2002) with permission from National Academy of Science, U.S.A.

Solid freedom fabrication and ink-jet liquid polymer printing

Solid freedom fabrication and ink-jet liquid polymer printing are relatively new techniques and can produce features as small as 6µm (Friedman et al., 2002). 3D printing is one type of solid freedom fabrication and uses powder processing in a layer by layer manner (Park et al., 1998). This process, like other solid freedom

fabrication methods, creates a scaffold from a computer model and is able to create complex features, such as internal walls, porosity gradients and multiple material regions. The limitations of this approach lie within the high cost of the equipment.

Ink-jet printing has been used to create PLA scaffolds with desired thickness, dimensions and incorporated biomolecules. MicroFab Inc. in Plano, Texas designed the printer to produce bifurcated degradable polymer tubes with ridges to provide strength and thinner parts to allow nutrient exchange (Schmidt and Leach, 2003).

These techniques provide powerful tools for scaffold fabrication, although they range within the micrometer scale and recent research focuses on manipulating biomaterials on the nanometre scale.

Electrospinning

Electrospinning is used for fabrication of ultrafine nanofibres and for designing three-dimensional tissue scaffolds. The produced scaffolds have the advantage of resembling the ECM structure (e.g. collagen fibres) and support cell attachment, proliferation and differentiation (Rho et al., 2006).

Although this method has been known for more than 70 years in the production of textile yarns, its use for processing of large molecules started in the early 1990s (Doshi and Reneker, 1995). Electrospinning is a process where polymer nanofibres are produced or spun using electrostatic force, hence the name electrospinning (Doshi and Reneker, 1995). During the process the polymer solution is pumped through a syringe needle, where high voltage is applied (Fig. 2.7). The droplet of polymer solution, which is forced out of the needle tip, becomes highly electrified and distorted into a conical shape called the Taylor cone, named after its discoverer (Taylor 1969). Once the electrostatic force overcomes the surface tension, it forces the ejection of a liquid jet. The jet undergoes a stretching and whipping process leading to the formation of a long thin thread (Shin et al., 2001). The thread is collected on the grounded surface, while the solvent evaporates or solidifies.

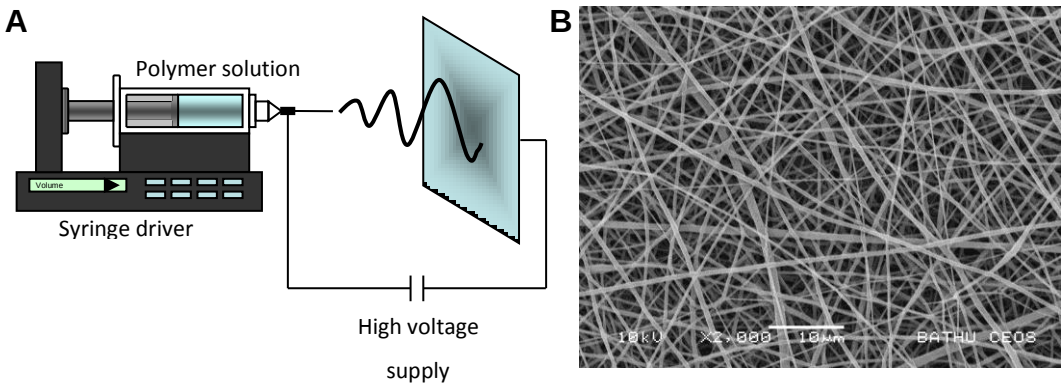

Figure 2.7 Schematic of electrospinning (A) and SEM image of electrospun PLGA (B). For electrospinning, the polymer is dissolved in a solvent and the solution is ejected through a needle by the electrostatic force (A). The solution evaporates and the charged polymer is collected on a grounded collector, forming a mesh of non-woven nanofibres (B). The advantage of this technique is the use of simple equipment and control over porosity, morphology and composition of the mat created

An important characteristic of electrospinning is the ability to produce fibres ranging from nanometres to a few microns in diameter (Li and Xia, 2004). Therefore the resulting fibrous mats have a large surface area per unit mass, making them usable for applications such as wound dressing, artificial blood vessels (Dong et al., 2008) and tissue engineering scaffolds (Martins et al., 2008).

For neural tissue engineering purposes, a wide range of polymers have been electrospun (natural and synthetic, degradable and non-degradable, biocompatible and non-biocompatible) to manufacture random and aligned scaffolds (Cao et al., 2009). For example, Patel and co-workers have produced random and aligned PLLA nanofibres and demonstrated their effect on directional neurite outgrowth of DRGs (Patel et al., 2007). Astrocytes and DRGs have been seeded on random and aligned poly(dioxanone) (PDS) (Chow et al., 2007). Human Schwann cells were cultured on random and aligned PCL nanofibres (Chew et al., 2008). Due to its potential, electrospinning is the focus of an increasing number of investigations (Li and Xia, 2004).

Self-assembling scaffolds

Self-assembling scaffolds, that form the desired structure after being injected into the injury site, are one the most recent developments (Tysseling-Mattiace et al., 2008). These isoleucin-lysine-valine-alanine-valine-epitope (IKVAV) containing

peptide amphiphile molecules self-assemble *in vivo* into nanofibres after being injected as a liquid into the tissue of interest. The self-assembly takes place due to the characteristics of the molecule which has a hydrophilic and a hydrophobic sequence and once the electrostatic repulsions are screened by electrolytes, the molecules are driven to assemble by hydrogen bond formation and by the unfavourable contact of the hydrophobic segments and water molecules (Silva et al., 2004), (Tysseling-Mattiace et al., 2008) (Fig 2.8). Great potential lies in this technique as implantation of the scaffold is simplified reducing side effects of the implantation procedure.

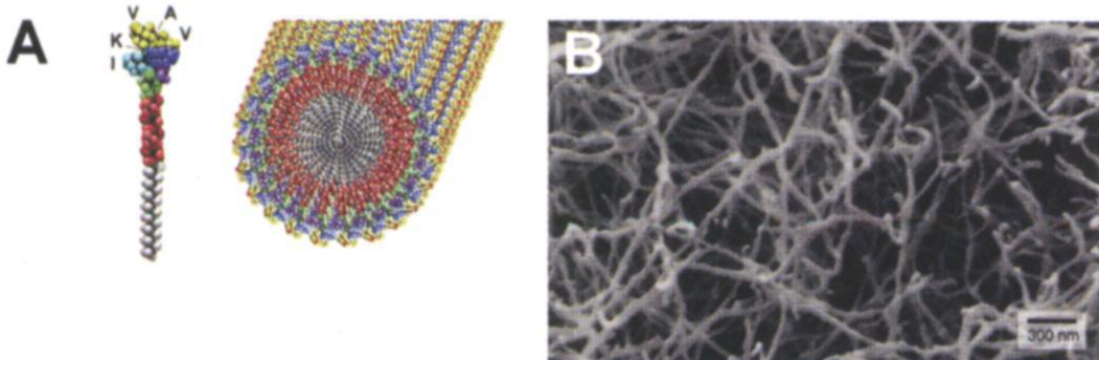

Figure 2.8 Molecular graphic illustration of an IKVAV-containing peptide amphiphile molecule, its self-assembly into nanofibres and SEM image of nanofibre network in vitro. Scale bar=300nm. (Silva et al., 2004)**.** Reprinted with permission from AAAS.

2.5.2 Material selection

The task of finding an optimal biomaterial for SCI has confronted tissue engineers with various challenges. Methods of fabrication have been discussed in the previous chapter and raise challenges themselves which to be further improved in order to address the challenges of scaffold design for SCI. For neural tissue engineering the challenges include several aspects such as mechanical strength, pore-size, hydrophilicity and conductivity. Most of these parameters are still sub optimal, as for example a PLA tubular scaffold collapsed after implantation into a rat spinal cord due to its low mechanical strength, preventing axonal outgrowth (Oudega et al., 2001). Various polymers have been tested and the most significant results are presented and discussed here (Table 2.3).

In order to increase the material's mechanical strength and pore-size and to decrease its hydrophobic surface properties, an introduction of bioactive molecules, manufacturing methods for porous structures and several hybrids with numerous materials have been developed. These materials have been processed into foams, films and fibres and seeded with Schwann cells, neural stem cells, PC12s and dorsal root ganglia cells (DGRs) in order to evaluate their regenerative potential (Table 2.3).

The family of poly(α-hydroxy) esters (PLA, PGA, PLGA) are approved for clinical use by the FDA. They are extensively used or tested for nerve regeneration strategies due to their biocompatibility and controllable biodegradability. These poly-esters have also been used as sutures (Yang et al., 2001), enforcement materials (Zong et al., 2005) and drug delivery devices (Aubert-Pouessel et al., 2002, Tatard et al., 2005). The materials have been applied in tissues such as skin (Kim et al., 2006a), (Blackwood et al., 2008), liver (Mayer et al., 2000), cartilage (Fan et al., 2006), blood vessel (Kaushiva et al., 2007), bone (Yang et al., 2001) and nerve (Bini et al., 2006).

Another biodegradable poly(ester), poly(caprolactone) (PCL), has also been tested as guidance scaffold and demonstrated potential for nerve repair applications (Ghasemi-Mobarakeh et al., 2008). In addition to poly(esters), other biodegradable materials, such as poly(organo phosphazene) (Nicoli Aldini et al., 2000), methacrylate-based hydrogels (Dalton et al., 2002), poly(3-hydrocyrutyrate) (Young et al., 2002) and poly(urethane) (Soldani et al., 1998), have also shown potential for nerve regeneration. Although the majority of these studies focus on PNS regeneration, lessons can be learned from these experiments as to how cells behave on biomaterial scaffolds.

Table 2.3 Summary of vairous polymers tested for regeneration of the spinal cord. 2D, two-dimensional; 3D, three-dimensional; NSCs, neural stem cells; PC12, pheochromocytoma cells; DRG, dorsal root ganglia; PA, Polyacrylamide; PLA poly(lactic acid); PLGA, poly(lactide-co-glycolide acid); PDMS, polydimethylsiloxane; PLLA, poly(L-lactic acid); PCL, Poly(carpolactone); PES, Poly(ethersulfone); PEG, Poly(ethylene glycol); PVF, poly(vinylidene fluoride); rNSCs, rat hippocampus-derived adult NSCs.

Material	Cell type	Type of scaffold	Findings	Reference
PA	PC12	2D gel coated with fironectin	Increased number of neurites, branching and length (10^2-10^4 Pa)	(Leach et al., 2007)
PCL	neonatal rat DRG	Random and aligned nanofibres	Fibre direction influences neurite outgrowth	(Xie et al., 2009)
PCL/gelatin	Neonatal mouse cerebellum C17.2 stem cells	Random and aligned nanofibres	Enhanced differentiation and proliferation, supported neurite outgrowth	(Ghasemi-Mobarakeh et al., 2008)
PEG	PC12	Hydrogel	Extend neurites, promotion of aggregation	(Dai et al., 1994)
	PC12	Film	Increased neurite density on medium wettability	(Lee et al., 2003)
PES coated with laminin	rNSCs	Electrospun nanofibres	Higher degree of proliferation and cell spreading on fibres with smaller diameter (< 300μm)	(Christopherson et al., 2009)
PLA	Primary sensory neuron, Primary motor neuron	Aligned nanofibres	Neurons survival and alignment	(Corey et al., 2008)
	Murine embryonic cortical neurons	Aligned nanofibres	Increased neurite extension	(Nisbet et al., 2007)
	chick DRGs, rat SCs	Aligned nanofibres	Cell and neurite orientation along fibres	(Wang et al., 2009)

Table 2.3 Summary of vairous polymers tested for regeneration of the spinal cord (continued).

Material	Cell type	Type of scaffold	Findings	Reference
PLA	NSCs	Random and aligned nanofibres with immobilised bFGF and EGF through heparin	Effect on cell orientation	(Yang et al., 2005)
	hECS-derived neural stem cells	Random and aligned nanofibres with immobilised bFGF and EGF through heparin	Heparin promoted axon growth	(Lam et al.)
	Schwann cells, DRG	Micropatterned grooves	SCs promote neurite alignment, outgrowth and neurite orientation	(Miller et al., 2001)
PLA with laminin	PC12	Electrospun random nanofibres	Longest neurites on blended laminin-PLLA	(Koh et al., 2008)
PLGA	Murine embryonic cortical neurons	Aligned nanofibres	Increased neurite extension	(Nisbet et al., 2007)
	SCs, rat mesenchymal stem cells	7-channel conduit	Cells attach, spread and proliferate	(He et al., 2009)
	C17.2 nerve stem cells	Random and aligned microfibres	Cells attach and differentiate	(Bini et al., 2006)
	PC12	Random microfibres	Shear stress of 0.5 Pa resulted in most aligned neurons	(Kim and Park, 2006)
	rat Schwann cells	Scaffolds with controlled, parallel-channel architecture	Axon regeneration	(Moore et al., 2006)
PLGA with hydrophobin II	Neural stem cells	Film	Promotes adhesion	(Li et al., 2009)

Surface topography

Surface topography has been shown to be an effective tool to enhance neurite outgrowth. Studies have been conducted using polymers of various chemical compositions, which have been micropatterned to contain grooves of different height, thickness and depth (Flemming et al., 1999, Fan et al., 2002b, Foley et al., 2005, Brunetti et al., 2010). It has been established that smaller channel widths (<100μm) in PLGA are more effective than larger channels in neurite guidance and result in longer neurite outgrowth and less secondary branching (Houchin-Ray et al., 2007). Studies combining topographical features with others such as biochemical or mechanical have demonstrated that the effect of topographical features seems to be most influential on neurite outgrowth (Haq et al., 2006). But the topographical effect can be supported, as controlled release of neurotrophic factors was shown to increase the effect of optimal topographical conditions (Houchin-Ray et al., 2007), especially when combining several neurotrophic factors, such as NGF and NT-3 which guided DRG a greater distance (12.5mm) compared to NGF alone (7.5mm) (Cao and Schoichet, 1999). All these studies demonstrated that even small changes to the surface of the scaffold can influence neurite behaviour and therefore topography can be used to desigh scaffolds which affect direcional neurite extention.

Conductivity

Research has also shown that electrical stimulation plays an important role in cellular differentiation for several cell types. For example, piezoelectric materials (i.e. materials that generate surface charge with small deformation) have been shown to significantly increase neurite extensions, such as poly(vinylidene fluoride) (PVDF) (Valentini et al., 1993, Makohliso et al., 1993), and poly(pyrrole) (Schmidt et al., 1997). PLGA has been coated with poly(pyrrole) to increase its conductivity which resulted in longer neurite extensions of PC12 cells (Lee et al., 2009).

Bioactive molecules

The scaffold's ability to support cell attachment has to be considered when designing an implant. Many polymers used in tissue engineering, such as PLGA, lack natural adhesion sites thus have to be manipulated using hydrolysis, aminolysis, blending and covalent attachment of adhesive peptides (Croll et al., 2004).

Modified poly(ethylene glycol) (PEG) polymers were shown to aid nerve regeneration, as PC12 cells extend neurites on PEG hydrogel when Arg-Gly-Asp (RGD), a cell adhesion motif, is covalently bound to the material (Dai et al., 1994, Schmidt and Leach, 2003). This motif is recognised by integrins, homologous transmembrane cell-ECM adhesion receptors which mediate cell attachment to surrounding tissues (Tomaselli et al., 1987). The RGD amino acid sequence is part of the integrin-interaction site of many ECM proteins. Other motifs that are recognised by integrins are YIGSR, IKVAV and can be found in laminin, collagen-I, fibronectin and vitronectin (Miceli et al., 1997).

Poly[N-(2-hydroxypropyl)methacrylamide] (pHPMA) hydrogel has been modified to contain RGD and was shown to support tissue development within the injured rat spinal cord (Woerly et al., 2001). PLGA films were coated with laminin, fibronectin or collagen, demonstrating that coating is essential for neural cortical cells to adhere and differentiate (Han et al., 2005). RGD was immobilized on various biomaterials, including but not restricted to chitosan, PLGA and PLLA (Gunn et al., 2005, Blewitt and Willits, 2007, Cooke et al., 2008, Mochizuki et al., 2007, Kim and Park, 2006), as it was shown to promote adhesion and neurite outgrowth from embryonic central, peripheral neurons and PC12 cells more efficiently than laminin (O'Shea et al., 1991). Other amino acid sequences, such as Tyr-Ile-Gly-Ser-Arg (YIGSR) and Ile-Lys-Val-Ala-Val (IKVAV) laminin derived penta-peptides, were shown to promote PC12 cell attachment when grafted to dextran-coated surfaces (Massia et al., 2004).

Neurotrophic factors

Neurotrophic factors are proteins with various functions. They enhance neurite outgrowth, proliferation, differentiation, axonal outgrowth and synaptic plasticity. They contribute to neuronal survival and differentiation during development and promote repair and recovery after injury to the CNS in the adult (Nomura et al., 2006). Administration of neurotrophic factors, such as NT-3, NT-4/5, or BDNF, into the injured spinal cord promotes regeneration and limits neuronal damage (Grill et al., 1997) (Lu et al., 2005) (Himes et al., 2001). In combination with Schwann cells or peripheral nerve, FGF-1, NT-3 or BDNF results in functional recovery due to anatomical connectivity after rat spinal cord transection (Menei et al., 1998), (Lu et al., 2005). Tubular PAN/PVC implants in combination with neurotrophic factors (especially NT-3, BDNF, GDNF) and Schwann cells seeded inside the tubular implant resulted in promising results in rat SCI model (Bunge, 2001). (Xu et al., 1997).

2.6 Conclusion

Over the past 20 years scaffold fabrication techniques have become more sophisticated allowing tissue engineers to manipulate the design of the scaffold down to nanometer level. The most promising scaffolds produced to date are scaffolds manufactures by electrospinning and self-assembly. The advantage of self-assembling scaffolds lies within the delivery method, as the peptide solution is injected into the site of injury using a syringe and self-assembles at the site of injury, reducing further damage which may occur during implantation. On the negative site, only random scaffolds can be produced using this method and only specifically designed molecules can be used, limiting the application of this method. The advantage of electrospinning is that various polymers can be electrospun into desired nanofibres with highly porous structures, and random and aligned nanofibres. Furthermore, by manipulating the settings, electrospinning can be used to produce droplets of polymer, called electrospraying, in which drugs can easily be incorporated, providing further applications for this method. Electrospinning has also its limitations; including the challenge of producing aligned nanofibres in tubular form resulting in a bigger implant, comparable to those produced using gas-

foaming and solid-liquid phase separation techniques. In the future, the optimum technique will be selected by time efficiency and low price in production and physiological optimum parameters.

Tissue engineering has increased the potential for SCI repair, leading to partial recovery in experimental SCI, still requiring more pre-clinical work for translation into humans. To date, synthetic guidance scaffolds by themselves have been unable to promote significant anatomical or functional recovery in SCI. Combinational approaches combining biomaterials delivering growth factors and cells (Schwann cells, OEG, stem cells) are the preferred strategy. However, various challenges remain, concerning both biomaterials and stem cells. Non-biodegradable scaffolds are not preferred as they do not degrade and remain at the site of injury. Biodegradable scaffolds may collapse and prevent regeneration by creating neuromas. On the positive side biodegradable scaffolds obviate the need for second surgery, but require detailed degradation studies, optimising degradation time as well as resulting in non-toxic products and be non-inflammatory. Despite the remaining challenges, there is some hope that the combination of biomaterial, cells and neurotrophic factors will result in functional repair of SCIs. The big questions that remain to be solved are:

1. Optimum scaffold. A scaffold that fulfils all the required parameters has yet to be developed including the question which modality is more beneficial under which traumatic circumstances.
2. Delivery of any neuroprotective or regenerative agents. Delivery, encapsulation, and release efficiency need to be further investigated.
3. Cell type. What type of cells can be successfully delivered to the site of injury to achieve the best outcome? What delivery method is most efficient and cell death preventative?
4. Timing of therapeutic interventions has still to be addressed.

All four parameters can influence each other and have to be investigated before proceeding to human clinical trials. And although there are still limitations to the

construction of the scaffolds, they can be used to investigate the points mentioned above, facilitate understanding and open new possibilities for recovery after SCI.

2.7 Aims and objectives of the project

The focus of the research presented here will be points 1 and 2 as these are the more fundamental questions of therapeutic interventions for spinal cord repair where essential data is still missing.

This multidisciplinary project aims to develop a scaffold for spinal cord repair using PLGA membranes as a guidance conduit for nerve regrowth and delivery of bioactive chemicals to overcome the inhibitory signals found at the site of spinal cord injury.

PLGA will be tested for its ability to support cell adhesion, proliferation and differentiation of nerve cells. PLGA flat sheet membranes will be the starting point for these tests. As well as being a physical support for cells, it will be established if PLGA effects neurite outgrowth in a positive or negative way. If necessary, PLGA will be treated with adhesive and neurite-promoting proteins such as laminin, or chemically modified with the YIGSR laminin fragment to improve its cytocompatibility.

In order to evaluate the PLGA scaffold, PC12 cells will be used as a model cell line. These cells were chosen as parameters such as cell counts, increased cell numbers and the increased length of neurites, are accepted as indicators of positive PC12 cell response to presented scaffolds. Once attachment is established, PC12 cells will be exposed to NGF in order to induce the neural phenotype and neurite outgrowth on the surfaces will be analysed. For this analysis PC12 will be exposed to NGF for up to seven days, after which their differentiation in terms of number of neurite bearing cells and neurite outgrowth will be characterised.

In parallel with the work on flat sheet membranes, the project will focus on investigating other scaffold producing methods, e.g. electrospinning, a method for production of nanoscale fibres. Various parameters affecting electrospinning such

as solution viscosity, polymer concentration, inner needle diameter and voltage will be investigated. The produced scaffolds will be evaluated for their ability to support PC12 cell attachment and differentiation as described above.

3. MATERIALS AND METHODS

3.1 Introduction

This chapter describes all methods used for the work carried out in this thesis. This chapter is subdivided into three sections: experimental methods, analytical methods and statistical analysis. A detailed list of materials can be found in the appendix (A1).

3.2 Experimental methods

All experiments were conducted at room temperature (20°C) unless otherwise stated. A washing step describes the addition of PBS to a well and its immediate aspiration.

3.2.1 Fabrication of PLGA films

Poly(lactic-co-glycolic acid) (PLGA) films were produced using a new method adapted from (Sharon and Puleo, 2008). PLGA solution (50µl, 10% w/w in dichloromethane and methanol (DCM:MeOH, [3:1]) was pipetted on to glass coverslips (squares 18x18mm, circle 13mm diameter) and allowed to air dry for 30 min and then vacuum dried overnight, both at 20°C. This allows a quick production of films with uniform surfaces. Surface roughness of films was analysed using atomic force microscopy (AFM) in the tapping mode (see 3.3.8).

3.2.2 Fabrication of PLGA flat sheet membranes

Biodegradable porous membranes were produced using the immersion precipitation method. 1-methyl-2-pyrrolidinone (NMP) was used as solvent whereas dH_2O was used as non-solvent. PLGA was dissolved in NMP at a concentration of 20% w/w and left to dissolve on a rotating drum at 80rpm for 24 hours. The polymer solution was poured onto a 15x25cm glass support and flattened out using a glass rod, controlling the thickness (200µm) with guide wires. The polymer solution was immersed in distilled water (enough water to cover the glass support with polymer solution, usually 500-1000ml) for 2-3 min. The resulting membrane was lifted off the glass support and left in 500–1000ml distilled water for two days, changing the water twice a day.

3.2.3 Electrospinning

PLGA nanofibres were produced using electrospinning. Polymer solution was prepared by dissolving PLGA in several solvents at a concentration of 10% w/w, including dimethylformamide (DMF), tetrahydrofuran (THF), DMF and THF at ratios 3:1 and 1:1, isopropanol (Meng et al., 2007), dichloromethane (DCM) (Nie et al., 2009), chloroform ($CHCl_3$) and methanol (MeOH) at ratio 3:1 and NMP, which was previously used for fabrication of PLGA flat sheet membranes (Ellis and Chaudhuri, 2008). From each solution, 5ml was transferred into a 10ml Hamilton glass syringe fitted with a needle, which was controlled by a syringe pump at a feeding rate of 0.5-5ml/h. The feeding rate was chosen based on experience with the setup, favouring slower feeding rates, as it was shown to result in decreased fibre diameter and a less broad diameter distribution. The distance between the needle tip and the collector, was adjusted to 11cm.

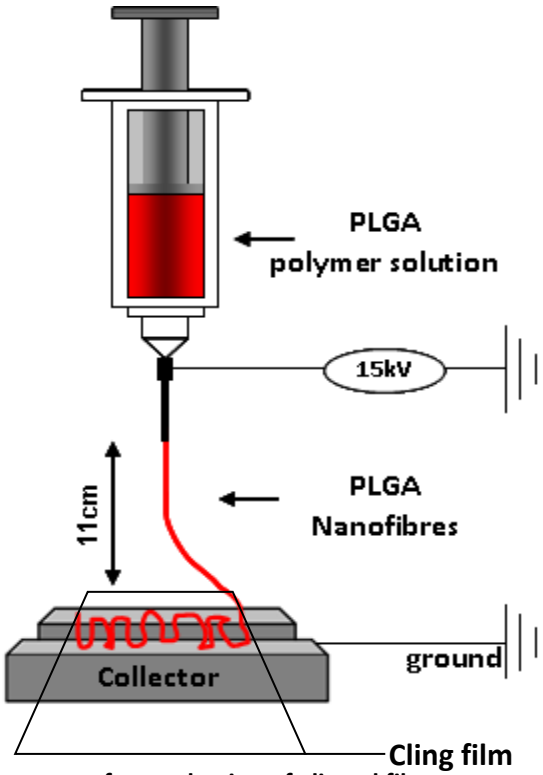

Figure 3.1 Electrospinning set up for production of aligned fibres.

For collecting random fibres, aluminium foil was used as collector. In order to produce aligned fibres the aluminium foil was replaced by two aluminium rods covered with cling film (Fig 3.1). A high voltage of 15kV was applied to the needle by

a voltage regulated power supply. The resulting fibre mats were placed in a desiccator for at least 24 h or until use.

3.2.4 Preparation of emulsions for electrospinning

In order to incorporate poly-L-lysine (PLL) into the electrospun nanofibres, emulsions were prepared as follows. A 10% w/w PLGA solution was prepared in $CHCl_3$:MeOH (3:1). The aqueous solution, consisting of dH_2O in which the substance of interest was dissolved, was added drop-by-drop (drop volume of 50µl) to the PLGA solution under constant stirring at 750rpm to ensure thorough mixing of the aqueous solution, to a final ratio of 1 part water phase to 18 parts of organic phase. The solutions was rigorously stirred at 750rpm for a minimum of 10 min, vortexed, pipetted into the syringe and electrospun as quickly as possible avoiding separation of the two phases. For samples produced using a surfactant, 50µl of Span80 were added to the electrospinning solution, and stirred thoroughly at 750rpm. For fluorescent nanofibres the aqueous phase consisted of 1.1mg/ml PLL and 42µg/ml PLL-FITC in water/oil phase ratio 1/18. For non-fluorescent PLGA-PLL nanofibres PLL-FITC was not added.

3.2.5 Surface modification

Prior to surface modification samples of PLGA flat sheet membranes were cut into round pieces with a diameter of 21mm. The cut samples were placed in 12 well plates and retained at the bottom well with silicon rings. The standard volume of substances added to 12 well plates was set at 1.5ml. For surface modification sodium hydroxide (NaOH) (0.05M, 0.1M and 0.2M) in dH_2O or ethylenediamine (EDA) (0.1%, 0.2% and 0.5%) in propanol were added to the samples and incubated for 15 min, followed by two washes with PBS. Aminolysed films were used for cell culture without further modification. Hydrolyzed PLGA films and membranes were treated with 0.05mM NaOH for 15 min, washed with PBS and incubated in freshly made solution of 10mM 1-ethyl-3-(3-dimethylaminopropyl)carbodiimide hydrochloride (EDC) and 5mM *N*-Hydroxysuccinimide (NHS) in 2-(*N*-morpholino)ethanesulfonic acid (MES) buffer (pH 6.5) for 30 min. After a further

wash with PBS, the polymer was incubated with 1ml of YIGSR-peptide solution (100µg/ml) for 24 hours. Treated films were washed twice with PBS.

3.2.6 Ozone surface treatment

PLGA flat sheet membranes were treated with ozone in order to induce peroxide formation on the membrane's surface (Ho et al., 2007). PLGA flat sheet membranes were cut into 1.5x1.5cm squares and suspended in 20ml of dH_2O, where a stream of ozone and oxygen (O_3/O_2) mixture was bubbled through continuously. The O_3/O_2 mixture was generated by passing oxygen gas through the ozone generator. The operating conditions were set at room temperature at 5ml/h oxygen flow rate, variable control at 10 resulting in ozone production of 8.5gm/h or 50mg/l. The membranes were exposed to ozone for 10, 30, 60, 120, 180 and 240 min at 20°C. Water contact angle measurements was used to analyse the treated flat sheet membranes.

3.2.7 Cell culture

The PC12 cell line was used for all cellular experiments. Cell culture work was performed under sterile conditions in Class II microbiological safety cabinets. PC12 cells were maintained in tissue culture flasks coated with 0.01% PLL in PBS and RPMI 1640 medium, which was supplemented with 1mM sodium pyruvate, 1% antibiotic/antimycotic solution and 10% foetal calf serum (FCS). Cells were grown in incubators in a humid atmosphere at 37°C and 5% CO_2. For subcultivation, after reaching 75% confluence, cells were detached from 75cm^2 flasks by addition of 3ml 0.25% trypsin/0.1g/l EDTA. Detachment was observed under the microscope and after maximum 15 min 9ml of cell culture medium was added, the mixture was collected, placed in a tube and centrifuged for 4 min at 1500rpm. After centrifugation, the cell pellet was resuspended in 2ml fresh culture medium and cell density was established using a haemocytometer. Then cells were pipetted back into 75cm^2 flasks, which contained 10ml of fresh culture medium and was precoated with 0.01% PLL, or seeded onto the PLGA scaffolds at a density of $3x10^5$ cells cm^{-2}.

3.2.8 NGF induced differentiation of PC12 cells

For differentiation, PC12 cells were exposed to differentiation medium. For this the RPMI 1640 medium was supplemented with 1mM sodium pyruvate, 1% antibiotic/antimycotic solution, 1% FCS and 40ng/ml NGF. The cells were differentiated for up to 7 days. Medium was removed and replaced with fresh medium every second day.

3.3 Analytical methods

This section describes the methods used for analysis of experiments described in section 3.2. The analytical methods include the analysis of the scaffold, cell culture experiments and microscopy.

3.2.1 Viscosity of PLGA solutions

The viscosity of PLGA solutions was measured using a Rheometer (Bohlin, C-VOR). A cone with 40mm diameter and 4° angle was used. Shear stresses between 0.5-10 (force/area) were applied with a delay of 10 s and an integration time of 10 s.

3.3.2 Wettability of scaffolds

For water contact angle measurements, 300µl of polymer solution was electrospun onto glass cover slips of 13mm diameter which were placed on top of the aluminium foil. Flat sheet membranes were cut into 1x1cm squares and fixed on glass slides using tape. The glass cover slips and glass slides were placed onto the testing plate. Subsequently, a 5µl droplet of distilled water was deposited carefully onto the specimens. The water contact angles between water and electrospun fibre mats were measured using photos taken at various time periods (0, 30, and 60 s). The images were analysed using ImageJ (obtained from http://rsbweb.nih.gov/ij/) plug-in drop_analysis (obtained from http://bigwww.epfl.ch/demo/dropanalysis/). The output window provided data about the contact angle, drop volume (mm^3), surface of contact (mm^2) and drop surface (mm^2). Nine measurements of each sample were carefully conducted while placing the droplet in different places on the

surface of the samples. The reported values were mean value with the error bar representing the standard error of the mean.

3.3.3 Quantification of nanofibre alignment

For fibre alignment measurement phase contrast images were taken digitally using a microscope and analysed using Fast Fourier Transform (FFT) and Oval Profile plug-in in ImageJ (Alexander et al., 2006). The FFT output reflects the degree of fibre alignment present in the selected area. The pixel intensity of the FFT image is summed along a straight line radiating at the angle, from the centre to the edge of the image. A graphical representation of the alignment is obtained by plotting the summed pixel intensity. A totally random picture would result in constant pixel intensity independent of direction, which would be plotted as a horizontal line. On the contrary, an image that is perfectly aligned in one direction would have higher intensity in that direction, resulting in peaks. FFT analysis of 6 randomly selected images (512x512 pixels) gave information about gross image orientation in form of pixel intensity.

3.3.4 Vybrant CFDA SE cell tracker

Prior to use, a 10mM CFDA SE stock solution in high-quality DMSO was prepared. The stock solution was diluted in PBS to obtain a 5µM working solution. The cells were stained in suspension. A cell pellet was resuspended in pre-warmed (37°C) CFDA SE working solution. After an incubation of 15 min at 37°C, the cells were re-pelleted by centrifugation (4 min, 1500rpm) and resuspended in 2ml fresh pre-warmed medium (37°C). To ensure complete modification, the cells were incubated for another 30 min at 37°C. Stained cells were seeded on PLGA and left to attach for 4 h. For fixation, the cells were washed with PBS (1.5ml in 12 well plates) and fixed in formalin (1.5ml in 12 well plates) for 15min. After a final wash with PBS the cells were analyzed by fluorescence microscopy using a standard fluorescein filter sets.

3.3.5 Quantification of cell attachment

The PicoGreen Quant –iT^{TM} PicoGreen dsDNA kit allowed the detection of double stranded DNA using an ultrasensitive fluorescent nucleic acid stain and was used

according to the manufactures instructions. For extraction of DNA 1ml of TE buffer (10mM Tris-HCl, 1mM EDTA, pH 7.5) was added to each well, frozen down to -80°C for a minimum of two hours or until analysis. To thaw, the samples were heated up to 37°C for one hour. When completely thawed, TE buffer was pipetted up and down to allow thorough mixing. 1ml of the aqueous working solution of the Quant-iT PicoGreen reagent was added to each sample incubated for 2-5 min at room temperature and protected from light. After incubation the fluorescence of the samples was measured using a fluorescence microplate reader at standard fluorescein wavelengths (excitation ~480nm, emission ~520nm). The concentration of the DNA sample was established using the standard curve.

3.3.6 Quantification of cell survival

Live/Dead staining was performed to visualise the fraction of cells in a cell population that were viable or non-viable. For this 1mg/ml Hoechst (stains the DNA in the nuclei) in dH_2O, 4mM calcein acetoxymethyl (AM) (green = viable), 2mM ethidium homodimer (red = non-viable) were mixed into cell culture medium at a dilution of 1/200 for calcein AM and ethidium homodimer and 1/400 for Hoechst. This medium was added to the samples, usually cells that are seeded on tissue culture plastic (TCP) or polymer samples, and incubated at 37°C for 20-30 min. The incubation step was followed by a wash with PBS and a fixation step in 10% formalin for 20 min. After one washing step, fresh PBS was added and samples were analysed under a fluorescence microscope, using excitation 495nm and emission at 515nm for calcein AM, for ethidium homodimer excitation 530-585nm and emission 615nm and for Hoechst excitation 346nm and emission 460nm.

3.3.7 Neurite characterisation

Number of neurites per cell, neurite length and neurite alignment were measured using ImageJ software. Analysis was performed on cells which were exposed to NGF for 7 days, then fixed and stained as described in section 3.3.6. For this a minimum of 30 images of cells stained with Hoechst, calcein AM and ethidium homodimer were recorded. Four sets of images were taken, a phase contrast image and three fluorescent images visualising the three stains.

Number of neurites per cell was recorded by counting all cells per image and then counting all neurite bearing cells, where a neurite was considered when it was longer than the cell body diameter. Counting was performed using CellCounter plug-in for ImageJ.

Neurite length was analysed using the tool “Straight Line” in ImageJ. Before starting the analysis the scale for the image was set, using the image acquisition parameter from the microscope. Then the “Straight Line” tool was selected and a line was drawn along the visible neurite. In cases of non-straight neurite outgrowth the “Straight Lines” tool was replaced with the “Segmented Lines” tool. The data was collected using the Analyse plug-in, where the option “Measure And Label” was selected. For angle measurements the “Straight Line” tool was used starting at the cell body and drawing a line to the end of the longest branch of the neurite.

When using the “Straight Lines” tool in combination with the “Measure And Label” tool, the output gave not only the neurite length but also the angle of the neurite (Fig 3.2). This was used for measuring neurite alignment along electrospun fibres. For this the orientation of the fibres was set as zero, the image was rotated accordingly. Images of cells on random fibres were not rotated as no directional dominance was present. The negative and positive data was summarized and presented as positive data only as there was no difference between the two. Cells with neurites extending beyond the boundary of the image were excluded from the data.

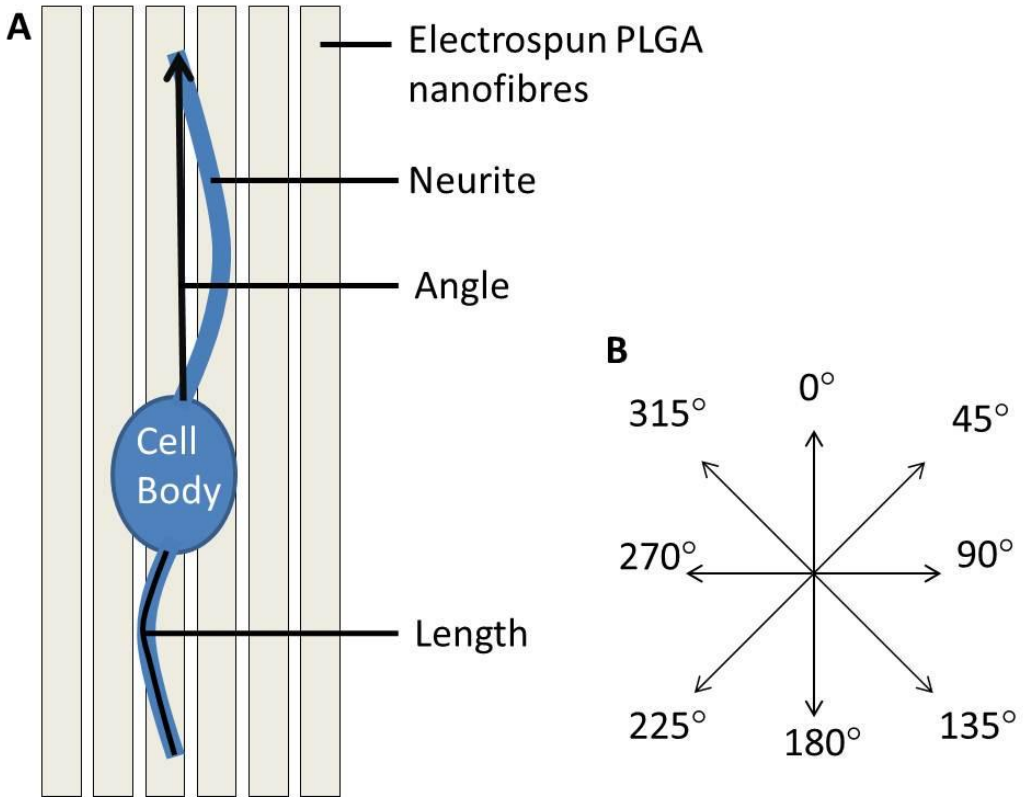

Figure 3.2 Neurite characterisation. (A) Model of obtained image for analysis. (B) Arrows indicate the angle of neurite outgrowth measurement; the cell body is the starting point of measurements. Nanofibres and cells are not to scale.

3.3.8 Atomic force microscopy (AFM)

PLGA films were analysed using AFM (Digital Instruments nanoscope IIIA) as follows. Tapping mode was performed in ambient air using a laser incorporated Nanoscope III SPM (wavelength 670nm, maximum power 1mW) from Veeco Instruments, Inc. A J-scanner was used with a maximum 125x125µm^2 x–y scan range, with a 512x512 pixels recorded for each image. On each sample, a series of areas (n=3) were recorded in tapping mode.

3.3.9 Scanning electron microscopy (SEM)

The morphology of electrospun PLGA scaffolds as well as the morphology of cells seeded onto the scaffolds were studied by SEM (JEOL, JSM-6480LV). Prior to SEM, scaffolds were gold coated using a sputter coater (Edwards Sputter Coater 5150B).

Preparation of cultured cells for SEM started with replacing culture medium with wash medium (normal strength culture medium without serum). Wash medium was

removed and replaced with 2.5% glutaraldehyde (GDA) in normal strength medium and fixed for 2 h at 37°C. After fixation the samples were washed with wash medium three times and postfixed with aqueous 1% osmium tetroxide for 1 h in the fume hood at 20°C. This was followed by three washes with distilled water and staining with filtered 2% aqueous uranyl acetate for 1 h in the dark. The samples were washed three times and freeze-dried overnight. The freeze dried samples were gold coated just before the SEM session.

3.3.10 Fluorescence and Light Microscopy

All cell morphology analysis was observed and recorded using a Leica microscope (Leica DMI 4000B). Pictures of aligned electrospun fibres were recorded using the same microscope.

3.4 Data analysis and Statistics

All collected data was analysed using Microsoft Excel. The data presented in this study is expressed as mean ± standard error of mean (SEM). Each parameter was conducted with a minimum of three samples (n=3). The statistical significance between two sets of data was calculated using Student's t-test. Differences were considered to be significant when a P value of 0.05 or less was obtained, with *denoting $P < 0.05$, ** denoting $P < 0.01$ and *** denoting $P < 0.001$.

4. POLY(LACTIC-CO-GLYCOLIC ACID) - A SUITABLE BIOMATERIAL FOR NERVE REGENERATION?

4.1 Introduction

In an effort to study the suitability of PLGA for neuronal applications, experiments were conducted to assess the polymer's ability to support neural cell attachment, proliferation and differentiation. PC12 cells were used as a model cell line for neural differentiation. The use of flat sheet membranes allowed testing the interaction between polymer and cells on a 2D surface, which previously has been proven efficient for human bone derived cells (Ellis and Chaudhuri, 2008).

PLGA flat sheet membranes were produced by phase inversion where precipitation of the polymer results from the movement of the solvent into a non-solvent. The membrane structure is determined by the rate and mechanism of precipitation (Mulder 1992). The roughness of the asymmetric flat sheet membrane was analysed using AFM, as this factor has previously been shown to play a major role in cell attachment (Fan et al., 2002a).

Surface modification has been widely used to improve polymer hydrophilicity, thus potentially increasing the bioactivity of the polymer. Increased hydrophilicity is due to the introduction of highly polar groups (e.g. hydroxyl, carboxyl, or amine) on the surface of the polymer to which the cells can attach. Low hydrophilic surface characteristics were shown to result in lower cell attachment compared to highly hydrophilic surfaces for neuronal cells (Park et al., 2008). The experiments conducted include surface treatment with ethylenediamine (EDA), peptide modification, and ozonation. These treatments have been previously used (Cao et al., 2004) and were applied to PLGA flat sheet membranes in the studies presented here.

4.2 Seeding efficiency of PC12s on PLGA flat sheet membranes

In order to assess PLGA as a scaffold material, PC12 cells were seeded onto flat sheet membranes and cell attachment was compared to membranes coated with poly-L-lysine (PLL), or tissue culture plastic (TCP) coated with PLL.

The results show that PC12 cells attached to PLGA flat sheet membranes, but in low numbers (Fig 4.1). On untreated PLGA, 20$\pm$7% of seeded cells attached to the

polymer, on PLGA coated with PLL 23±14% of seeded cells attached, and on TCP-PLL 69±12% of cells attached to the surface. Cell attachment numbers for PLGA and PLGA coated with PLL samples were not significantly different from each other (P>0.05), implying that coating with PLL did not have a positive effect on cell attachment. This data shows that attachment to PLGA flat sheet membranes is very low, less than 30% of seeded cells attached to the polymer. Cell numbers were counted using a haemocytometer, a method used for determining the concentration of cells in a suspension. For this, the number of cell in suspension as well as the number of cells attached, which were detached prior to counting using trypsin/EDTA, were counted. Here, only the numbers attached are presented. It was possible that using the haemocytometer the cell number count was not accurate as cells had to be detached from the surface. This was avoided by thorough washing of wells and control under the microscope to assure no cells remained in the well. Furthermore, this experiment was repeated with PC12 cells stained with Vybrant CFDA SE cell tracker and PLGA flat sheet membranes were analysed under a fluorescent microscope to assure all cells were detached from the flat sheet membranes. Nevertheless the error bars could not be reduced.

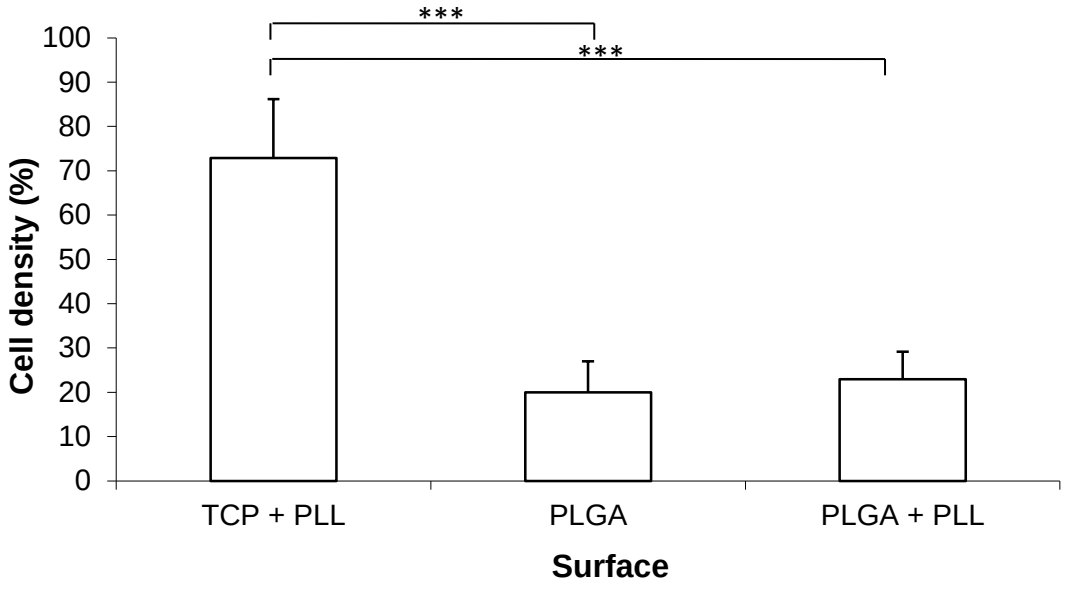

Figure 4.1 Attachment of PC12 cells to PLGA flat sheet membranes 4h after seeding. PC12 cells attachment to PLGA, PLGA coated with PLL and TCP coated with PLL (positive control) (TCP: tissue culture plastic, PLL: poly-L-lysine). Numbers are represented in number of cells attached in percent compared to the number of cells seeded (100%). Data represent the mean ± SEM (n=4) and were analysed using Student's t-test. *** P<0.001.

PC12 cells can form aggregates in suspension and on the polymer's surfaces making the creation of a single cell suspension a challenge. It is possible that the seeded cell number was not as accurate as expected, though cell suspension was controlled using the haemocytometer and a sufficient number of experiments was conducted.

No increase in cell numbers attaching to PLGA after coating with PLL can be explained with the lack of charges on the surface of PLGA. The positively charged PLL cannot bind to any charges on the PLGA surface and is likely to be washed off. In order for PLL to be efficient in increasing cell attachment the surface of PLGA needs to be modified in order to introduce negative surface charges.

The lack of interaction between PC12 cell and PLGA may be cell specific as other cells have been shown to attach to PLGA in higher numbers. Ellis and colleagues have shown that 75% of the initially seeded immortalised osteogenic 560pZIP.neo cells attach to PLGA flat sheet membrane (Ellis and Chaudhuri, 2007), which is three times more efficient than what was achieved with PC12s. Human bone derived cells also attach to PLGA flat sheet membranes with an efficiency of 65% (Ellis and Chaudhuri, 2008), which is also higher compared to 20$\pm$7% of seeded PC12 cells. Park and colleagues have shown that Schwann cells and olfactory ensheathing cells (OECs) attached to PLGA films (Park et al., 2008). As the size of the PLGA film was not mentioned in their publication, quantification of attachment efficiency and thus comparison with the work presented here is not possible. Other studies focused on cell attachment to PLGA microspheres, showing how for example undifferentiated mouse type cell line P19 cells attach to PLGA microspheres (Nojehdehian et al.). The efficiency of cell attachment was not clearly demonstrated in this recent publication thus it is difficult to compare it to the results here, but it demonstrates that PLGA as a polymer is of high interest in tissue engineering research. An additional interesting observation was made when these microspheres were coated with PLL. The coating with PLL resulted in higher cell number attaching to the coated microspheres compared to non-coated (Nojehdehian et al.). This effect was not observed when PLGA flat sheet membranes were coated with PLL (Fig 4.1). PLGA microspheres produced by Nojehdehian and colleagues were loaded with retinoic acid which was gradually released into the medium. As PLGA microspheres without retinoic acid

were not included in the controls the effect of retinoic acid on PLL may only be suspected and needs further investigation. A study by He and co-workers presented qualitative data of rat Schwann cells attaching to the lumen of PLGA multiple-channel conduits supporting the use of PLGA for nerve tissue engineering and proving its biocompatibility after implantation into rat spinal cords (He et al., 2009). Quantitative cell adhesion data was not presented and cannot be compared to cell adhesion data here. A study published by Valmikinathan and co-workers describes the attachment of rat Schwann cells to a PLGA microsphere-based spiral scaffold with a nanofibrous surface (Valmikinathan et al., 2008). Unfotunately, this publication does not list any cell attachment numbers but absorbance data obtained from MTS experiments, demonstrating increased absorbance at 490 nm after 4 days of incubation.

All things considered, PC12 cells attach to PLGA flat sheet membranes but in low numbers in comparison to the literature. In order to increase cell attachment efficiency various surface modification methods were performed and evaluated.

4.3 Aminolysis

Aminolysis is a technique which is used in the textile industry to improve wettability and dyeability of synthetic polyesters (Wei and Gu, 2001). It has also been applied for tissue engineering in order to modify polymer surfaces (Zhu et al., 2002). The advantage of using aminolysis as a modification method are the resulting amine groups on PLGA films, which provide a stable pH environment during degradation as opposed to modification with magnesium hydroxide (Houchin et al., 2007). Here, a low number of seeded cells attached to non-modified PLGA (Fig 4.1), thus the polymer's surface was modified in order to achieve higher adhesion efficiencies. The aim of surface modification using ethylenediamine (EDA) is to introduce primary and secondary amine groups to the surface of the polymer, as PLGA does not possess any functional groups for attachment of biologically active molecules. Theoretically, after modification, cells seeded onto the polymer are more likely to attach to the presented amine groups.

On untreated PLGA, 20±7% of seeded PC12s attached (Fig 4.2). PLGA treated with propanol and EDA dissolved in propanol did not provide a more favourable surface for cell attachment resulting in low attachment of 23±12%, 19±14%, 10±10% and 9±6% on PLGA treated with propanol, 0.1% EDA, 0.2% EDA and 0.5% EDA, respectively. Statistical analysis of the results revealed that cell attachment to TCP-PLL was significantly higher compared to non-treated and treated PLGA ($P<0.01$) and attachment to PLGA treated with 0.5% EDA was significantly lower compared to PLGA ($P<0.05$). These results suggest that the introduction of amine groups was not successful or the number of groups introduced was not high enough to result in higher cell attachment of PC12s. Plus, it appears that treatment with 0.5% EDA did prevent cell attachment.

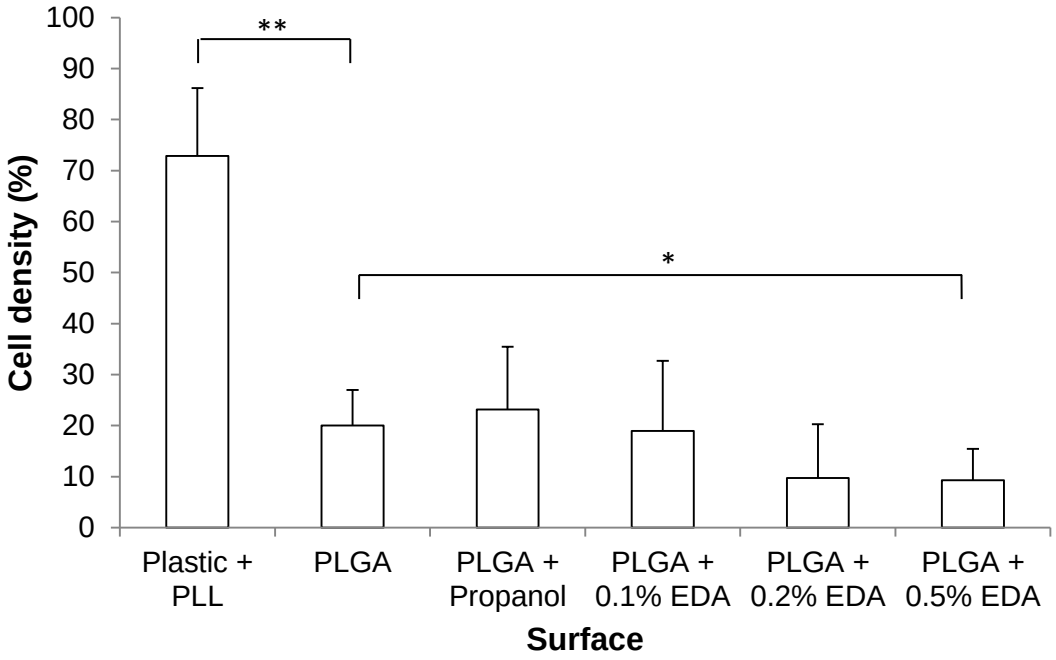

Figure 4.2 EDA modification of PLGA flat sheet membranes does not promote cell attachment. PC12 cell attachment to PLGA treated with propanol, 0.1%, 0.2% and 0.5% EDA. Data represent the mean ± SEM (n=3) and was analysed using Student's t-test. * $P<0.05$, ** $P<0.01$.

Propanol, similar to ethanol, can act as adhesive which can lead to coglutination of the polymer and consequently to loss of surface structure and surface chemistry inhibiting cell attachment. The question is then, why only the highest EDA

concentration sample resulted in lower cell attachment as propanol was used on its own and as solvent for other EDA concentrations. Thus EDA is likely to be responsible for significantly lower cell attachment at a concentration of 0.5% but not at lower concentrations.

Other proteins present in the medium, e.g. components of the FCS, may have a higher affinity for the amine groups compared to PC12 cells, thus blocking the polymer from the cells. Fibronectin and vitronectin are most abundant cell attachment proteins in the FCS (Hayman et al., 1985) and their influence on PC12 attachment behaviour is an interesting point to investigate.

In order to confirm the success of aminolysis, Zhu and colleagues used rhodamin B isothiocyanate (RBITC) to label the amino groups on the aminolysed PCL followed by the ninhydrin analysis method to quantitatively detect the amount of NH_2 groups on the polymer's surface (Zhu et al., 2002). This quantification was not applied here as in the end aminolysis was intended to increase cell attachment. As the presence of amine groups on PLGA flat sheet membranes was not performed two conclusions can be drawn, either the modification worked but did not result in higher cell attachment or the modification did not work and thus did not result in higher cell attachment. But some sort of reaction took place as the highest EDA concentration resulted in the lowest cell number attaching. Either way cell attachment was not increased and requires further investigation as to which scenario is correct. For this, other treatment methods such as plasma treatment can be investigated and the use of other amine precursors can be attempted.

Aminolysis has previously been shown to be an effective surface modification method (Croll et al., 2004, Djordjevic et al., 2008). Nevertheless cell culture studies were not conducted on those surfaces making this the first report describing cell culture studies for aminolysed PLGA flat sheet membranes.

One report supports our findings; Zhu and co-workers modified polycaprolactone membranes using aminolysis (Zhu et al., 2002). They observed that attachment of fibroblasts was not improved but they found that proliferation was improved by 10% compared to non-treated membranes. Nonetheless the extent of proliferation was small compared to TCP (up to 70%). These publications show that aminolysis is

a promising technique. However, modification of PLGA flat sheet membranes did not result in higher cell attachment and remained below numbers of cells attaching to TCP. As there was no increase in the cell numbers attaching, aminolysis was excluded from further investigation.

4.4 Peptide modification

The aim of peptide modification is to introduce peptide groups to a polymer's surface, for example laminin fragments, in order to increase the biocompatibility of the polymer. The method described here results in peptides attached to the polymer via covalent bonds. Aqueous carbodiimide chemistry uses 1-Ethyl-3-(3-dimethyl-aminopropyl)carbodiimide hydrochloride (EDC) as a zero-carbon-crosslinker, which reacts with carboxylic acid groups to form an *O*-acylisourea intermediate which is replaced by a primary animo group. The amino group forms a peptide bond with the original carboxyl group and an EDC by-product is released as soluble urea derivative. N-hydroxysuccinimide (NHS) is introduced to improve the efficiency of the reaction. EDC couples NHS to carboxyls which results in formation of an NHS ester which is more stable than the *O*-acylisourea intermediate and more efficient at physiological pH (Thermo Fischer Scientific Inc, 2011). Self-polymerisation cannot happen in this system as there are only surface immobilised activated carboxylic acids which react only with free amine groups present in the peptides the polymer was incubated with. Figure 4.3 illustrates the peptide immobilisation process. This method has been used to immobilise peptides on for example alginate (Dhoot et al., 2004), chitosan (Yu et al., 2007) and PCL (Santiago et al., 2006).

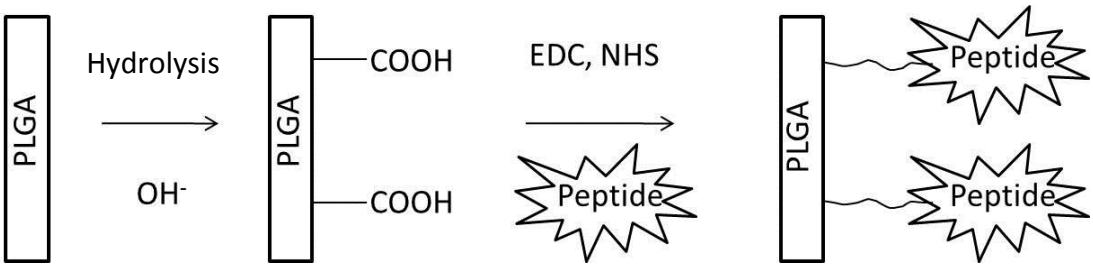

Figure 4.3 Schematic representation of hydrolysis and further immobilization of biomolecules on PLGA. EDC, 1-Ethyl-3-(3-dimethyl-aminopropyl)carbodiimide, hydrochloride; NHS, N-Hydroxysuccinimide.

For the results presented in this chapter, PLGA flat sheet membranes were modified in order to attach YIGSR-peptide groups to the surface. This peptide sequence was chosen due to its characteristics of mediating neural cell attachment and migration (Massia et al., 1993, Ranieri et al., 1994, Dhoot et al., 2004, Santiago et al., 2006).

As the results show in figure 4.4 20±7% of seeded cells attached to the non-modified surface and 14±6% of seeded cells attached to the modified surface. Using Student's t-test, no significant difference in cell attachment was observed between non-treated and treated PLGA flat sheet membranes ($P>0.05$). Thua, peptide modification did not result in higher cell attachment as anticipated and previously reported.

From the experiment conducted here it is not clear whether the peptide modification has been successful or not as analysis of the modified surface was not performed. The cell attachment numbers did not increase indicating the latter but further confirmation of the modification is necessary. Confirmation can be performed using for example the BCA protein assay in order to measure the amount of protein. Furthermore, X-ray photoelectron spectroscopy (XPS) can be used to characterise the surface chemical changes of the flat sheet membranes before and after peptide modification.

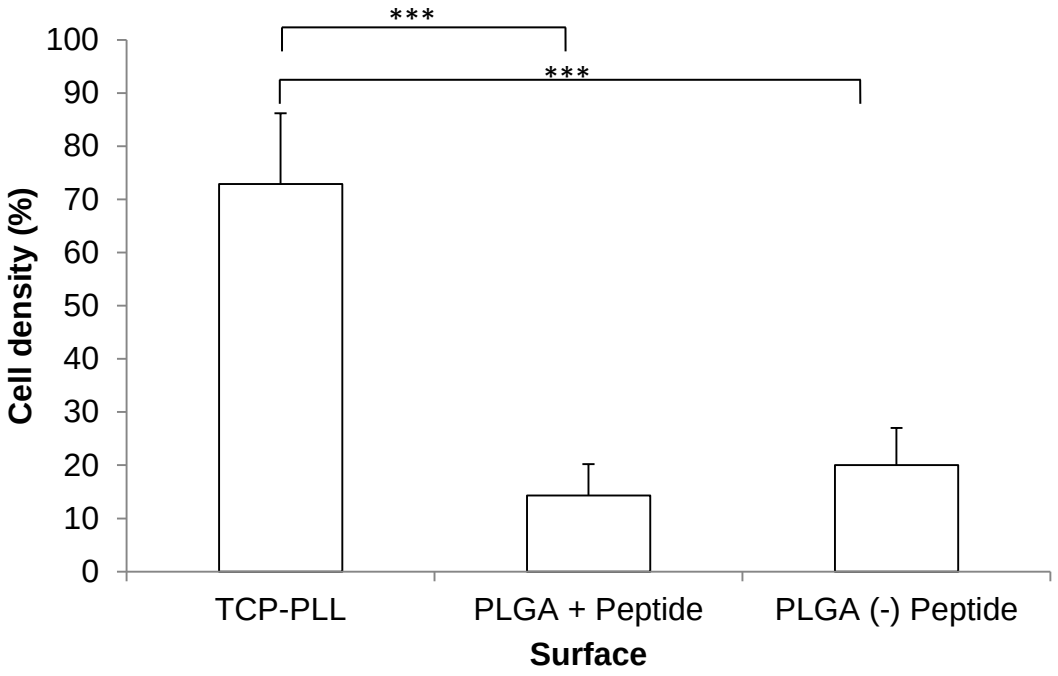

Figure 4.4 Peptide modification does not affect cell attachment. PC12 cell attachment to non-modified and modified PLGA flat sheet membranes. Peptide modification does not result in higher cell numbers attaching to the modified surface. Data represent the mean ± SEM (n=3) and was analysed using Student's t-test. *** P<0.001.

This experiment investigated one laminin fragment, the YIGSR peptide, and its effect on cell attachment after immobilisation on PLGA. There are indications that cells attach differently to different laminin fragments (Santiago et al., 2006). Although this penta-peptide laminin sequence has been shown to mediate cell attachment and migration (Massia et al., 1993), it is important to test various laminin fragments to find the one most suitable for each cell line. Santiago and co-workers seeded human adipose cells onto PCL scaffolds showing a significantly higher cell attachment to modified surfaces compared to non-modified ones. They also presented some evidence that other laminin sequences such as IKVAV are more likely to result in higher cell adhesion (Santiago et al., 2006). Dhoot and colleagues attached the YIGSR laminin sequence to alginate prior to gel formation resulting in five-fold increase in cell attachment and higher rate of differentiation of NB2a neuroblastoma cells (Dhoot et al., 2004). Yu and colleagues modified chitosan with the peptide sequences GQAAS**IKVAV** and GDPG**YIGSR** which resulted in higher

cell attachment of rat superior cervical ganglion neurons (Yu et al., 2007). Ranieri and colleagues have attached the IKVAV laminin sequence to fluorinated ethylene propylene (FET). Although quantitative cell attachment data was not presented the qualitative data clearly demonstrated the selective cell attachment behaviour of PC12 cells as the cells remained exclusively attached to the 300 μm wide peptide pathways (Ranieri et al., 1994).

The sole publication on PLGA modification with laminin was published by Huang and co-workers, where laminin-PLGA films were produced using oxygen plasma treatment (Huang et al., 2007). Although it was shown that laminin was successfully grafted on PLGA films, no cell attachment data was presented making comparison of cell attachment impossible.

Generally, there are not sufficient publications present in the literature that can be compared to the data presented here, as either a different polymer is used or no cell attachment data is published. Peptide modification here did not result in higher cell attachment and was excluded from further investigation. It is clear that more research into grafting methods is necessary in order to facilitate the use of various protein sequences.

4.5 Characterization of PLGA flat sheet membranes

Unfortunately surface modifications did not have a positive effect on cell attachment. To ensure that the characteristics of the PLGA flat sheet membranes were not compromised its surface was analysed. AFM was performed to evaluate the effect of surface modification on roughness of flat sheet membrane.

PLGA flat sheet membranes were treated with 0.2M NaOH, 0.5% EDA or ethanol. Analysis with an AFM in the tapping mode revealed that the surface treated with NaOH was the roughest surface with an arithmetic average of the absolute values of the surface being R_a=11.26±2.36nm and a maximal vertical distance between the highest and lowest data points of R_{max}=108.70±17.58nm (Table 4.1). This was also confirmed by 3D root mean square (RMS) height mode images, which were obtained by using an oscillating tip that “taps” the surface (Fig 4.5). The smoothest

surface was the non-treated one with R_a=0.18±0.01nm and R_{max}=3.37±1.27nm. As ethanol was used to sterilize the films, its effect on surface modification was also analysed with AFM, showing a similar roughness as surfaces treated with EDA (Table 4.1). Statistical analysis confirmed that treatment with 70% ethanol, 5% EDA and 0.2M NaOH increased surface roughness as R_a and R_{max} were significantly higher compared to non-treated PLGA flat sheet membranes ($P<0.05$). The results show that NaOH treatment resulted in a 8-10 fold increase in surface roughness to the extent that with prolonged exposure to NaOH the polymer sample degraded completely, making NaOH treatment the most invasive of the three.

An optimum surface roughness of R_a=20-100nm, a much higher value than was achieve for PLGA here, has been established for silicon and was shown to promote cell adhesion and longevity of rat cortical neurons (Khan et al., 2005), which is much higher than was achieved for PLGA here. In order to increase the surface roughness to the extent it was done for silicon the polymer has to be exposed to more invasive treatments, which would result in the polymer's degradation and would affect its mechanical strength making it unusable in cell culture studies. Fan and co-workers have established an average surface roughness of 20–70nm for silicon wafers which significantly affected adhesion and viability of central neural cells (substantia nigra) (Fan et al., 2002a) which overlaps with data published by Kahn and colleagues (Khan et al., 2005).

Table 4.1 Roughness of PLGA flat sheet membranes. R_a= the arithmetic average of the absolute values of the surface height deviations measured from the mean plane; R_{max} = maximum vertical distance between the highest and lowest data points in the image; Data represent the mean ± SD (n=3).

	R_a (nm)	**R_{max} (nm)**
No treatment	**0.18** ± 0.01	**3.37** ± 1.27
70% EtOH	**1.12** ± 0.29	**12.06** ± 1.99
5% EDA	**1.47** ± 0.06	**15.10** ± 0.90
0.2M NaOH	**11.26** ± 2.36	**108.70** ± 17.58

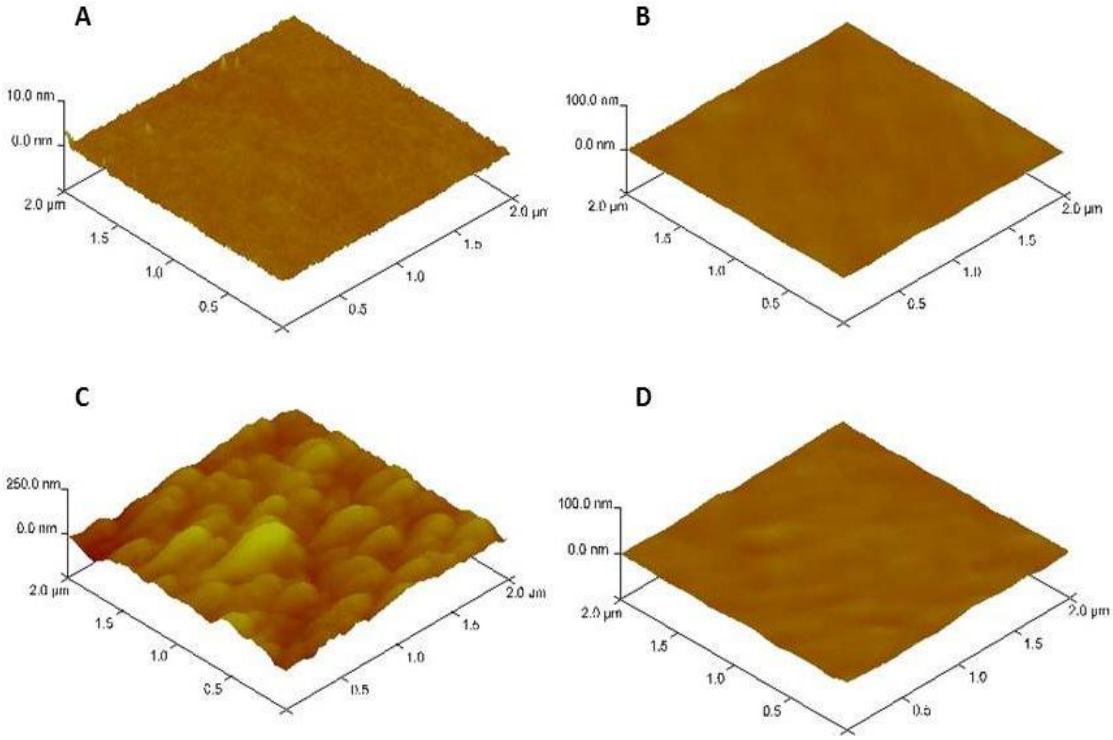

Figure 4.5 Roughness of PLGA films. Images of PLGA films were obtained by atomic force microscopy (AFM). Roughness of (A) PLGA non treated membrane, (B) 70% ethanol for 15 min, (C) 0.2M NaOH, (D) 0.5% EDA. EDA, ethylenediamine; NaOH, sodium hydroxide.

The highest value for surface roughness obtained here was 11.26±2.36nm after NaOH treatment, which is below the minimum of 20nm established by Kahn and Fan and therefore, the surface of PLGA flat sheet membranes might not be optimal for cell adhesion. Brunetti and co-workers have investigated the response of the human neuroblastoma cell line (SH-SY5Y) to gold surfaces with different levels of roughness, demonstrating very high sensitivity to nanoscale features (Brunetti et al., 2010). Contrarily to Fan and Khan, Brunetti and co-workers observed a decrease in cell adhesion with increased surface roughness (R_a from 36 to 100nm), with 10-15% of cells attached but 90–95% underwent necrosis at R_a of 80–100nm and at R_a of 36nm approximately 50% of adherent cells underwent necrosis. But again, the surface roughness range investigated by Brunetti was higher than the surface roughness achieved here.

Characterisation of surface roughness revealed that all treatments (EtOH, EDA, NaOH) significantly increased surface roughness, showing that all surface treatments changed the characteristics of the PLGA films. Unfortunately the increased surface roughness did not have an effect on cell attachment as neither EDA (section 4.3) nor NaOH treatment (section 4.4) of PLGA flat sheet membranes yielded higher cell densities indicating that the surface roughness achieved was sup-optimal to promote attachment of PC12s.

4.6 Ozone treatment

The final surface modification included exposure of the flat sheet membrane to ozone. Ozone was used because it is inexpensive and uniformly introduces peroxides on the surface of the polymer (Fujimoto et al., 1993). The effect of the ozonation procedure on the polymer was measured by evaluating water contact angle, drop volume, surface of contact and drop surface.

The contact angles in table 4.2 and figure 4.6 show that exposure to ozone resulted in insignificant changes in contact angle compared to untreated PLGA. The contact angles ranged from 76.61°±2.06° when exposed to ozone for 60 min to 67.62°±5.91° after exposure to ozone for 180 min. On average, the contact angle was 73.05°±3.90°. Although this observation was surprising, other reports show that ozonation does not always results in contact angle decrease. For example, Suh and co-workers treated PLLA membranes with ozone which did not result in increased wettability as the contact angle remained unchanged (Suh et al., 2001). Cell attachment data was not reported. On the other hand, Ho and colleagues published data where ozone treatment of PLLA resulted in a water contact angle decrease of 7° (Ho et al., 2007). Furthermore, Ko and co-workers reported a decrease in contact angle after ozone treatment for silicone, polyethylene and polyurethane (Ko et al., 2001). To date, there are no publications reporting the ozonation of PLGA flat sheet membranes or any other PLGA scaffold.

Other parameters, such as drop volume, surface of contact and drop surface were included into the measurement to assure accuracy of the procedure. As results

show in table 4.2 the droplet characteristics did not change drastically. It is known that contact angle is not only dependent on hydrophilicity but is also influenced by other factors such as surface roughness, surface porosity, pore size and its distribution. Plus, the crystallinity of the polymer might prevent the introduction of active groups via ozone treatment on the polymer's surface. Without further supportive data, it is difficult to find an explanation for the unchanged contact angle.

Table 4.2 Analysis of PLGA flat sheet membranes treated with ozone.

Time (min)	Contact angle (°)	Drop volume (mm^3)	Surface of contact (mm^2)	Drop surface (mm^2)
0	73.90 ± 2.24	0.24 ± 0.00	0.97 ± 0.04	1.51 ± 0.03
10	75.51 ± 2.10	0.21 ± 0.03	0.83 ± 0.02	1.32 ± 0.07
30	76.07 ± 2.87	0.21 ± 0.02	0.86 ± 0.05	1.38 ± 0.07
60	76.61 ± 2.06	0.25 ± 0.06	0.91 ± 0.06	1.48 ± 0.09
180	67.62 ± 5.91	0.28 ± 0.05	1.21 ± 0.26	1.73 ± 0.27
240	68.59 ± 8.24	0.18 ± 0.03	0.88 ± 0.18	1.28 ± 0.16

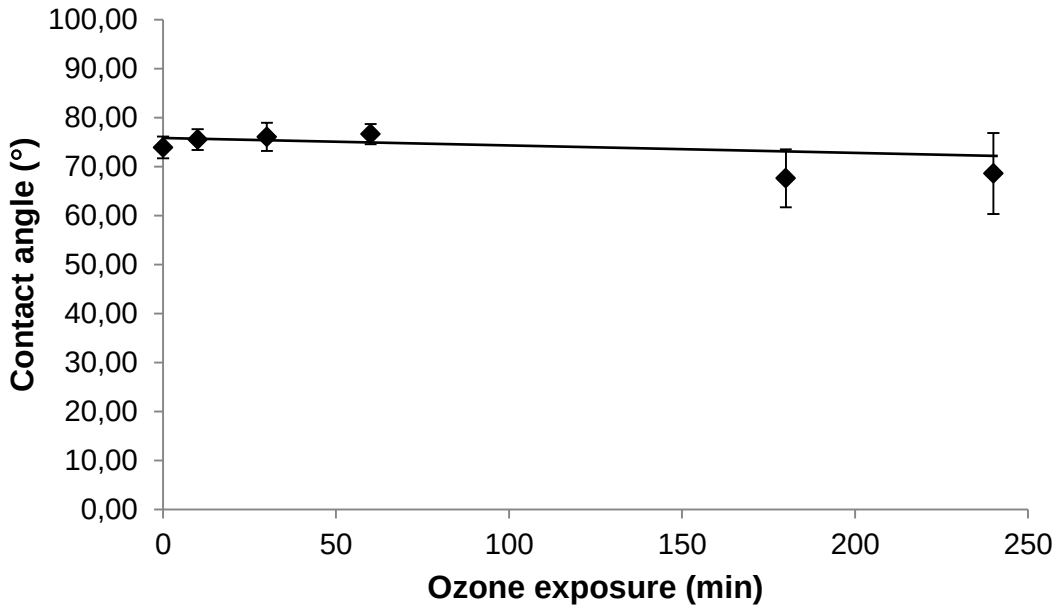

Figure 4.6 Contact angle does not change with increased exposure to ozone. PLGA flat sheet membranes were exposed to ozone for 0, 10, 30, 60, 180 and 240 min, followed by contact angle measurement of treated membranes. Data represent the mean ± SEM (n=6) and were obtained using the Student's t-test. Although the trendline indicates a decrease in contact angle with increased exposure to ozone there is no significant difference between timepoints (P>0.05).

Additionally to measurement of contact angles, the amount of polymeric peroxides introduced onto the treated membranes was measured by the iodide spectrophotometry method (Fujimoto et al., 1993, Ko et al., 2001). This method uses the oxidation of sodium iodide by peroxides in the presence of ferric chloride. The treated films were kept at 60°C for 10 min in benzene-isopropyl alcohol solution (1:6) which also contained saturated sodium iodide and 1ppm ferric chloride. Water was added to stop the reaction and the absorbance of oxidized iodine as triiodide anion was measured at 360nm. Unfortunately, no difference between ozone treated and non-treated membranes was detected which leads to the assumption that the ozone treatment was not successful. Nevertheless, the effect of ozone was visible by corrugation of the flat sheet membrane. The corrugation showed as folding and groove formation of the membrane exposed to ozone. The degree of deformation increased with the time the polymer was exposed to ozone.

The ozone experiments conducted in this project did not result in measurable contact angle changes or in measurable increase of peroxide groups. Nevertheless, it was necessary to investigate if ozone treatment results in higher cell attachment. To assess the effect of ozonation on cell attachment, PC12 cells were seeded onto treated and untreated PLGA flat sheet membranes. As shown in Figure 4.7 higher cell attachment numbers were not achieved on ozone treated flat sheet membranes, with a quantified average cell density of 14±4%.

The cell attachment experiment was conducted six times; still the error bars remained very big, adding another factor for the exclusion of this method from future experiments. The cells on PLGA flat sheet membrane were not evenly distributed but formed clumps on the edges and retracted from the centre of the flat sheet membrane. Although the edge effect is a very widely observed phenomenon, ozone treatment did not eradicate it. Furthermore, corrugation of flat sheet membranes did not support even distribution of cells. Every flat sheet membrane sample showed a different pattern of corrugation resulting in different cell attachment patters which contributed to the big error bars in the cell attachment data (Fig 4.7).

Because of the corrugation effect of ozone treatment on PLGA flat sheet membranes as well as the lack of increased cell attachment ozonation was not further pursued during this project.

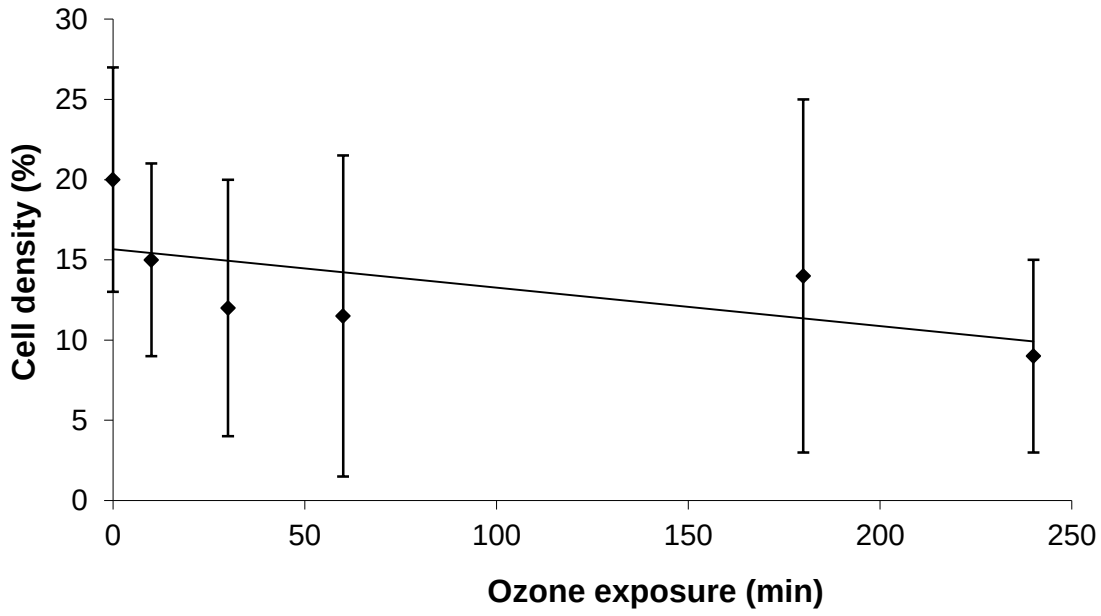

Figure 4.7 Ozone treatment does not affect attachment of PC12s to PGLA flat sheet membranes treated with ozone. PC12 cells were seeded onto PLGA flat sheet membranes and left to attach for four hours. Cell density was analysed using Picogreen. Cell density is represented as the number of cells attached of the number of cells seeded. The linear trendline illustrates a decrease in cell adhesion. Cells were seeded at 50,000 cells/cm^2. Data represent the mean ± SEM (n=6) and was analysed using Student's t-test.

4.7 Effect of foetal calf serum on PC12 cell attachment

The results described so far in this chapter support the fact that PLGA has some disadvantages when aiming to attach PC12 cells in high numbers. To further investigate PC12 adhesion to PLGA, cell attachment behaviour of PC12 cells on TCP was investigated in relation to the amount of foetal calf serum (FCS) present in the media.

In order to investigate the effect of FCS on cell attachment, PC12 cells were seeded onto uncoated TCP and left to attach for 4 h. TCP was chosen as a control before seeding cells onto the polymer in order to exclude polymer-cell interactions. Cell numbers were quantified using the Picogreen assay.

The first interesting observation was made when removing FCS from the cell culture medium. When using medium supplemented with 10% FCS, 7.4±0.7% of cells attached to TCP (Fig. 4.8). Cell attachment was significantly greater for medium supplemented with 5% FCS ($P<0.05$) compared to 10% FCS medium, with 10.7±0.6% of seeded cells attached, and even greater when using 2.5% FCS medium, 14.0±1.4% of seeded cells ($P<0.001$). When using 1% FCS medium 16±1.7% of cells attached and 50.4±9.0% of cells attached when FCS was completely removed from the culture medium. Both figures, for 1% and 0% FCS medium, are statistically significantly greater compared to medium containing 10% FCS ($P<0.001$).

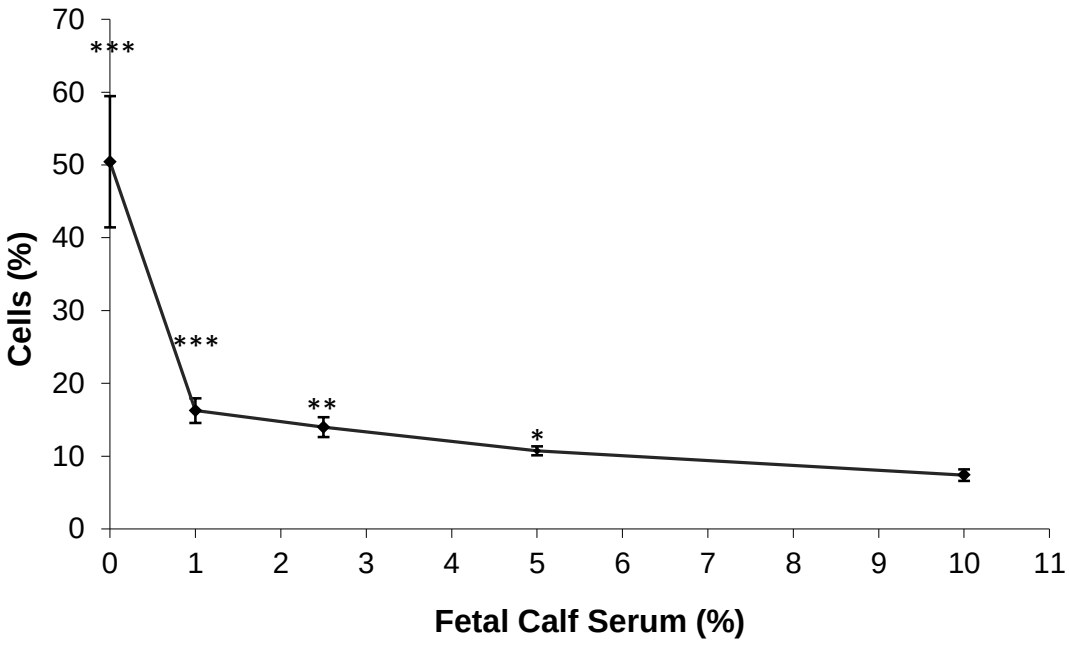

Figure 4.8 Effect of foetal calf serum on attachment of PC12 cells to TCP. In medium cells (50,000 cells/cm^2) were seeded onto tissue culture plastic (TCP) and left to attach for 4 hours. Cell number of the attached cells was analysed using Picogreen assay. 100% represents total number of cells seeded. Data represent the mean ± SEM (n=6) and were analysed using Student's t-test. *P<0.05, **P<0.01, ***P<0.001.

Whether the same effect was present when seeding cells onto PLGA, was investigated by seeding PC12s onto PLGA films, because those films are easily and quickly produced but still demonstrate the interactions of the cells with the material. It was observed that FCS has a negative effect on PC12 attachment to PLGA surfaces (Fig. 4.9) to the same extent as it does on TCP. Cells seeded in the

absence of FCS showed higher affinity to PLGA than those incubated with FCS. A significantly greater number of PC12s (60±15%) attached to PLGA films when using medium without FCS compared to 11±5% when using 10% FCS medium ($P<0.001$) (Fig 4.10). No significant difference was observed between attachment of PC12s to TCP, 50±9% and 7±1% without and with FCS respectively, and to PLGA films ($P>0.05$). There was no significant difference between attachment of PC12s to PLGA films compared to PLGA flat sheet membranes, where 20±7% of seeded cells attached (Section 4.2), justifying the use of PLGA films instead of flat sheet membranes.

FCS is normally added to the medium because many of its components are essential for cell survival and growth. It is also known to promote cell attachment by adsorption of serum proteins, such as fibronectin (Korkmaz et al., 2003). The negative effect of FCS on cell attachment contradicts previous findings, where FCS had a positive effect on PC12 cell attachment to chitosan films blended with PLL (Mingyu et al., 2004). Mingyu and colleagues “primed” their cells by addition of 50mg/ml NGF 24 h before seeding. This effect was also investigated in this study with no observed effect onto cell attachment. This suggests that it may be the material to which the cells attach that influenced their behaviour. The absence of FCS in the media might increase the interactions between the PLGA and the PC12 cells, as the polymer’s surface is not blocked by proteins present in the FCS. Further experiments are necessary to investigate this aspect. As a consequence, all subsequent attachment experiments were conducted using culture medium without FCS for four hours which was then replaced with culture medium supplemented with 10% FCS.

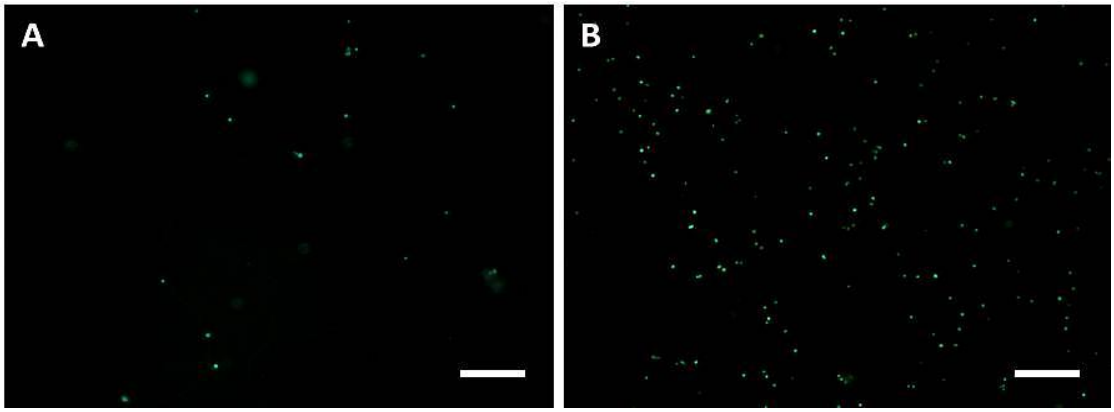

Figure 4.9 Effect of serum on attachment of PC12 cell to PLGA films. Cells were stained with cell tracker (Vybrant). With 10% FCS (A) only very few cells attach to the polymer. Removing FCS increased the number of attached cells (B) Scale bar=500 µm.

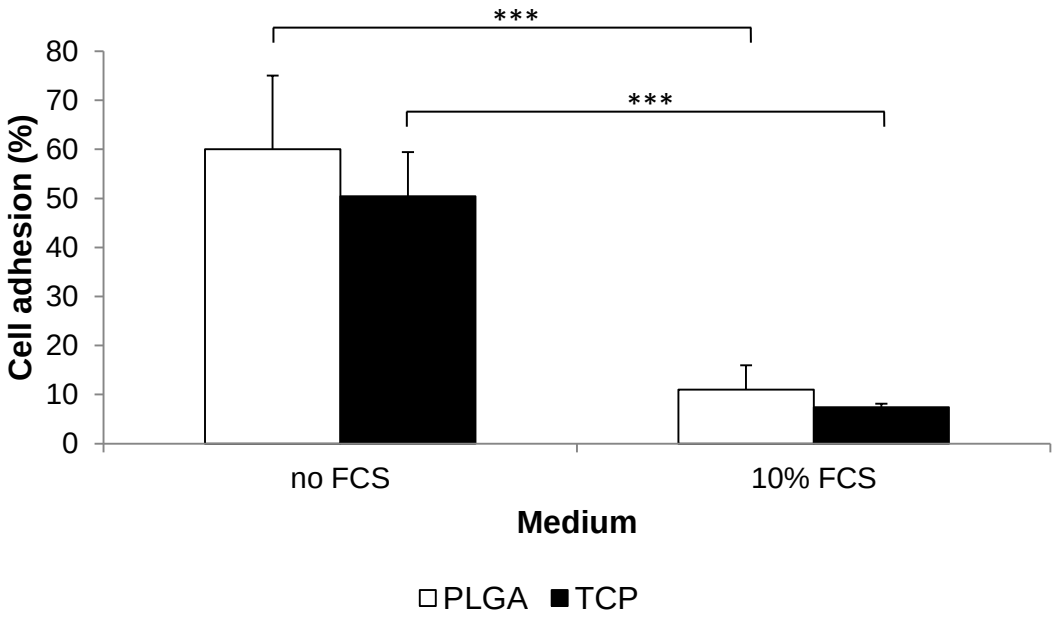

Figure 4.10 Cell adhesion of PC12 cells to PLGA films in absence and presence of 10% FCS. 100% represents total number of cells seeded (100%). Data represent the mean ± SEM (n=6) and were analysed using Student's t-test. ***P<0.001. FCS, foetal calf serum.

The effect of serum on cell attachment has also been described in relation with cerebellar cells and spinal cord cells, which do not attach to substrates in the presence of 5–10% serum in the medium (Kleinfeld et al., 1988). Kleinfeld and colleagues have cultured rat cerebellar and mouse spinal cord cells on chemically patterned silicon substrate showing that cell adhesion to *n*-tetradecane patterned silicon is inhibited in the presence of serum in the medium compared to ethylenediamine propane patterned surface. Furthermore, it has been reported

that non-adhesive proteins such as BSA are likely to reduce the adhesion of neurites to fibres (Lochter et al., 1995). Therefore serum could reduce neurite alignment but support neurite growth on less adhesive substances, supporting neurite jumps from one fibre to another and consequently cell migration. This is true for Schwann cells (Thompson and Buettner, 2004) and dorsal root ganglia (Lochter et al., 1995). These studies support the decision to remove FCS from cell attachment studies during the first four hours of attachment.

4.7 Conclusion

In conclusion, the results clearly show that none of the surface modification techniques were successful in creating more effective cell attachment. These results partly correlate with the literature where it is widely reported that the PC12 cell line requires surface coatings prior to seeding. It is questionable if surface modification is particularly suitable for soft tissue engineering applications, as it can be invasive and distorting for delicate scaffolds. NaOH modification in particular degrades the membrane and the polymer's exposure has to be kept to a minimum and at low concentrations, otherwise it results in polymer degradation.

The removal of FCS from the culture media during PC12 cell attachment resulted in significant higher cell attachment to uncoated TCP. This is a major finding which has not been reported previously. This knowledge was included in any further experiments conducting cell attachment.

Although the results obtained from surface modification were discouraging, PLGA as a polymer for tissue engineering has great advantages in terms of ease of process, biocompatibility and degradation rate. Furthermore, it has been shown that PC12 cells do attach to PLGA. This makes PLGA a suitable material to develop further as a scaffold for spinal cord injury repair. Thus the next chapter describes the fabrication of a PLGA scaffold using electrospinning, a method which produces fibres on nanometre scale.

5. FABRICATION AND CHARACTERISATION OF ELECTROSPUN PLGA NANOFIBRES

5.1 Introduction

For biomedical applications, nanofibres have been produced with synthetic and natural polymers using predominantly one out of three methods, including phase separation, self-assembly and electrospinning (Zhao et al., 2007). All of these methods produce three dimensional fibrous scaffolds suitable for tissue engineering applications. Phase separation requires only simple equipment (Liu et al., 2005); the self-assembly method can form very thin fibres (Hartgerink et al., 2001); but electrospinning is the most versatile, flexible and widely adopted technique. Using electrospinning, fibres can be produced ranging from 6 to 3000 nm in diameter, processing a wide range of polymers, including blends and emulsions (Li and Xia, 2004, Liang et al., 2007).

In order to establish the electrospinning process for PLGA in the laboratory, parameters including choice of solvent and process settings (applied voltage, solution feeding rate, collector-to-needle distance, solvent, solution viscosity) have been examined and the results are presented and discussed in this chapter.

5.2 Polymer concentration affects fibre formation

The first parameter of interest was the polymer concentration in the electrospinning solution. For this, three PLGA (75:25, MW=76,000-116,000) solutions were prepared each with 8, 10 or 15% (w/w) of polymer in dimethylformamide (DMF) and tetrahydrofuran (THF) in a ratio of 1:1 (Li et al., 2002). These solvents were chosen because they were found to be most dominant in the literature. The solutions were electrospun while keeping all other parameters, such as flow rate (1.5ml/h), voltage (15kV) and distance of collector to the needle constant (10cm). Analysing the nanofibre mats using SEM allowed the characterisation of the produced nanofibres according to the nanofibre diameter and the presence of a 3D network. The desired scaffold would be a porous fibre mesh which allows the diffusion of external growth factors.

First results indicated that a slight concentration change from 8 to 10% (w/w) PLGA in a 1:1 mixture of DMF and THF had an effect on fibre formation. After electrospinning of the samples with 8 and 10% (w/w) polymer concentration, the morphology was analysed using SEM (Fig 5.1). When the 8% polymer solution was electrospun, only droplets were collected. By increasing the polymer concentration by 2% it is apparent that fibres started to form. Using the solvents DMF and THF did not result in uniform fibres, even when increasing the polymer concentration. The solution containing 15% of PLGA did not result in fibres, as it blocked the tubing and the needle, and thus no polymer was collected.

The process of droplet formation is called electrospraying (Gupta et al., 2009). Electrospraying occurs due to insufficient chain entanglements which lead to instability in the jet forming droplets (Kose et al., 2003). Consistent fibre size across the mat (i.e. no beads) results in relatively consistent porosity, which also results in consistent cell spreading and diffusion of external growth factors (Cui et al., 2010). These factors make bead-free fibres more favourable. Furthermore, an additional reason to avoid beads, is their uptake of essential space where neurons could potentially migrate and attach, making the beads a physical barrier. On the other hand, electrospraying can be used to produce beads with encapsulated drugs, providing a new drug delivery scaffold. New heterogeneous scaffolds consisting of fibres and beads can be created, in which case fibres and beads can be electrospun in layers and/or consist of different polymers, depending on the application. The advantage of bead-free fibres is the control of porosity. It is more difficult to control the pore size of the scaffold when random beads are present.

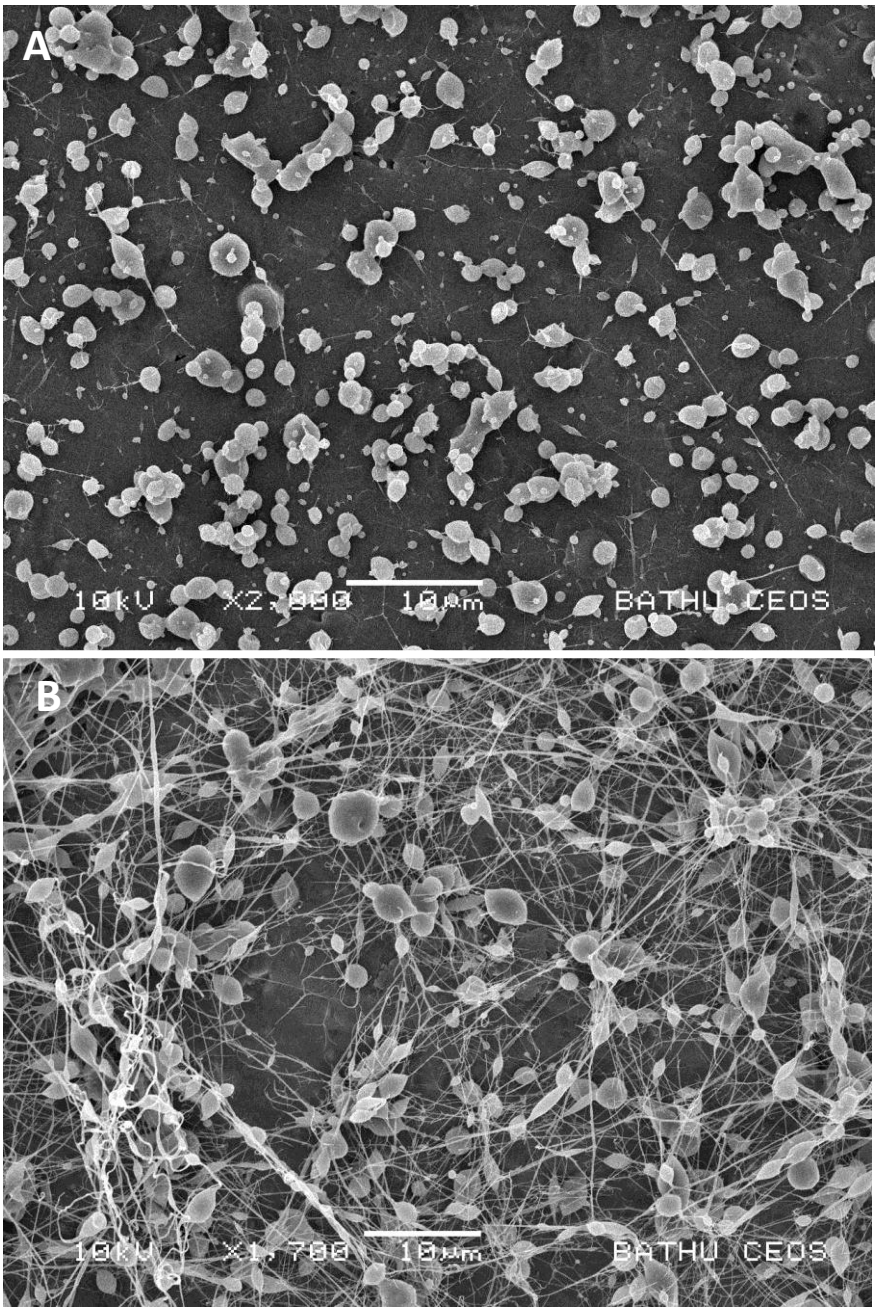

Figure 5.1 Polymer concentration in the solution effects fibre formation during electrospinning. (A) 8% PLGA in DMF:THF (1:1), (B) 10% PLGA in DMF:THF (1:1). Electrospinning parameters were identical for both samples: flow rate 1.5ml/h, applied voltage of 15kV, 10cm collector-to-needle distance.

The process of electrospraying can be overcome by increasing the polymer concentration in the solution until a critical concentration is obtained. In the present study it was found that a 10% polymer solution resulted in fibre formation. When using 8% polymer solution only beads were obtained and when using 15%

solutions clogging of the needle was interfering with fibre formation. According to Fong and colleagues, bead formation is influenced by solution viscosity, net charge density carried by the electrospinning jet and surface tension of the solution (Fong et al., 1999). Further, a probable competition between surface tension and viscosity influences the gradual change from beads to smooth fibres (Katti et al., 2004). In this case the surface tension tries to reduce surface area per unit mass, leading to beads, whereas the viscoelastic forces resist this facilitating the formation of fibres. The use of THF and DMF as solvents did not result in bead-free fibres likely due to the strong surface tension which cannot be overcome by the viscoelastic forces of the solution. As THF and DMF did not result in bead-free fibre formation other solvents were investigated.

5.3 Effect of solvent on fibre formation

In order to carry out electrospinning, the polymer has to be in solution. The property of the solution strongly affects the electrospinning process and the resulting fibre morphology (Fong et al., 1999). The polymer solution is drawn from the tip of the needle and parameters such as viscosity, surface tension and rate of evaporation effect the stretching of the solution. It was observed that polymer concentration had an effect on fibre formation when using DMF:THF as solvent. But it was not the only factor, as further manipulation of other setting parameters (including applied voltage, flow rate and needle-collector-distance) did not produce any fibres. In order to establish whether the solvent itself has a dominant influence on the electrospinning process, other solvents were chosen for further experiments.

The solvents tested were DMF, THF (Nisbet et al., 2007, Zhao et al., 2008), DMF and THF at ratios 3:1 and 1:1, 1-methyl-2-pyrrolidinone (NMP) (Ellis and Chaudhuri, 2008), isopropanol (Meng et al., 2007), dichloromethane (DCM) (Nie et al., 2009) and chloroform ($CHCl_3$) and methanol (MeOH) at ratio 3:1 (Panseri et al., 2008). These solvents were chosen as they were previously described in the context of scaffold fabrication using PLGA. NMP was used to produce PLGA flat sheet membranes by our group, whereas DMF and THF are the most common solvents

used for electrospinning PLGA. Isopropanol was previously used as a solvent for electrospinning a combination of poly(3-hydroxybutyrate-co-3-hydroxyvalerate) and type-I collagen (Meng et al., 2007). The results indicated that with the other parameters kept constant, the morphology of the fibres changed according to the solvent used (Fig 5.2). NMP and DMF:THF did not result in fibres but droplets only (Fig 5.2 A), and were excluded from further experiments. Isopronanol did result in fibres but they were not continuous and showed many beads (Fig 5.2 B). DCM resulted in continuous fibres but the uniformity was distorted by beads (Fig 5.2 C). The best results were obtained using the CHCl3:MeOH (3:1) solution (Fig 5.2 D), as the fibres were bead free. The fibre diameter of fibres produced using DCM and CHCl3:MeOH were analysed as these solutions resulted in most promising nanofibres.

Using $CHCl_3$:MeOH as solvent resulted in continuous uniform fibres without beads with an average fibre diameter of 530$\pm$140nm (n=31) (Fig 5.3). These fibres were significantly different from those obtained using DCM ($P<0.05$) with fibre diameter of 860$\pm$420nm. Lee and co-workers have electrospun thinner nanofibres using PLGA in hexafluoro-2-propanol (HFIP) which resulted in fibre diameters of 250$\pm$110nm for random and 360$\pm$130nm for aligned fibres (Lee et al., 2009). As a different solvent than $CHCl_3$:MeOH was used and the molecular weight of the polymer is not mentioned in the publication, it is very difficult to compare the data to the results presented here. Nisbet and co-workers have used THF:DMF (1:1) as a solvent, which resulted in random fibres with diameter of 760$\pm$300nm. They used PLGA with the molecular weight of 160,000 in 10% (w/w) solution which was higher than the molecular weight of PLGA used here, Mw 76,000–116,000.

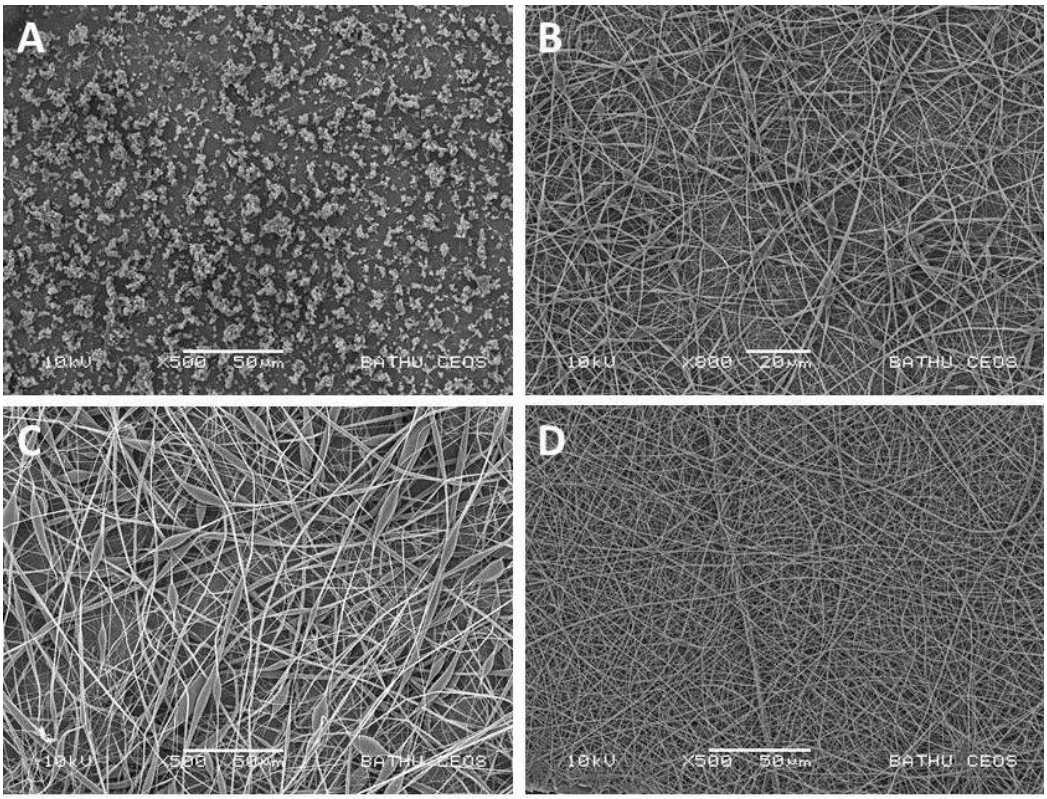

Figure 5.2 Effect of solvent on fibre formation. Electrospun PLGA dissolved in dimethylfomamide (DMF) and tetrahydrofuran (THF) (3:1) (A), isopropanol (B), Dichloromethane (C), chloroform ($CHCl_3$) and methanol (MeOH) (3:1) (D).

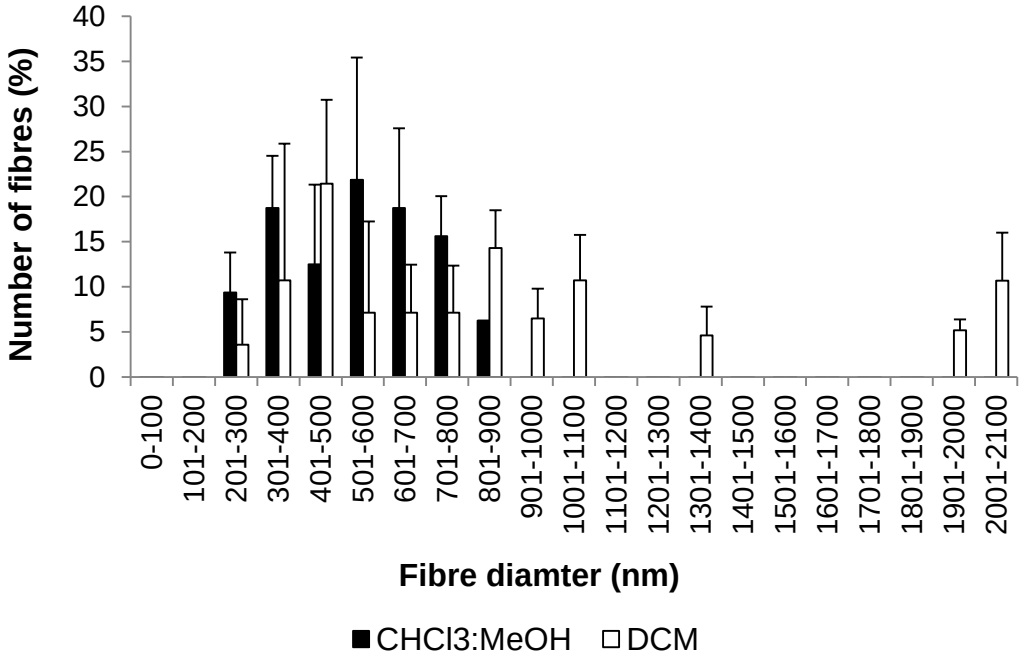

Figure 5.3 Solvent affects fibre diameter. Diameter distribution of fibrous mats fabricated by electrospinning were compared. Comparison of fibre diameter of electrospun PLGA when using $CHCl_3$:MeOH (3:1) and DCM, 10% (w/w). 10 random images of the fibrous mat were taken per sample with a minimum magnification of 4000x. Fibre diameter analysis was conducted using ImageJ, analysing a minimum of 30 fibres per image.

Zhao and co-workers demonstrated that the fibre diameter can be manipulated by changing the electrospinning parameters. They electrospun PLGA (50/50, MW=40,000) in THF:DMF (3:1). By varying the concentration of the polymer (0.15 to 0.3g/ml), the applied voltage (7.5 to 15kV) and the feeding rate (0.4 to 1.2ml/h), it was shown that optimal settings were 0.2g/ml for PLGA concentration, 0.4ml/h for feeding rate and electric field strength of 13.75kV. These parameters were impossible to reproduce with the PLGA used in this study. The flow rate had to be increased to 3ml/h as well as the applied voltage to 15kV, although the concentration of the polymer was lower, 0.1g/ml. The reason for the different settings is on one hand the use of different PLGA, the ratio of lactic to glycolic acid is 50/50 and not 75/25, and on the other hand the fact that the experiment were conducted in a different laboratory using different equipment and being exposed to different ambient settings, such as room temperature, humidity and air flow. Electrospinning is a very sensitive process making the reproducibility of settings difficult and only to some extent comparable to each other. Panseri and co-workers have electrospun PLGA/PCL in order to create a tubular implant for peripheral nerve repair using $CHCl_3$:MeOH (3:1) as a solvent. Their fibres ranged from 280 to 8000nm in diameter (Panseri et al., 2008), whereas here the fibres were more uniform making the outcome of electrospinning more predictable.

Although there are studies that have obtained fibres of different size diameter, there is also data in the literature correlating with the results presented here. For example, Li and co-workers obtained random electrospun PLGA (85:15, unknown molecular weight) fibres in the range of 500 to 800nm, the same size fibres as described here (Li et al., 2002).

Fibre diameter is considered carefully as it has been reported that cells recognize nanometric topologies of microporous structures (Nisbet et al., 2008). With decreased fibre diameter fibre density is increased which in turn affects cell behaviour. Kwon and colleagues have electrospun poly(L-lactide-co-caprolactone) (PLCL, 50/50) with different fibre diameters and studied the behaviour of human umbilical vein endothelial cells (HUVECs) (Kidoaki et al., 2005). The results showed

that cells attached and proliferated on small fibre diameter (300nm and 1100nm) whereas reduced cell attachment and proliferation were observed on large diameter fibres (7000nm). This was probably due to the low fibre density and high fibre distance, which prevented adhesion across neighbouring cells.

The needle which was used for electrospinning is a further parameter that has to be considered when creating a new set-up. The needle used here had an inner diameter of 0.4mm. This parameter was set and not changed during the further experiments. It has been shown that the diameter of the needle used has an effect on the diameter of the resulting fibre. As a rule it can be said that the bigger the needle the thicker the fibre. Needles ranging between 0.4mm (Bini et al., 2004) to 0.84mm (You et al., 2006) result in fibres between 380nm and 760nm. The smaller diameter needle was chosen because there is preliminary evidence that cells attach better to small diameter fibres compared to larger ones and a smaller needle results in smaller diameter fibres (Duan et al., 2006).

5.4 Viscosity affects the electrospinning process

The solvent has a definite effect on fibre formation, but what characteristics exactly play the most important role? It was observed that, while preparing the solutions for electrospinning, the consistency of the solutions showed differences, such as 10% w/w PLGA in NMP appeared more viscous than in chloroform. Thus, the next parameter investigated was the viscosity of the polymer solution. The same solvents as mentioned in section 5.3 were chosen to measure the viscosity of the polymer solution as well as clogging of the needle and amount of polymer collected. The viscosity of all solutions ranged between 0.039$\pm$0.003Pa.S and 0.088$\pm$0.012Pa.S (Fig. 5.4). Solutions prepared using $CHCl_3$:MeOH or chloroform were easily electrospun causing the least processing difficulties, e.g. no needle clogging. Their viscosity ranged from 0.066$\pm$0.014Pa.S to 0.07$\pm$0.005Pa.S. These changes in solution viscosity make it important to choose the correct settings to ensure the reproducibility of electrospun samples. Additionally, it can be concluded that when choosing a solvent for electrospinning, its effect on viscosity has to be considered,

as it has a negative effect on the electrospinning process when either too high or too low. The results obtained here correlate with previously published data, where a 10% PLGA solution in hexafluoropropylene (HFP) had a viscosity of 0.07Pa.S and was successfully electrospun (You et al., 2006). Although a different solvent was used by You and colleagues, the viscosity was the same as measured here.

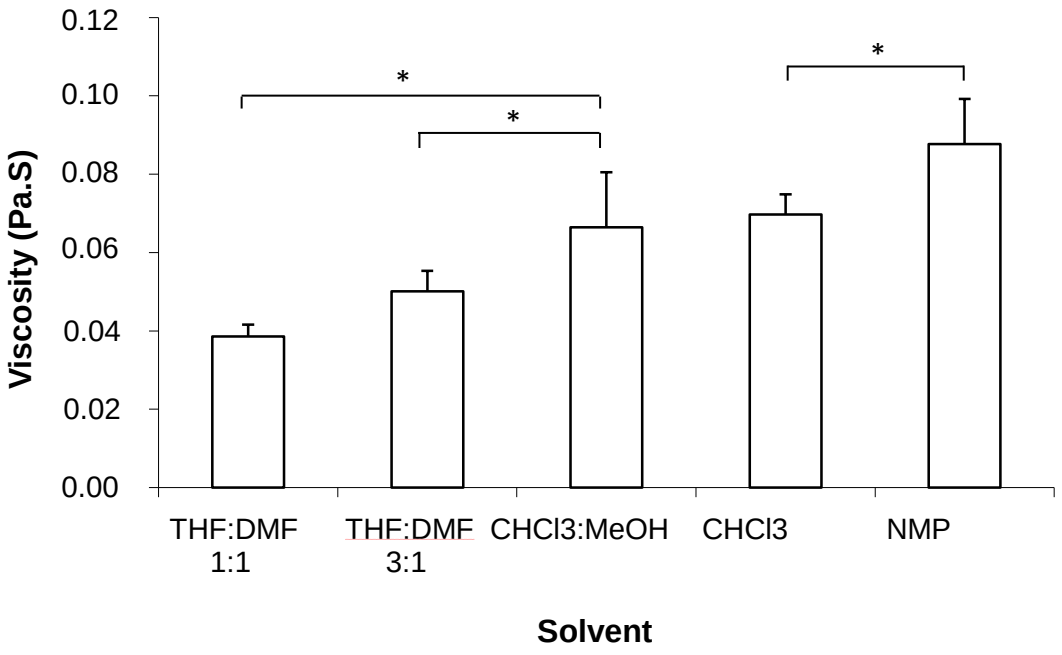

Figure 5.4 Viscosity of 10 % (w/w) PLGA solutions changes with the solvent. The graph represents the viscosity of 10% PLGA solutions used for electrospinning. $CHCl_3$:MeOH and chloroform on its own result in the same viscosity which is significantly different to the other samples (*P<0.05). Measurements were repeated three times with freshly made up solutions for each repeat, with three measurements per solution (n=3). $CHCl_3$, chloroform; MeOH, methanol; NMP, N-Methyl-2-pyrrolidinone; THF, tetrahydrofuran; DMF, dimethylformamide.

During electrospinning the solvent has to evaporate by the time the jet reaches the collector. Depending on the solvent, evaporation may not occur quickly enough and fibres may not be formed at all, instead depositing a thin film of polymer solution on the collector. Evaporation can happen too quickly which may result in the absence of a polymer jet as the needle gets clogged by the polymer. Table 5.1 gives an overview of the solvents used and the problems experienced with each.

Table 5.1 Summary of electrospinning observations. The table summarizes the observations made during electrospinning of various 10% PLGA solutions. Viscosity of DCM was not obtained as it evaporated too quickly. $CHCl_3$, chloroform; MeOH, methanol; DCM, dichloromethane; DMF, Dimethylformamide; NMP, N-methyl-2-pyrrolidinone; THF, tetrahydrofuran. (-) no, (+) low, and (+++) high amount of polymer collected.

Solvent	Viscosity (Pa.S)	Clogging of needle	Amount of polymer collected	Fibres
THF:DMF (1:1)	0.039 ± 0.003	No clogging	+	Droplets
THF:DMF (1:3)	0.05 ± 0.005	No clogging	+	Droplets
CHCl3:MeOH (3:1)	0.066 ± 0.014	No clogging	+++	Continuous homologous fibres
Chloroform	0.07 ± 0.005	Minor clogging	+	Continuous homologous fibres
NMP	0.088 ± 0.012	Medium clogging	+	Droplets
DCM	/	Major clogging	-/+	Non homologous fibres

The clogging can be attributed to the viscosity of the polymer solution, as the solution with the highest viscosity resulted in clogging. Moreover, the volatility of the solvent used may have an effect on the electrospinning procedure. When using DCM, the needle was blocked very quickly after starting electrospinning, which was due to the fact that the solvent evaporated very quickly and the residual polymer blocked the needle. The boiling point of DCM is 40°C, which makes it highly volatile. Chloroform on the other hand has a boiling point of 61.2°C, which makes it less volatile, thus more suitable for electrospinning, as it does not evaporate as quickly as DCM and the needle remains unblocked. Conversely, NMP has a very high boiling point of 202-204°C, which contributes to its unsuitability, as it does not evaporate quickly enough and big droplets are formed instead of fibres. Plus, the viscosity of NMP is relatively high, also preventing fibre formation. Volatility of the solution is not only effected by the boiling point of the solvent but also by vapour pressure, specific heat, surface tension of liquid and air movement above the liquid surface.

All these parameters may influence the physics of electrospinning and should be investigated in future work.

An additional fluid parameter, the dielectric point of the solvent, also influences the electrospinning process. The dielectric constant represents the ratio of the electrical conductivity of a dielectric material to free space (Table 5.2). Generally, the solvent with a greater dielectric constant results in less bead formation and a reduced fibre diameter as it reflects the polarity of the molecules (You et al., 2006). The dielectric point can also be used as predictor for the productivity of the electrospinning process as solvents with a higher dielectric constant are more likely to give higher electrical susceptibility and a higher electrostatic field, which also helps to increase the throughput of the solution from the spinneret (Wannatong et al., 2004). Nevertheless, systematic study of the effect of polarity of solvent on the fibre diameter is still missing. Chloroform has a relatively low dielectric constant (4.8). Methanol, with a dielectric constant of 32.6, is added to increase the spinnability of the solution.

Table 5.2 Boiling point and dielectric constant of solvents.

Solvent	Boiling Point (°C)	Dielectric constant
Chloroform, $CHCl_3$	61.2	4.81
Dichloromethane, DCM	40	8.93
Dimethylformamide, DMF	153	36.71
Methanol, MeOH	64.7	32,6
N-methyl-2-pyrrolidinone, NMP	202-204	32
Tetrahydrofuran, THF	66	7.47
Isopropanol	82.5	18
Water	99.9	80.2

A further factor that affects the viscosity is the molecular weight of the polymer. Polymers with high molecular weight will result in higher viscosity compared to those with lower molecular weight when the volume of the solvent is kept constant. Bhattarai and co-workers have used polyethylene oxide (PEO) to decrease the viscosity of a chitosan solution and increase its spinnability (Bhattarai et al., 2005).

PEO interacts with chitosan through hydgrogen bonding increasing the solubility of chitosan and the spinnability of the solution. For electrospinning to occur the polymer must be of sufficient molecular weight and reach a critical concentration, e.g. minimum concentration for entanglements to occur. These parameters influence each other and the resulting fibres. Consequently, the parameters have to be adjusted accordingly when choosing a new polymer and/or solvent.

For electrospinning, the charges of the polymer solution have to be high enough to overcome the surface tension of the solution. While the jet is accelerated on the way from needle tip to collector the polymer solution is stretched and the viscosity of the solutions prevents the breaking of the jet, which can result in electrospraying or bead formation within the fibre (Morozov et al., 1998). For a pure liquid system the surface tension would decrease with increasing temperature. From a molecular point of view with higher temperature the molecules within the liquid gain more energy and move faster in the space, which results in decreased bondage between the molecules and lower surface tension, resulting in non-continuous fibres.

As has been demonstrated in this section, viscosity has a high impact on the electrospinning process. As viscosity is affected by the solvent, the solvent also affects the electrospinning process and the resulting fibres.

5.5 Distance to collector

In order to analyse the effect of distance between the tip of the needle and the collector, distances of 10cm and 20cm were used, while not changing any of the other parameters, including 3ml/h feeding rate, 15kV applied voltage, 300µl polymer solution volume, and earthed aluminium foil as collector.

The distance between the needle and the collector has less effect on fibre characteristics but on fibre density; the closer the collector is to the needle the more electrospun polymer is collected (Fig. 5.5). This indicates that the surroundings, for example the stand, the flow hood etc., may influence and distort the polymer jet which results in fibre deposition on surrounding objects and hence loss of polymer. The only measure that can be taken to avoid this effect is having

minimal air disturbances and non-conductive material around the electrospinning area.

When placing the collector 10cm away from the needle much more polymer can be collected in comparison to 20cm distance (20±7mg after 15 min electrospinning compared to 5±3mg). The reason for this may be the electrostatic force which is not strong enough to carry the polymer over the distance of 20cm. On the other hand, if the collector is placed too close to the needle, the fibre formation process is interrupted as the jet is not accelerated enough to form fibres (data not shown as no fibres were formed). At shorter distances the solvent has less time to evaporate which can lead to fibre merging on the collector. Longer distances can cause more polymer stretching or a decreased electrostatic field which leads to thinner or thicker fibres respectively. In the literature, distances between needle tip and collector range from 5cm (You et al., 2006) to 32cm (Panseri et al., 2008). The majority of publications report about distances around 10-15cm (Qi et al., 2006, Carroll and Joo, 2006, Yang et al., 2008, Zhao et al., 2008). The established distance for the set up used in this project is 11cm which falls within the range provided by previous publications. When the distance between the spinneret and the grounded target was less than 5cm the solvent did not evaporate and the polymer solution was deposited on the collector. On the other hand, the polymer jet was deflected and deposited on surrounding objects and not on the collector when the distance between spinneret and grounded target was too long resulting in lower quantity of fibres collected and waste of polymer.

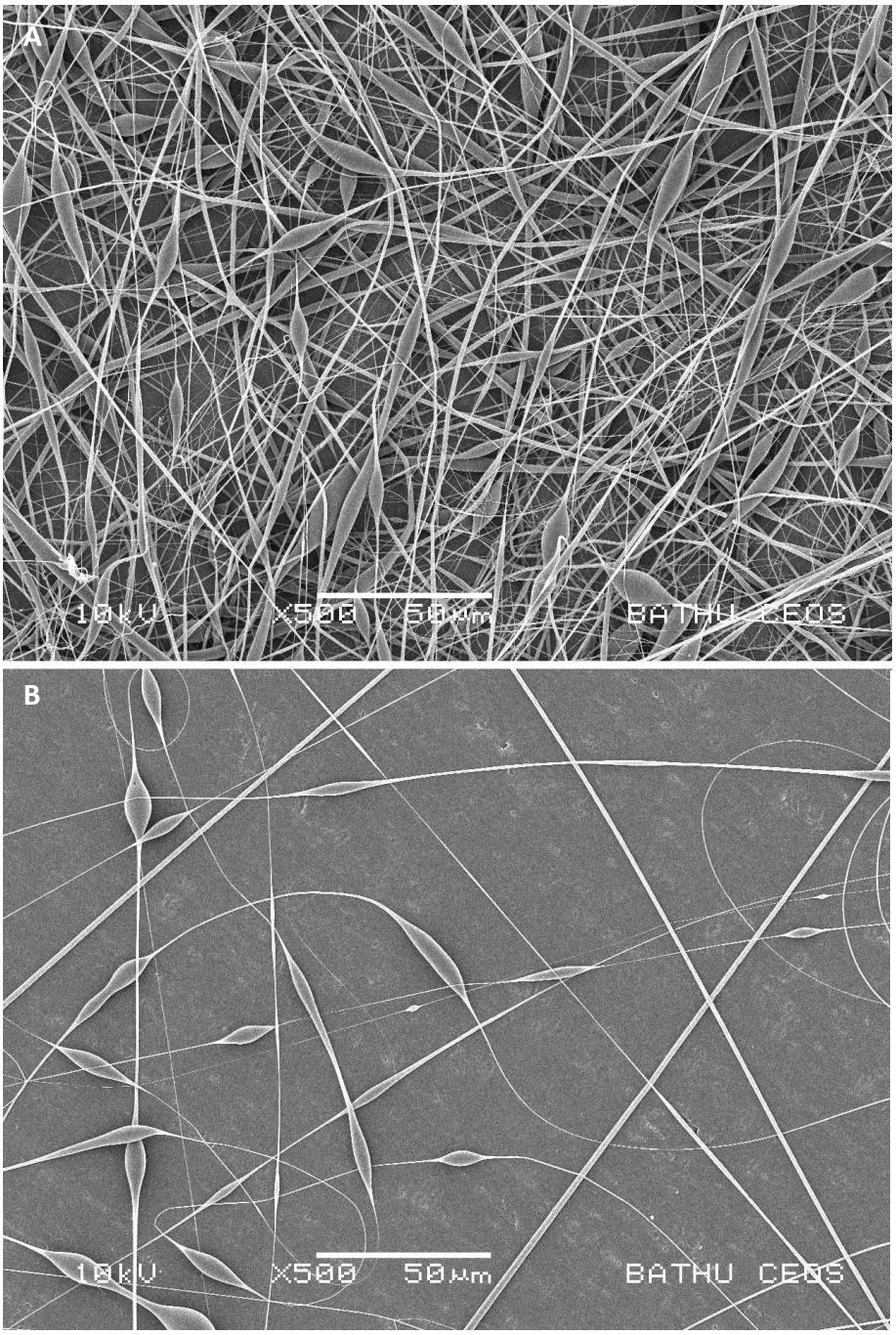

Figure 5.5 Needle-to-collector distance effect. The distance between collector and needle tip influences fibre density on the collector. (A) 10cm and (B) 20cm needle-to-collector distance. 10% (w/w) PLGA in DCM was electrospun onto aluminium foil. Settings used for electrospinning: 3ml/h feeding rate, 15kV applied voltage, 300µl polymer solution volume.

5.6 Effect of applied voltage

The applied voltage is the key to electrospinning. It affects the formation of the Taylor cone and fibre formation. When the voltage is too low the polymer jet does

not form. When the voltage is too high, the jet ruptures and becomes non-continuous, which affects the thickness of the fibres and homogeneity of the fibre mat. On the other hand, more of the polymer is deposited on the collector when the applied voltage is set high. This results in thicker polymer mats, and reduces the amount of polymer lost to surroundings of the electrospinning set up, which is an important factor to consider as PLGA is expensive. For all these reasons, the optimal settings must be chosen taking in consideration feeding rate, collector-to-needle distance and polymer concentration. Following the observations made during electrospinning, the flow rate was reduced to 2ml/h, the distance was set at 11cm and the voltage was tested at 10kV and 15kV. The voltage was not raised higher than 15kV as the syringe pump discharged at higher settings. Voltages tested rage between 5kV and 18kV (Fig 5.6) (Nisbet et al., 2007), although voltages in the range of 0-30kV have been tested (Zong et al., 2003, Zong et al., 2005).

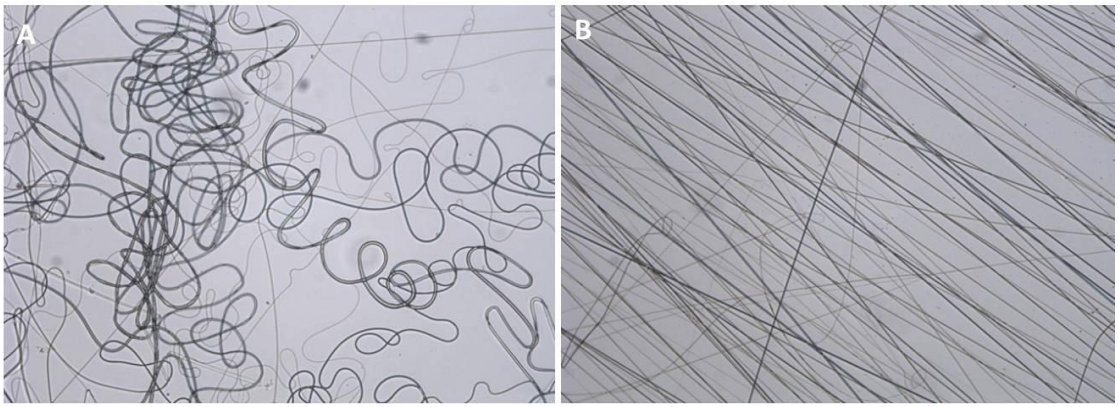

Figure 5.6 Applied Voltage affects fibre formation. 10% (w/w) PLGA electrospun onto glass cover slips using 10kV (A) and 15kV (B) applied voltage. Other parameters were kept constant at 2ml/h and 11cm.

Higher voltage favours the formation of fibres without beads, as well as the formation of thinner fibres as the polymer jet is exposed to stronger electrostatic forces. As surface tension is responsible for the formation of beads, reduced surface tension results in fibres without beads. In a recent publication, Fridrikh and colleagues presented an analytical model to determine jet diameter taking into consideration surface tension, flow rate and electric current in the jet (Fridrikh et al., 2003). In this model, the diameter strongly depends on the relation between surface tension and electrostatic repulsions.

5.7 Feeding rate

In order to determine the optimum feeding rate of the polymer solution feeding rates ranging from 0.5ml/h to 5ml/h were tested (Tab 5.3). Feeding rates of 0.5, 1 and 5ml/h were too slow or too fast leading to no fibre formation or deposition of drops of polymer solution and consequently to fibre merging on the collector. Feeding rates of 2 and 3ml/h did result in fibre deposition and drop formation without clogging.

Table 5.3 Feeding rates tested. (-) no drop formation, (+) drop formation

Feeding rate (ml/h)	Observations	Drop formation at needle tip	Clogging of needle
0.5	Too slow to push solution out	-	Clogging
1	Too slow to push solution out	-	Clogging
2	Slow initial formation of polymer solution drop at the needle tip, no solution deposition on collector	+	No clogging
3	Initial formation of polymer solution drop at the needle tip, no solution deposition on collector	+	No clogging
5	Too fast, polymer solution drops onto collector before evaporation, resulting in fibres merging	+	No clogging

The feeding rate influences the size of the fibre as a higher feeding rate results in an increase of fibre diameter (Zhao et al., 2007). To achieve smaller diameter (<800 nm), the flow rate was reduced so far that it was enough to push the solution out of the needle and not to interrupt the fibre formation process. This was achieved with 2ml/h resulting in the highest efficiency of fibre density to polymer solution electrospun. Both higher and lower settings generated fewer fibres on the collector. Any lower setting was not successful as it was not strong enough to force the polymer solution out of the needle. Also with a higher feeding rate the solvent had less time to evaporate completely, resulting in thicker fibres and deposition of polymer solution on the collector resulting in merging of nanofibres. When the amount of solution jet per unit time is excessive the jet has does not whip and

stretch, resulting in non-straight fibres. Additionally, during the elongation process the solvent may not evaporate in time which results in bead formation and polymer solution deposition on the collector.

The flow rate found to be optimum here was 2-3ml/h which is in correlation with the literature where reported feeding rates range from 0.4ml/h (Zhao et al., 2008) to 4 ml/h (You et al., 2006).

5.8 Quantification of fibre alignment

The main focus of the previous results and discussions was on producing random electrospun fibres with settings that result in reproducible samples. The next step was to produce aligned electrospun fibres. For this, all process settings remained the same except the collector was replaced with two parallel aluminium rods with an air gap (0.5, 1, or 1.5cm) (Fig 3.1).

When examining the literature, many publications mention the use of rotating drums. These drums have different sizes and shapes and rotate at different speeds, making it difficult to choose a standard method (Tong and Wang, 2007, Duan et al., 2006). This is also an obstacle when comparing data published in the literature. It was also attempted to use a rotating drum in this work, but the fibres obtained were not aligned, although all parameters (i.e. the rotating speed) have been varied excessively, still only random fibres were obtained. Instead two aligned aluminium rods were used. The use of two conductive electrodes with a void gap of variable widths has been previously reported to result in aligned fibres (Li et al., 2005). The use of two aligned electrodes changes the configuration of electrostatic forces resulting in fibres spanning across the gap.

To assess the alignment of the produced fibres, a thin layer of polymer was electrospun onto glass cover slips. In order to quantify the orientation of fibres, analysis of fibre alignment was carried out using ImageJ, an open source image analyses software. For this, original images were transformed using Fast Fourier transform and alignment quantified using Oval_Profile a further ImageJ plug in (Fig. 5.7).

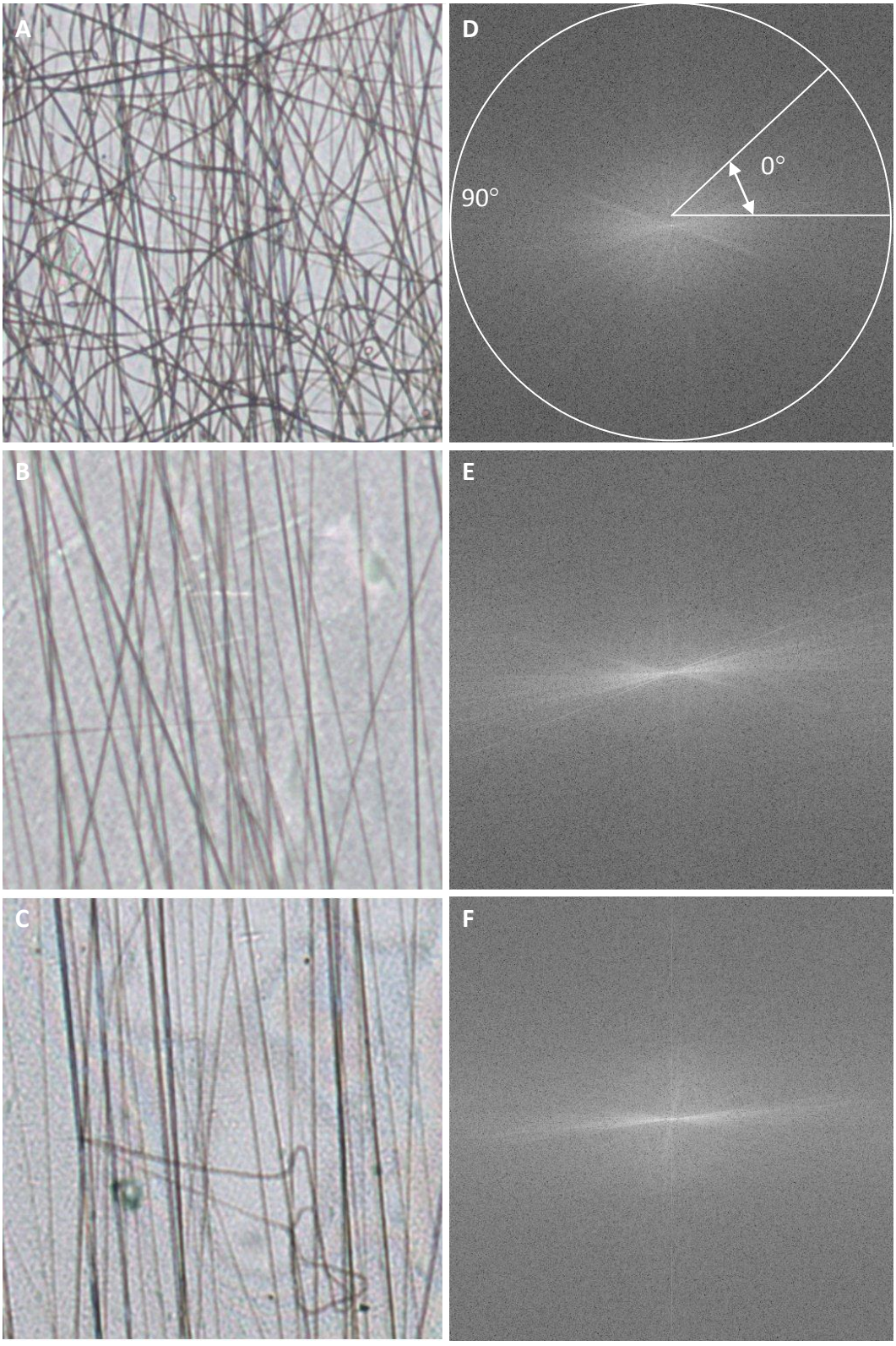

Figure 5.7 Analysis of alignment of electrospun PLGA nanofibres. Representative phase contrast images of electrospun fibres (A-C) and fast fourier transformation (FFT) output images (D-F). (D) structure which was used to retrieve the oval profile data. Collector distances were 0.5cm (A +D), 1cm (B + E) or 1.5cm (C + F).

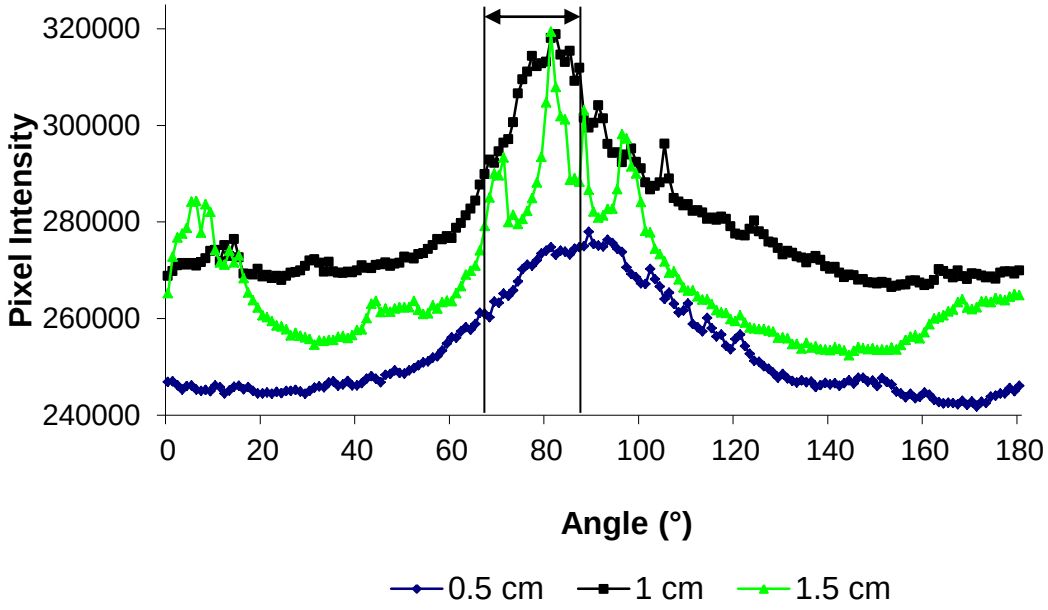

Figure 5.8 Angular fibre alignment of electrospun PLGA. Pixel intensity plots against the angle of acquisition of fibres collected onto two parallel stainless steel rods with 0.5, 1, and 1.5cm air gap. Note the single distinctive peak produced by the image output containing aligned formation.

When the two aligned aluminium electrodes were placed 0.5cm apart hardly any alignment was present (Fig. 5.7 a). After increasing the distance to 1cm fibre alignment improved drastically (Fig. 5.7 b). Once the distance between the electrodes was too far, random fibres start to appear again. The pixel intensity plots (Fig 5.8) show the pixel intensity orientation of the analysed images. A single distinctive peak in the graph represents the pixel intensity and thus orientation of the image.

It has been reported that the fibre orientation changes from aligned to random after 30 min of electrospinning at a flow rate of 1ml/h (Yang et al., 2005), which may be due to residual charges. The residual charges of the electrospun polymer seem to be efficient to exercise a repel force on the next depositing fibre and changing its orientation, leading to pores or voids between aligned fibres. This was also observed when producing the aligned samples here. For this reason the scaffolds were electrospun for only 30 min at a flow rate of 2ml/h. If required, the thickness of the final scaffold can be increased by placing fibrous mats on top of each other.

Several previous publications dealt with electrospinning PLGA, although only one reports about the production of aligned PLGA fibres which were additionally modified with polypyrrole to increase electrical conductivity trying to overcome the non-conductive properties of PLGA (Lee et al., 2009). This makes this report the first describing the production of aligned PLGA nanofibres. Yang and co-workers have produced aligned PLLA fibres for neural tissue engineering applications (Yang et al., 2005). These fibres show a high order of alignment and they were collected on a rotating disk, which was rotating at 1000rpm. The alignment was only demonstrated with SEM images and was not quantified making a quantitative comparison difficult. Jose and co-workers produced aligned poly-(lactic-co-glycolic acid)/hydroxyapatite fibres on a rotating drum at a speed of 6000rpm (Jose et al., 2009). These fibres show a lower order of alignment with the majority of fibres within 30° from the orientation axis compared to the work presented here, where fibres were within 20° from the orientation axis (Fig. 5.8). The advantage of using two electrodes lies within the simplicity of the electrospinning set-up. The disadvantage is the size restriction of the produced fibrous mats, which were on average 7.5cm^2 of aligned fibre area. The size of a human SCI is in the range of 2-4cm (Gros et al., 2010), making the produced sample too small for implantation in humans but they could be tested in animals.

Another advantage is that the mats can have both random and aligned fibres, random fibres on top the electrodes and aligned fibres spanning the gap if left for 30 min. This can be used to study cell behaviour on both topographies simultaneously with potential applications in tissues other than the spinal cord.

5.9 Further considerations

In general, the produced nanofibre mats were very fragile indicating low mechanical strength. The low mechanical strength might limit the application diversity of the produced scaffold. Ways in which the scaffold can be packed and stored prior to implantation have to be investigated. Also, being produced at room temperature the fibres tend to shrink when exposed to 37°C in the incubator, which makes it

difficult to predict the polymer's behaviour. This loss of initial size of electrospun fibre mats during incubation is due to thermally induced relaxation of stretched amorphous chains and results in formation of a much denser structure. Unfortunately, this also results in loss of porosity. This effect has been previously described by Zong and colleagues (Zong et al., 2003) and was confirmed in this study. This shrinkage effect is very undesirable for biological application, as it may result in faster release of encapsulated drugs or shock the cells embedded in the scaffold. It would be useful to control or prevent this behaviour. This was partly achieved by Zhon and colleagues who used PLGA 10:90 instead of 75:25. Preventing the shrinkage, the altered ratio of PLA to PGA resulted in a faster degradation rate, instead of up to six months (Zhou et al., 2004), the polymer degraded within one month (Zong et al., 2003). This makes it less favourable for long term application, such as implantation within the nervous system.

5.10 Conclusion

In this chapter various parameters of electrospinning were described and the characterisation of electrospun PLGA nanofibres was presented. It was shown that those parameters influence the electrospinning process and thus the fibre formation process as well as morphology of the fibres. The parameters include the concentration of the polymer solution, the solvent used, voltage applied, feeding rate of the polymer solution, collector-to-needle distance and type of collector, aluminium foil for random fibres and two aluminium rods.

The most suitable fibres, with an average fibre diameter of 530±140nm, were obtained using a 10% w/w PLGA polymer solution in $CHCl_3$/MeOH (3:1) with an optimum viscosity of 0.07Pa.S which was electrospun using a needle with 0.4mm inner diameter and 15kV applied voltage. The polymer was collected onto aluminium foil for random fibres and on two parallel aluminium rods for aligned nanofibres. Both collectors were placed 11cm away from the tip of the needle through which the polymer solution was pumped at a feeding rate of 2-3ml/h.

These conditions were used to produce polymer samples for further cell attachment experiments.

After the production of the scaffold and intense investigation of parameters influencing the electrospinning process, the assessment of the scaffold in terms of cytocompatibility was investigated and the results are presented in chapter 6.

6. INTERACTIONS OF PC12 CELLS WITH ELECTROSPUN PLGA SCAFFOLDS

6.1 Introduction

After a spinal cord injury the damaged neurites retract and cannot find their distal targets because the glial scar blocks axonal outgrowth. A tissue engineering approach to this problem involves the provision of physical cues in terms of implantation of a scaffold. Here, a scaffold made from an electrospun PLGA was tested for its suitability to promote cellular attachment, proliferation and differentiation. This chapter describes the assessment of these characteristics, focusing on PC12 cells on random and aligned PLGA fibre mats. Parameters examined include the number of cells attaching to the scaffold after 4 h followed by proliferation of the cells over 120 h, the number of neurite-bearing cells, the number of neurites per cell, the length of neurites and the alignment of neurites along nanofibres.

6.2 Attachment of PC12 cells to random PLGA nanofibres

Many cell lines, excluding those which grow in suspension, cannot grow without being attached to a surface, each other or to other cell types. The attachment is mediated through cell adhesion molecules, e.g. cadherins, integrins and selectins. These transmembrane cell-matrix adhesion receptors activate intracellular signalling pathways that communicate to the cell the character of the extracellular matrix (ECM) (e.g. laminin, fibronectin, fibrinogen, vitronectin or other proteins) upon which the cell adjusts its behaviour. A simplified version of the ECM would consist of many randomly oriented bundles of nanofibres, representing collagen, which is the most abundant protein in mammals (Di Lullo et al., 2002). By using electrospinning it is possible to produce synthetic nanofibres, which can be used as an implant material.

In order to study the effect of electrospun fibres on cell attachment, PC12 cells were seeded on sterilised random and aligned PLGA nanofibre mats and left to attach for 4 h. After attachment, cells were fixed and analysed using fluorescent microscopy and SEM. PC12 cells were shown to attach to the electrospun

nanofibres and also to divide on the surface, as can been seen in figure 6.1 where two cells are in the end phase of cell division. The cells were small, 10.76±1.28µm (n=6), and of very round appearance, which is in accordance with previous work (Fujita et al., 1989). The cells were in contact with the surface through microvilli and cilia, membrane protrusions which are involved in absorption, secretion, mechanotransduction and also increase the surface area of cells. These features of surface morphology were first described by Connolly and colleagues who analysed PC12 cells on PLL coated glass coverslips (Connolly et al., 1979). The qualitative surface morphology results relate to the data presented here which also confirms that the invasive SEM cell preparation procedure did not affect the surface morphology. These findings indicate that the electrospun scaffold does not affect PC12 cell behaviour negatively making it suitable for further investigations and for nerve regeneration applications.

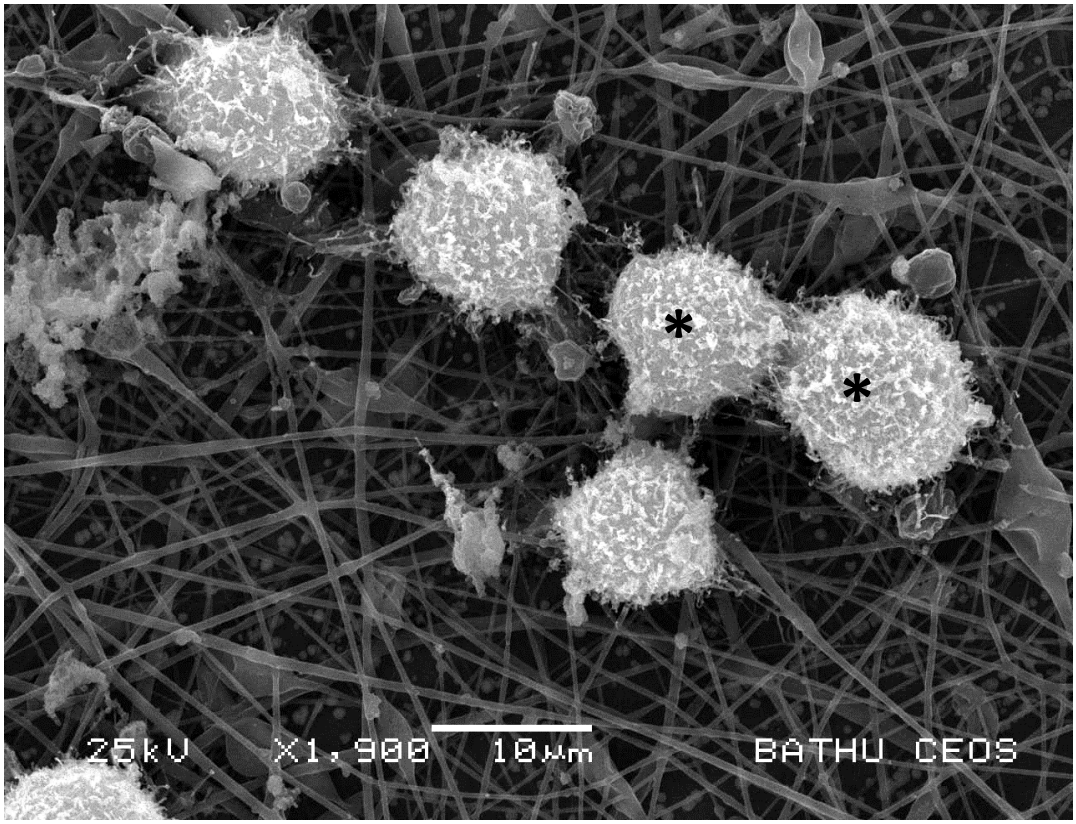

Figure 6.1 PC12 cells on random electrospun PLGA nanofibres. * indicates cells that may be in the final stages of cell division.

Further qualitative evidence of cell attachment also demonstrated that the nanofibres provide topographical cues for the cells. The results in Figure 6.2 (D-F) show that cells attach to the polymer according to the orientation of the electrospun nanofibres, that is along the fibres in a row, compared to TCP coated with PLL where cells accumulate in random clusters on the surface as no topographical signals are provided (Fig 6.2 A-C). The random attachment pattern was also observed for random fibres. This was the first promising result indicating that the surface provided by the nanofibre mats had an effect on PC12 cell attachment behaviour. The results indicated good attachment of PC12 cells to the polymer as cell remained attached after staining and treatments that precede SEM analysis. Living cells were present (green labelled cells, stained with calcein AM) compared to the absence of dead cells (red labelled cells, stained with ethidium homodimer) indicating the non-toxic characteristics of the PLGA scaffold (Fig. 6.2 E+F). Additionally, images obtained by light microscopy showed cells attached to fibres in no particular orientation on random PLGA nanofibres and along nanofibres on aligned PLGA nanofibres (Fig 6.3).

PC12s do not attach to TCP, thus coating is essential for adherent cultures (Lhoest et al., 1996). This provides an obstacle when trying to conduct cell attachment studies. PLGA is a relatively hydrophobic material. This means that PC12 cells, which are unlikely to attach in the first place, will not be likely to attach to a polymer which does not actively support cell attachment by being hydrophobic and by the absence of functional groups on the surface to promote cell attachment. This was the case when using PLGA flat sheet membranes (Chapter 4). Only a minimal number of cells attached to the polymer and cells were easily washed off during washing and staining steps. Cell attachment experiments revealed that 18±7% of seeded cells attached to random and aligned PLGA nanofibres with no significant difference between random and aligned nanofibres ($P>0.05$) (Fig 6.4). Although the numbers indicated that cell attachment to electrospun nanofibres is not more efficient than to flat sheet membranes (20±7%), analysis of the samples under the microscope indicated a higher proportion of cells were on the sample. The major

challenge when quantifying cell attachment on electrospun PLGA nanofibres was the successful detachment of cells from the polymer in order to allow accurate cell counting. Thus only conservative numbers were included into the final analysis resulting in low cell attachment efficiency. Cell numbers on flat sheet membranes were obtained using a haemocytometer where cell numbers on electrospun samples were obtained using PicoGreen assay. There may be discrepancies between the two methods which cannot be ruled out.

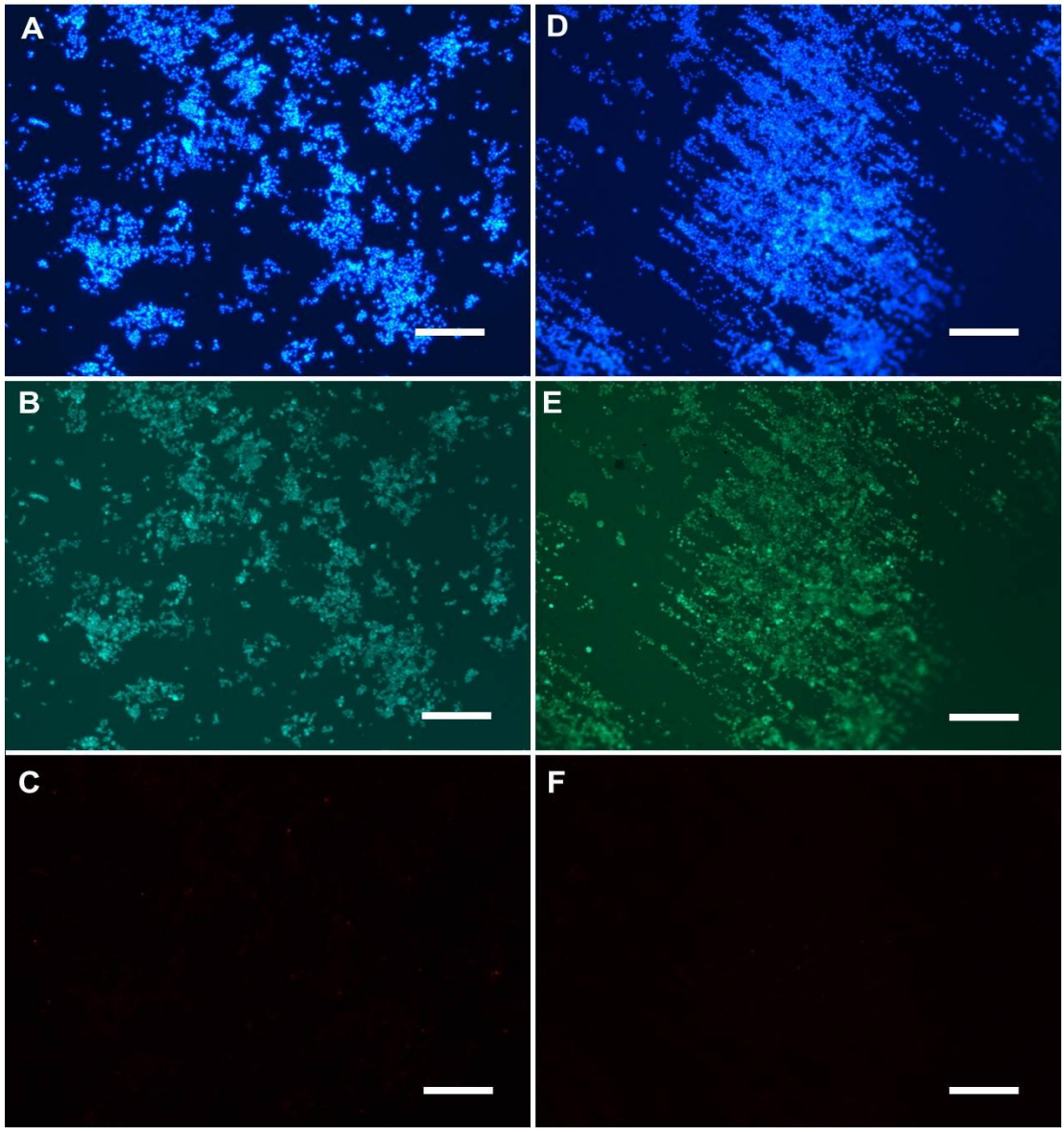

Figure 6.2 PC12 cells attach along PLGA nanofibres. PC12 cells on TCP coated with PLL (A-C) and electrospun PLGA nanofibres (D-F) stained with Hoechst (blue, A+D), calcein AM (green, B+E) and ethidium homodimer (red, C+F). Cells did not die after attachment to either TCP or PLGA fibre mats. The linear structure that is visible in D, E, and F are cells which align according to topography presented to them. Scale bar=200µm.

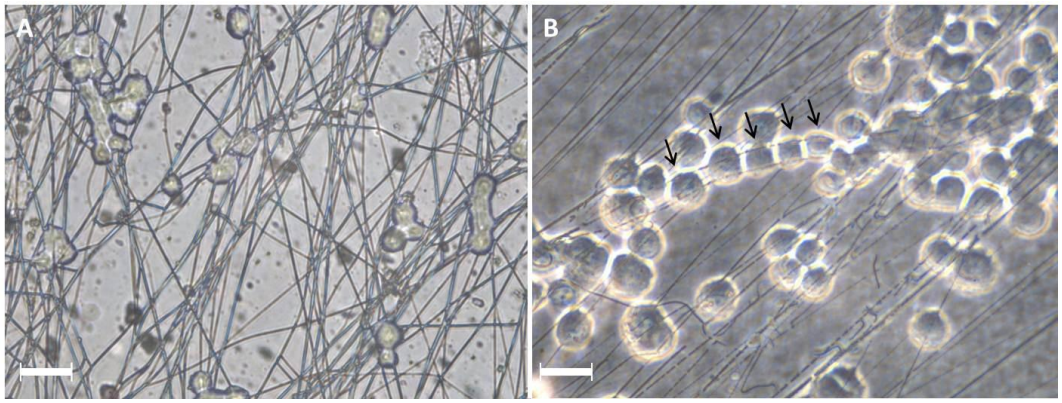

Figure 6.3 PC12 cell distribution along nanofibres. Cells were seeded on random (A) and aligned (B) PLGA nanofibres. PC12 cells attach to both random and aligned PLGA fibres. When seeded on aligned fibres cells attached along nanofibres. Scale bars=25µm

6.3 Proliferation of PC12s on electrospun PLGA nanofibres

After examining the attachment of PC12s to electrospun PLGA nanofibres, proliferation of the cells was examined, comparing TCP-PLL, random PLGA nanofibres and aligned PLGA nanofibres. Following seeding, the cell number was established using the PicoGreen assay after 4, 24, 48, 72 and 120 h of incubation. The results showed that the cells seemingly stopped dividing on the polymer scaffolds, whereas they proliferated on TCP-PLL (Fig. 6.4). There was no significant difference in initial cell attachment (4 h) between random and aligned PGLA nanofibre mats , but a significantly higher percentage of cells attached to TCP-PLL ($P<0.001$). The cells proliferated on all surfaces within the first 48 h, followed by a 24 h phase where no proliferation took place as the cell numbers did not increase between the 48 h and the 72 h time points ($P>0.05$). This was followed by further proliferation on TCP-PLL (time point 120 h), no proliferation on aligned PLGA nanofibres and a decrease in cell numbers on random PLGA nanofibres.

No cell migration into the scaffold was observed. Although the surface topography is 3D, cells attach to the surface only which indicates that either the cells perceive the nanofibrous surface as 2D or cell migration into the scaffold requires more time. Although cell migration into an electrospun scaffold has been previously observed with human adipose derived stem cells (Heydarkhan-Hagvall et al., 2008), PC12 cells did not show such behaviour and remained on the surface of the nanofibrous mat during proliferation.

According to previous research, the rate of proliferation and differentiation of cells on a material depend on the successful initial attachment of cells on the surface of the material (el-Ghannam et al., 1995). Here, initial cell attachment was relatively low thus leading to relatively poor growth of PC12 cells.

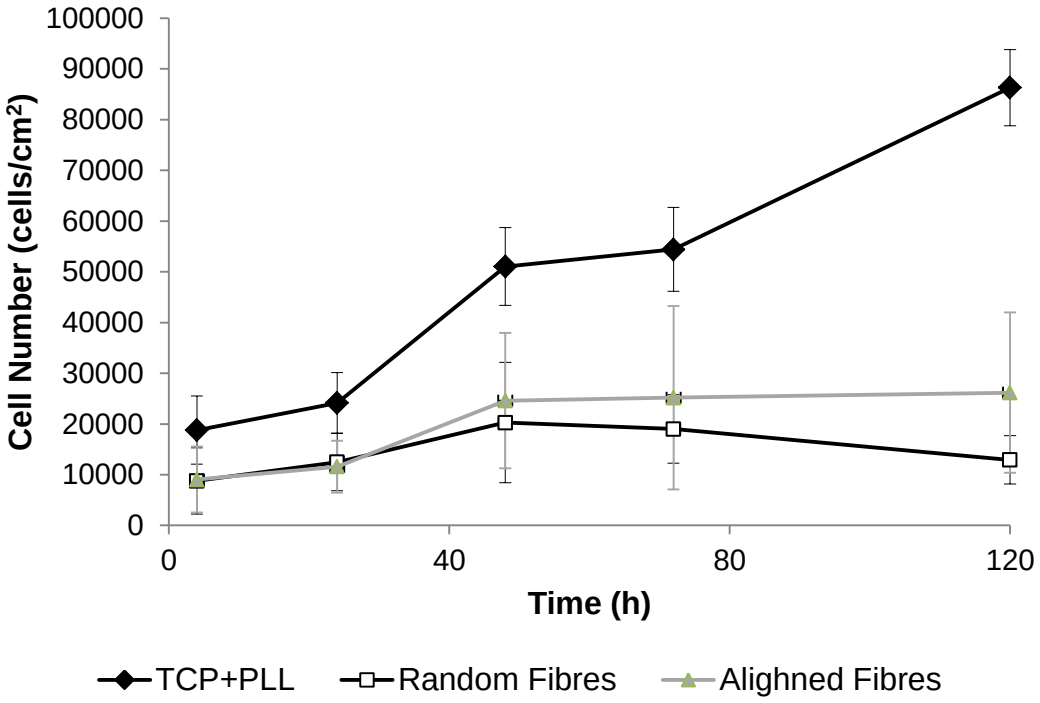

Figure 6.4 Proliferation of PC12 cells on TCP-PLL, random and aligned PLGA nanofibres. Cell numbers were obtained using Picogreen quantification kit. Data represent the mean ± SEM (n=4) and were analysed using Student's t-test.

As the aim of this experiment was to promote neurite outgrowth, proliferation of neuronal cells was not the major aim and for that reason not considered a major drawback. Additionally, in the damaged spinal cord cell division of damaged cells is not taking place, instead extension of axons along the scaffold is highly desirable. Nevertheless proliferation was present during the 4-48 h period after seeding. It would be interesting to know why the cells did not proliferate. Normally, these cells stop dividing and start growing neurites after addition of NGF, which was not the case here. It is possible that the cells may perceive the topography of the scaffold as a cue for differentiation and stop dividing, although there is no evidence in the literature for PC12s behaving in such a way. Thus, this effect needs to be further investigated.

6.4 Differentiation of PC12s on electrospun PLGA nanofibres

Once attachment and proliferation of PC12s on electrospun PLGA was analysed, their differentiation on random and aligned PLGA nanofibres was investigated. The parameters recorded included the number of neurite bearing cells, the number of neurites per cell, the length of neurites and the angle of neurites outgrowth along nanofibres. In order to measure neurite outgrowth on electrospun fibres, cells were seeded onto random and aligned PLGA fibres at a density of 50,000 cells/cm^2. After 4 hours attachment in FCS-free medium, medium containing 1% FCS and 40ng/ml NGF was added and cells were allowed to differentiate for seven days. After seven days, cells were stained with ethidium homodimer, calcein AM and Hoechst and fixed with formalin. The cells were stained in order to quantify cell survival as well as for visualisation of neurite extension as calcein molecules diffuse across the membrane, get trapped inside and give out strong green fluorescence (Gatti et al., 1998). The length of neurites was analysed using ImageJ.

When comparing neurite outgrowth on random fibres and aligned fibres, it was very clear that neurites grew along aligned fibres (Fig 6.5, 6.6 and 6.7), showed less branching and were longer than those on random fibres. These three parameters were quantified. Figure 6.5 shows a whole image obtained using fluorescence microscopy. The cells were stained with the nuclear stain Hoechst and calcein AM which fluoresced green and visualised the cell body and the neurites. Figure 6.6 (A+C) shows two PC12 cells which differentiated on random nanofibres. These cells had two or three neurites which extended in random directions. Additionally, the neurites showed intensive branching. Figure 6.7 shows PC12 cells which differentiated on aligned PLGA nanofibres. These cells had predominantly one to two neurites per cell, longer neurites (for detailed quantification of neurite length see Fig. 6.8) and extended along the orientation of the fibre (for detailed quantification of alignment see Fig. 6.9).

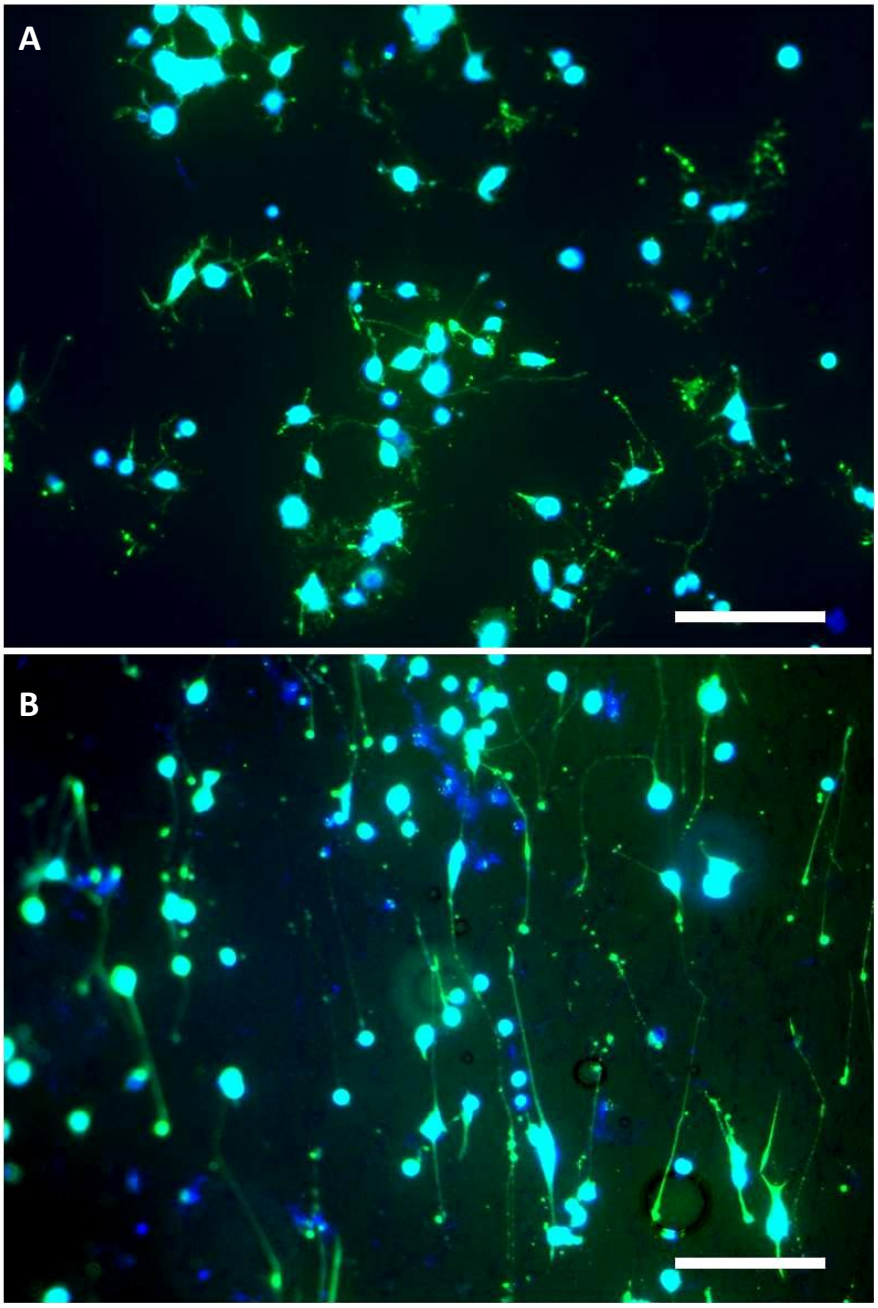

Figure 6.5 Neurite outgrowth of PC12s. Neurite outgrowth of PC12s was compared (A) on random and (B) on aligned PGLA nanofibres. Cells were allowed to differentiate in cell culture medium supplemented with 1% FCS and 40ng/ml NGF. Cells were stained with hoechst (blue), calcein AM (green) and ethidium homodimer (red). Scale bar=200µm.

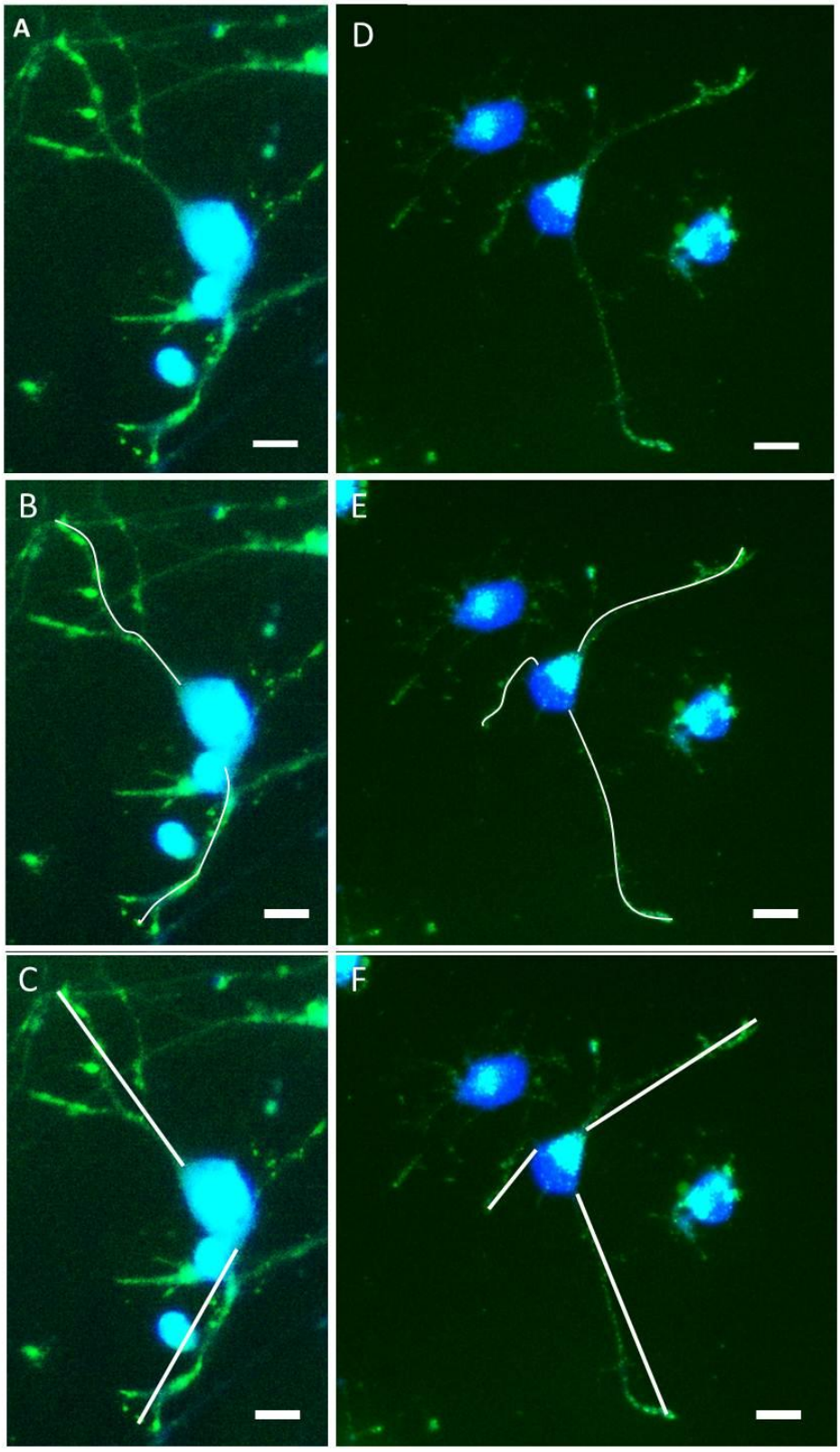

Figure 6.6 PC12s on random PLGA nanofibres. The measurement of neurite length (neurites longer than cell body diameter and longest branch were measured) (B + E) and angle of neurite outgrowth (C + F) were measured using ImajeJ. Cells were allowed to differentiate in cell culture medium supplemented with 1% FCS and 40ng/ml NGF for 7 days. Cells were stained with Hoechst (blue), calcein AM (green) and ethidium homodimer (red). Scale bar=10μm.

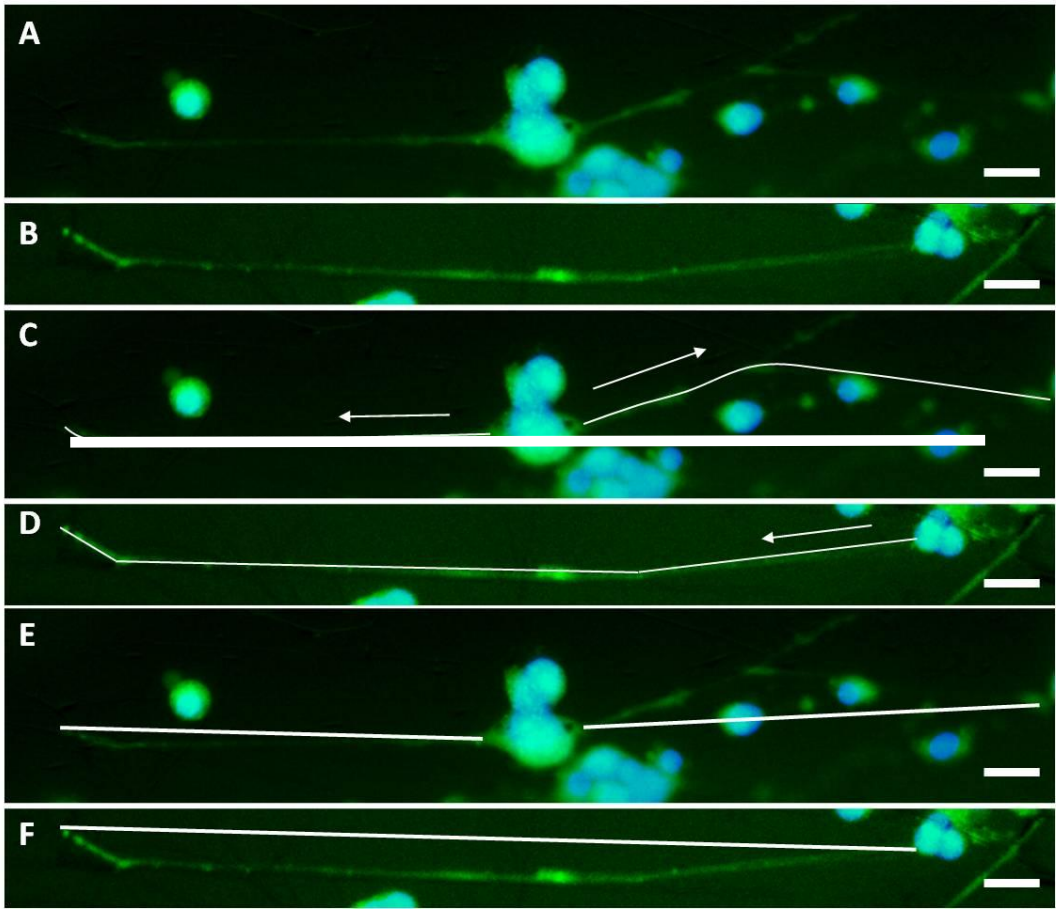

Figure 6.7 PC12s on aligned PLGA nanofibres. The measurement of neurite length (neurites longer than cell body diameter and longest branch were measured) (C + D) and angle of neurite outgrowth (E + F) were measured using ImajeJ. Cells were allowed to differentiate in cell culture medium supplemented with 1% FCS and 40ng/ml NGF for 7 days. Cells were stained with Hoechst (blue), calcein AM (green) and ethidium homodimer (red). A + C + E scale bar=10μm, B + D + F scale bar=20μm.

6.4.1 Electrospun PLGA nanofibres influence differentiation of PC12s

The differentiation of PC12 cells on random and aligned PLGA nanofibres was investigated.

Number of neurites

The first differentiation parameter of interest was the number of neurites per cell. For this, the total cell number and the number of neurite bearing cells on TCP-PLL,

random and aligned PLGA nanofibres were compared. The number of neurite bearing cells was 55±5% and 68±6% on random and aligned fibres, respectively, but only 16±8% on TCP-PLL (Fig 6.8), indicating a positive topographical effect on neural differentiation provided by the polymer scaffold. The data revealed that the number of neurite bearing cells was significantly higher on the polymer compared to TCP-PLL. These results also demonstrated that a significantly higher number of neurite bearing cells were present on aligned fibres compared to random fibres. This effect was also previously described by Lee and colleagues (Lee et al., 2009), who investigated PC12 cell differentiation on electrospun PLGA coated with polypyrrole (PPy).

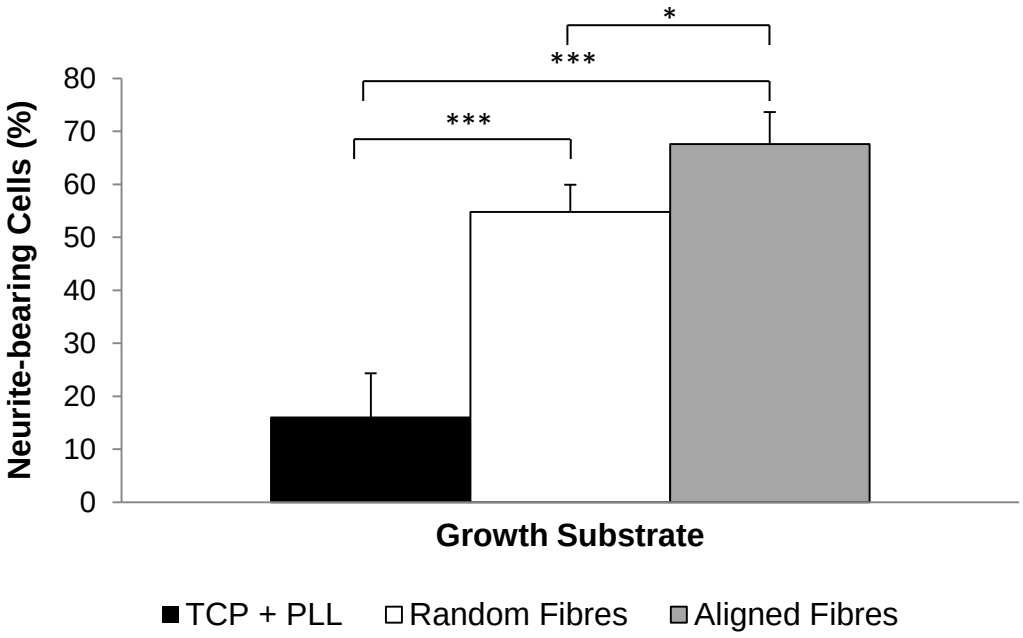

Figure 6.8 Proportion of neurite-bearing cells. Cells were grown on TCP coated with PLL, PLGA random and aligned fibres. After 7 days exposure to 40ng/ml NGF, pictures were taken of each sample and total number of cells and the number of neurite bearing cells were counted using "Cell Counter" an ImageJ plug in. Total number of cells/picture was set as 100% for each image. The experiment was repeated three times with three representative wells per surface. 10 random images were taken per well. *** P<0.001, * P<0.05.

After determining the number of neurite bearing cells, the number of neurites per cell was investigated on random and aligned PLGA nanofibres. The neurites per cell were counted after seven days of exposure to NGF. The cells differentiating on

aligned fibres have predominantly one to two neurites whereas cells on random fibres have up to eight neurites (Fig 6.9).

These data demonstrates the effect of topographical features on differentiation of PC12s. If given the chance, cells will grow in random directions, as is the case on random nanofibres. But if the topography provides distinct cues, as is the case on aligned nanofibres, PC12 cell will reduce the number of neurites according to the direction of nanofibres.

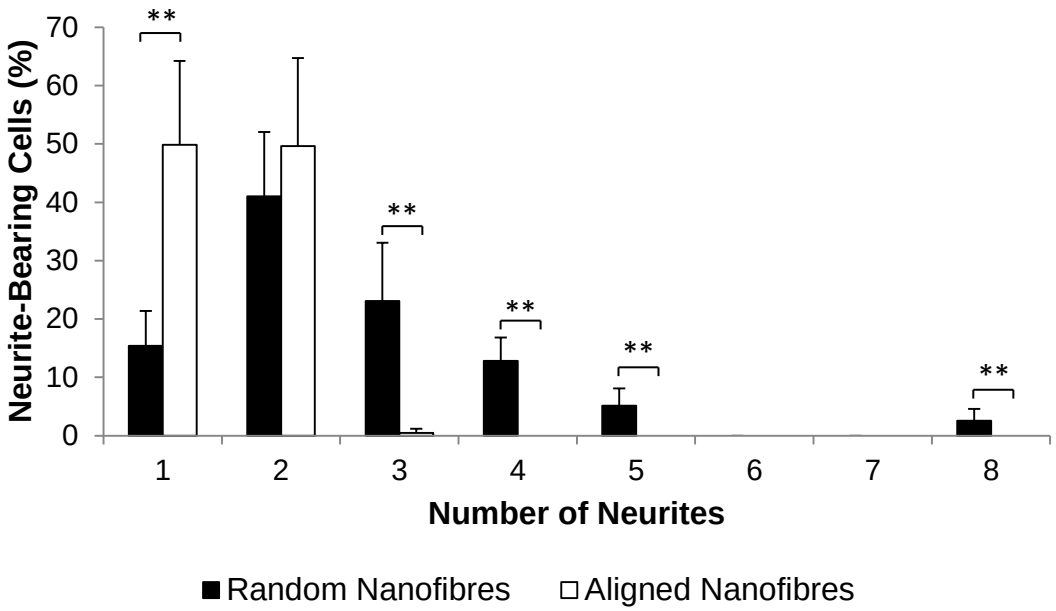

Figure 6.9 Aligned fibres reduce number of neurites per cell. Number of neurites per cell after 7 days exposure to 40ng/ml NGF. Cells on random fibres have up to eight neurites per cell, whereas cell on aligned fibres have only up to three neurites per cell. 10 random images were taken per well. **P<0.01. Data represent the mean ± SEM (n=3) and were analysed using Student's t-test.

Analysis of neurite length

The next parameter to be assessed was the length of neurites. Neurites on random fibres were shorter than those on aligned fibres (Fig. 6.10). On aligned fibres neurites extended up to 450µm after exposure to NGF for 7 days, whereas on random fibres neurites grew up to 200µm. The mean length of neurites on aligned fibres was 184±119µm, while on random fibres the mean length of neurites was 59±33µm. Similar results were obtained in other studies when seeding PC12 cells on

micropatterned laminin surfaces (Tai and Buettner, 1998, Leach et al., 2007, Kim et al., 2006b). Kim and co-workers showed that PC12 cells grow neurites of 80±40μm on aligned PLGA (50:50) microfibers (3-5μm diameter) after 4 days exposure to 50ng/ml NGF. The data presented here was recorded after 7 days exposure to 40ng/ml NGF, which is comparable to Kim (2006) where after half the time (4 days compared to 7 days used in this study) neurites reached nearly half (80±40μm) of the neurite length presented here (184±119μm). Neurite outgrowth could be explained with the rearrangement of proteins already present in the PC12s prior to NGF exposure thus longer neurites are not due to differences in protein synthesis. Longer neurites on aligned PLGA nanofibres can be explained by fewer neurites emerging from the cell than on random PLGA nanofibres. Previous published data described a twofold increase, from day 3 and day 9 of the experiment, in microtubule mass in parallel with neurite extension indicating the assembly of microtubules during differentiation (Drubin et al., 1985). Analysis was only performed for random neurite outgrowth and needs confirmation for outgrowth on aligned substances. Thus the lower number of neurites cannot be explained with the rearrangement of proteins already present within the cells prior to NGF exposure but could be due to the rate of protein production and the amount of protein available in combination with topographical cues.

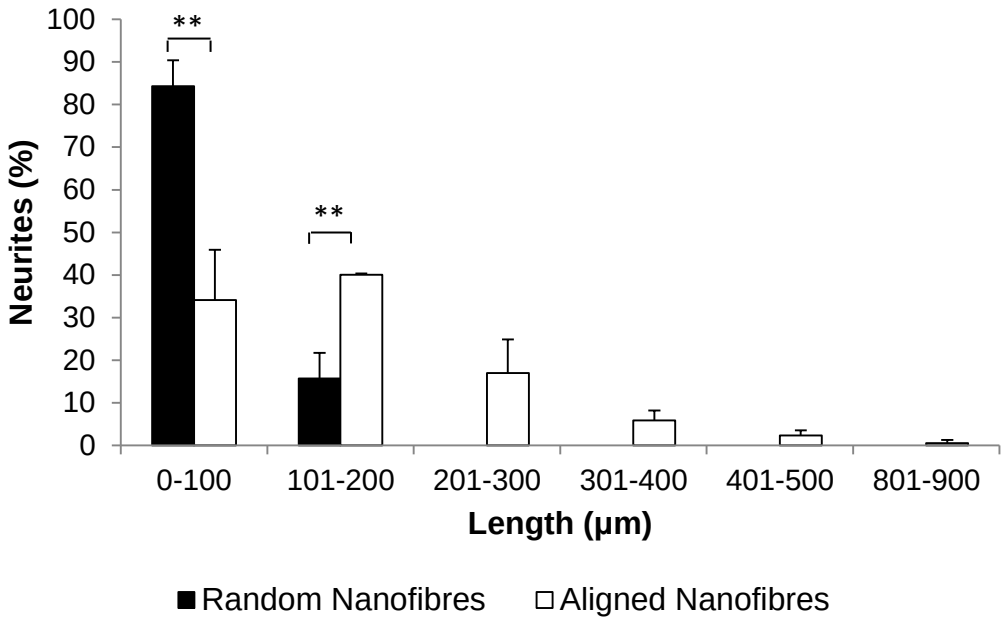

Figure 6.10 Random fibres restrict neurite extension. Length of neurites on random and aligned PLGA fibres was measured after 7days exposure to NGF. 10 random images were taken per well. **P<0.01. Data represent the mean ± SEM (n=3) and were analysed using Student's t-test.

Directional outgrowth of neurites

The most important effect of the electrospun fibres apart from the cell attachment effect was their influence on directional outgrowth of the neurites. The same data that was used to analyse the number of neurite bearing cells and number of neurites per cell was used to analyse the alignment of neurites along fibre orientation. The orientation of the electrospun fibres was set at 0°, and the angle of neurite extension was determined relative to this. As the data in figure 6.11 shows, the angle distribution of PC12 cell neurites on random fibres indicated no particular directional bias and differed significantly (P<0.05) from neurite angle distribution on aligned fibres, where a high proportion of neurites grew within 30 degrees of parallel.

When neurites start to sprout, a growth cone is formed out of which filopodia and lamellipodia emerge and explore the surrounding extracellular environment (Mahoney et al., 2005). The direction of neurite outgrowth is determined by traction which is formed by mictrotubules and actin filaments within the cytoskeletal structures. The strength of traction exerted by a filopodia determines

the direction of neurite outgrowth (Tan and Saltzman, 2002). Philopodia emerge from the cell uniformly in all directions when cells are cultured on glass surface, whereas parallel orientation to microchannels has been observed by Mahoney and colleagues suggesting that the topography, more precisely the walls of the microchannels, set the angles over which microtubules and actin filaments within the growth cone accumulate, assemble and orient to advance the extending neurite (Mahoney et al., 2005). It seems that not only channel walls but electrospun nanofibres have the same effect on neurite outgrowth of PC12 cells.

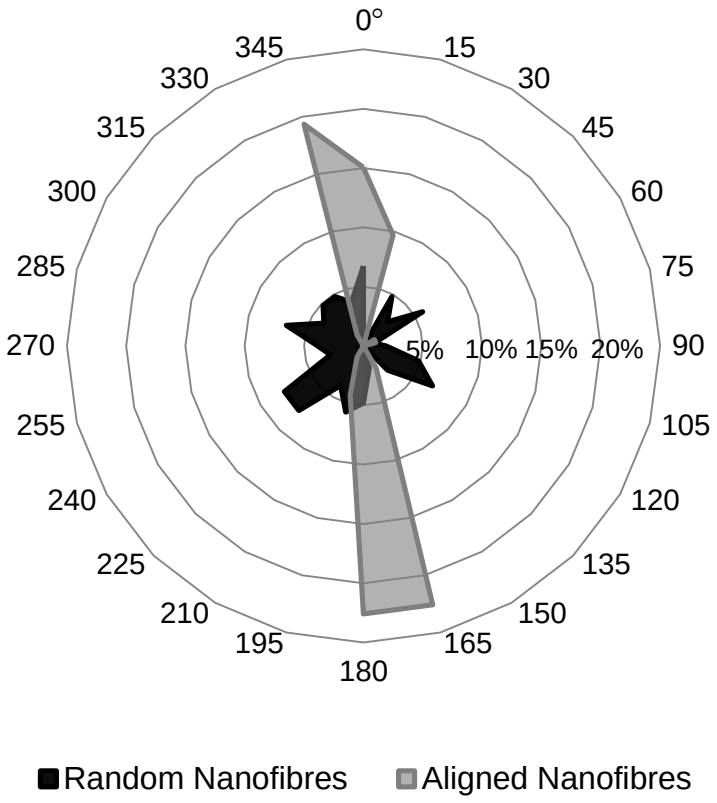

Figure 6.11 PC12 cell neurites extend along electrospun fibres. Number of neurites (%) is presented and their directional outgrowth on random and aligned PLGA nanofibres. The angle values were established in 15 degrees angle bins, with 0 and 180 degrees being completely parallel and 90 and 270 degrees being completely perpendicular. Data represent the mean values (n=3).The angle distribution of PC12 cell neurites on random fibres indicated no particular directional bias and differed significantly ($P<0.05$) from neurite angle distribution on aligned nanofibres, where a high proportion of neurites grew within 30 degrees of parallel. Data represent the mean (n=3) and were analysed using Student's t-test.

To date, there is only one study published on PC12 cell attachment to aligned PLGA fibres coated with polypyrole (PPy), an electroconducting polymer (Lee et al., 2009). Lee and co-workers have shown that PPy-PLGA supported growth and proliferation of PC12s. Upon stimulation with a potential of 10mV/cm and no addition of NGF, PC12 cells exhibited 40-50% longer neurites length and 40-90% more neurite formation compared to unstimulated cells on the same scaffold. Furthermore, stimulation on aligned PPy-PLGA fibres resulted in more neurite-bearing cells as well as longer neurites compared to random PPy-PLGA fibres. The work presented here is the first published study that investigated in detail the differentiation of PC12s on aligned, unmodified electrospun PLGA nanofibres. The work undertaken by Lee and colleagues supports the presented results here, even though the cells differentiate on polypyrrole and not on PLGA. This suggest that that the main factor affecting neurite length and number of neurite bearing cells is the topography of the scaffold, in particular the alignment of the PLGA nanofibres.

When taking into consideration the results from chapter 4, it becomes clear that there is a relation between surface chemistry and surface topography, both affecting the behaviour of PC12s.

6.5 Further considerations

At the present time in vitro experiments using primary sensory and motor neurons on PLLA (Corey et al., 2008), dorsal root ganglia (DRGs) on PLLA (Wang et al., 2009), chick DRGs on poly-caprolactone (Schnell et al., 2006) and neural stem cells on PLLA (Yang et al., 2004) have demonstrated the ability of aligned fibres to support directed neurite outgrowth compared to random fibres. Random axon outgrowth on random nanofibres was previously described by various publications (Yang et al., 2005, Foley et al., 2005) and was an expected outcome of this study. Yang and colleagues have demonstrated random and aligned neurite outgrowth of neural stem cells (neonatal mouse cerebellum C17.2 stem cells) on PLLA showing the effect of aligned nanofibres on a different neural cell line. Foley and colleagues demonstrated the effect of grooves and ridges of micro- and nanoscale (widths

ranging from 70 to 1900nm) on differentiation of PC12 cells. They observed that ridge widths of ≤400nm augmented neuritogenesis whereas ridge widths of ≥850nm suppressed neuritogenesis.

The reason for using electrospinning is to form a scaffold that mimics the ECM based environment as found in vivo as opposed to inhibitory cues present in the site of injury, including the glial scar. Work with electrospun materials has supported this purpose as the resulting nanofibres have a high surface to volume ratio, high porosity and high interconnectivity. All those parameters are necessary and indispensable for cellular attachment and proliferation (Li et al., 2002). This chapter describes the topographical effect of PLGA nanofibres on PC12 cells. Although not grooves, electrospun fibres have a similar effect on PC12 cells, they greatly affect neuritogenesis.

The behaviour of other neural cells has been investigated with the aim of evaluating an implant for PNS regeneration. It has been shown that aligned nanofibres support directional axonal outgrowth and glial cell migration (Schnell et al., 2007). A further publication describes the effect of aligned nanofibres on astrocytes' growth rate, morphology and alignment (Gerardo-Nava et al., 2009). Taking all the results together, electrospun PLGA nanofibres may be a promising start when manufacturing a spinal cord implant, as they provide topographical cues and promote neurite outgrowth in PC12s.

6.6 Conclusion

PC12 cells were used as a model for neurite outgrowth on electrospun random and aligned PLGA nanofibres. For that, cells were seeded onto random and aligned PLGA nanofibre mats and analysed to determine attachment, proliferation and differentiation. It was shown that the fibre mats did not support cell proliferation but they did support cell attachment and differentiation when compared TCP. When comparing random and aligned nanofibres, it was clear that neurite outgrowth was directed by the orientation of the nanofibres. Additionally, more neurite bearing cells were present on aligned fibres and cells extended longer

neurites on aligned nanofibres compared to random nanoifibres. As the aim was to create an implant that directs neurite outgrowth, minimising the distance for neurites to cover, aligned electrospun nanofibres are likely to be a material of choice for future nerve regeneration approaches.

7. ENGINEERING BIOMATERIALS: MODIFICATION OF PLGA NANOFIBRES BY INCORPORATION OF BIOACTIVE MOLECULES

7.1 Introduction

The work presented in this chapter focuses on incorporation of bioactive molecules into PLGA nanofibres and the potential of the newly created scaffold for nerve tissue engineering. PLGA is widely used in tissue engineering due to its ideal biocompatibility and degradation rate. Nevertheless it has some drawbacks such as its low hydrophilicity and conductivity. These characteristics can potentially be improved to make PLGA an ideal polymer, by for example surface modification, coatings or incorporation of substances into the scaffolds, such as other polymers or bioactive moieties. The process of electrospinning offers the option of spinning various mixtures. The newest development is the electrospinning of emulsions where aqueous and oil phases are mixed prior to electrospinning. The ability to introduce biological moieties into electrospun fibres opens a new opportunity for scaffold modification including delivery of therapeutically active agents to the site of injury. In this chapter, a water-in-oil emulsion was electrospun where the water drops contained poly-L-lysine (PLL) with an organic phase of PLGA dissolved in $CHCl_3$:MeOH (3:1).

7.2 PLL incorporation into PLGA nanofibres

PLL is used as a coating for cell culture and increases cell attachment of PC12 cells to TCP. Its effect on PC12 cell differentiation after incorporation into PLGA nanofibres was investigated. For this, random PLGA-PLL nanofibres were produced using emulsion electrospinning. Random nanofibres were used as they can be produced faster and on a larger scale than aligned fibres. In order to demonstrate the presence of PLL in the electrospun scaffolds, FITC-PLL was added to the aqueous phase. The FITC molecule emits light at 518nm (green fluorescence) when exposed to light at an excitation wavelength of 494nm. Nanofibres without FITC-PLL but with PLL did not fluoresce, whereas nanofibres with FITC-PLL displayed green fluorescence (Fig 7.1). As proteins and other biomolecules are susceptible to denaturation when exposed to solvents and high electrostatic forces, these assays confirm the presence of PLL after being exposed to solvents and electrostatic

forces, though further analysis, such as western blot, is necessary to investigate the presence of native protein.

The extent of labelling was 0.003-0.01 mol FITC per mol lysine monomer according to the manufacturer's information resulting in intensive green fluorescence fibres, also showing that more lysine has been incorporated than is possible to visualise using this labelling method. Theoretically, PLL that has not been labelled with FITC has also been incorporated, the exact amount of which still requires further quantification.

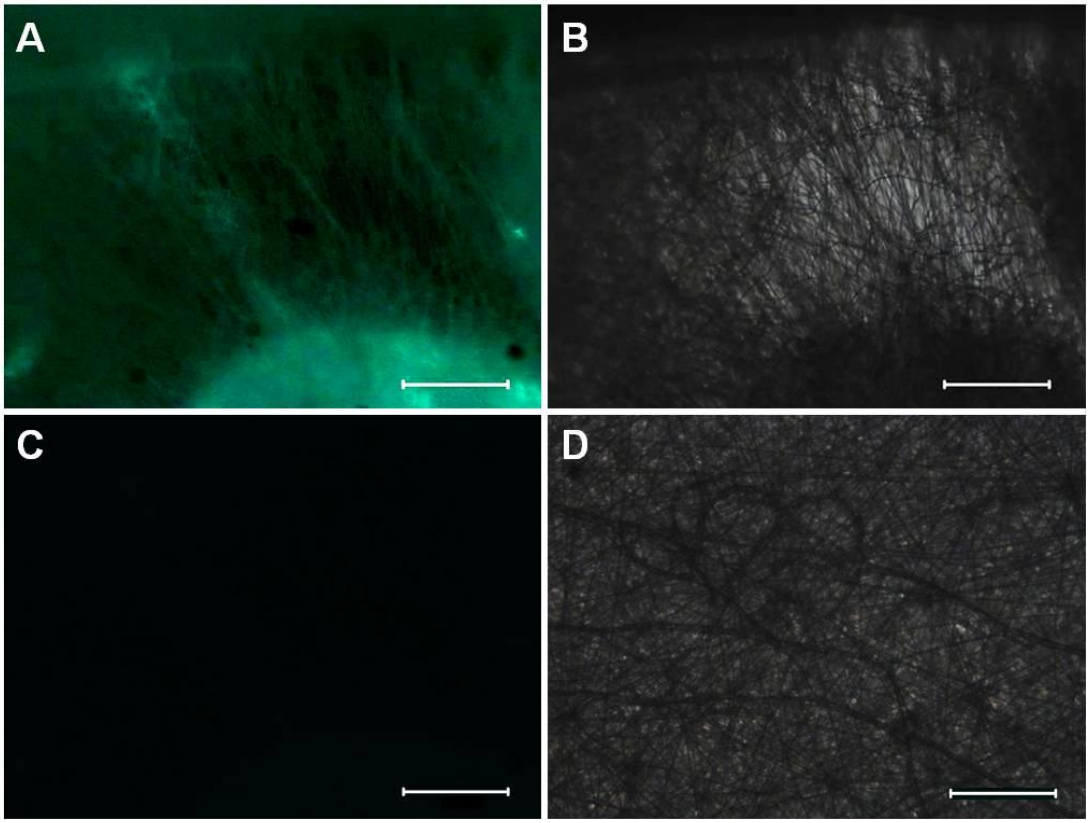

Figure 7.1 Visualisation of FITC-PLL in electrospun PLGA nanofibres. (A) Fluorescent image of electrospun fibres with FITC-PLL, (B) phase contrast image of same fibres as in A. (C) Fluorescent image of PLGA nanofibres with PLL. (D) phase contrast image of same nanofibres as in C. 10% PLGA in $CHCl_3$:MeOH (3:1), 1.1mg/ml PLL, 42ug/ml PLL-FITC (without PLL-FITC in C and D) in water/oil phase ratio 1/18. Scale bar=100µm.

7.3 Morphology of modified nanofibres

For incorporation of PLL into electrospun PLGA fibres, emulsions were prepared and compared to electrospun PLGA-dH_2O emulsions. The morphology of the resulting fibre mats was analysed using SEM (Fig 7.2). The resulting samples showed that

beads were present in the nanofibres when electrospinning PLGA-dH_2O. This indicates that the reduction of feeding rate from 3ml/h to 2ml/h resulted in bead formation. The feeding rate has to correspond to a given voltage to maintain a stable Taylor cone. A stable Taylor cone is maintained when the feeding rate is equal to the rate at which a solution is removed by electrical force. Beads can also be formed when the feeding rate is too high, making the investigation of an optimum feeding rate essential for uniform fibres (Gunn and Zhang, 2010). Furthermore it is possible that by adding water to the electrospinning solution the viscosity changes resulting in bead formation. The effects of viscosity are discussed in detail in chapter 5. The beads disappeared as soon as PLL was added to the water phase (Fig 7.2B). This is possibly due to the additional charges that the molecules (PLL) introduce into the electrospinning solution. The cations and anions present in the emulsion increase the elasticity of the whipping jet which stabilises and this prevents rupturing and droplet formation.

The fibre mats presented here were produced by electrospinning the polymer emulsion for no longer than 30 min. Phase separation of the water and oil phases occurred when the solution was left in the syringe for a longer period of time. As a solution, surfactants are normally used as means of stabilising the emulsion, which results in no separation or a longer period of time until separation occurs (Liao et al., 2008). This was attempted by incorporating Span80 into the emulsion. The surfactant did stabilise the emulsion, as it took up to twice as long for the water and phase to separate, but it had a droplet deposition effect on the resulting fibre mats (Fig. 7.3). This effect could not be eliminated by increasing the concentration of the polymer or modifying the process parameters, thus span80 was excluded from further experiments. Span80 is a non-ionic surfactant and emulsifier and should not have an effect on electrospinning in terms of providing additional charges to the solution. It may though have an effect on solution viscosity as it is an oily liquid with a viscosity of 1200-2000mPaS (Sigma-Aldrich). Further, it is possible that the surface tension of Span80 is stronger than the electrostatic force which fails to stretch the surfactant resulting in droplet formation.

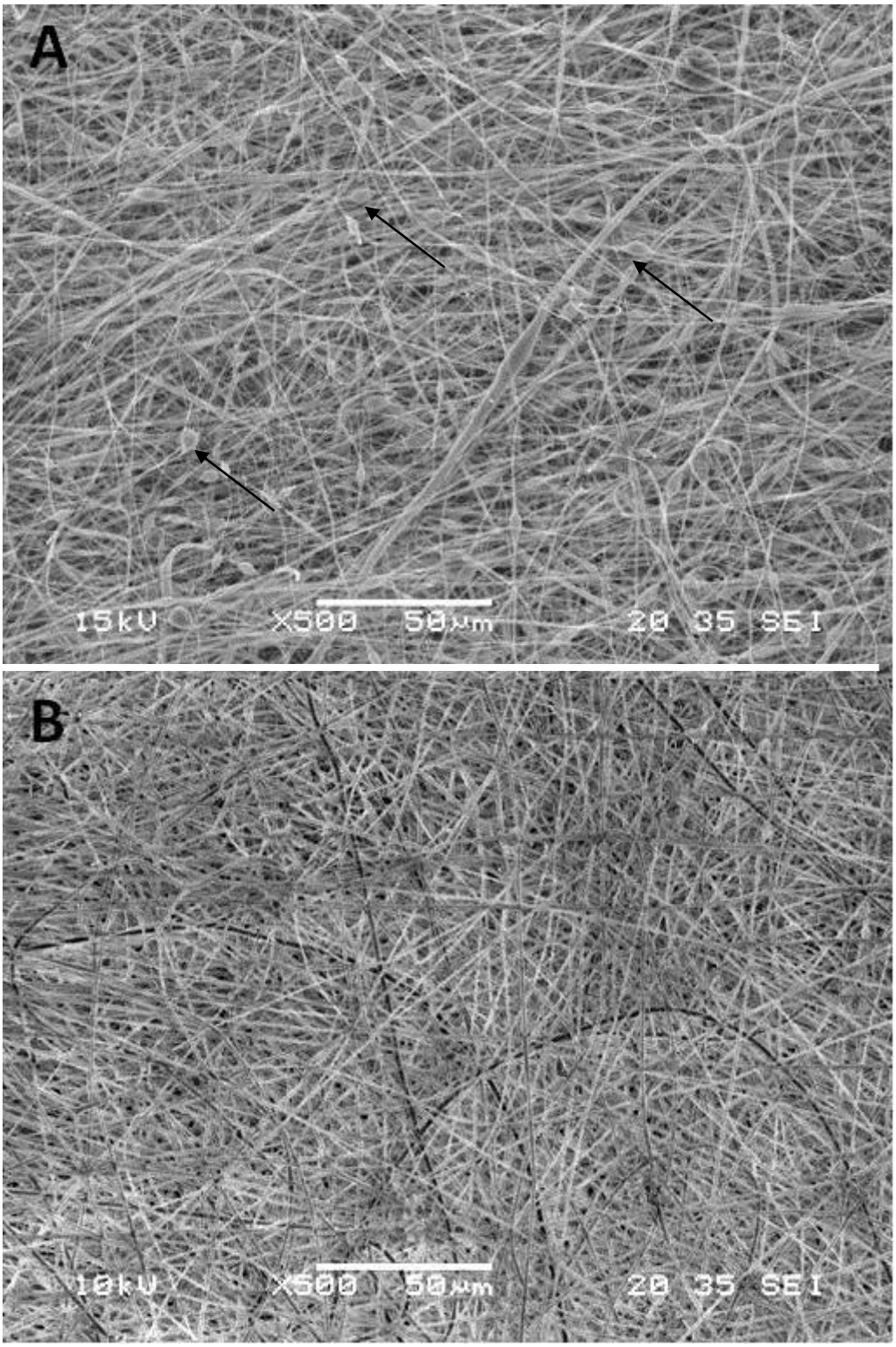

Figure 7.2 Morphology of electrospun naofibre mats produced from PLGA (A) and PLGA-PLL (C). The arrows point out the droplets formed during electrospinning of PLGA-dH_2O emulsion. The nanofibre mats were produced from emulsions with dH_2O (A) and PLL in dH_2O. Scale bar=50µm.

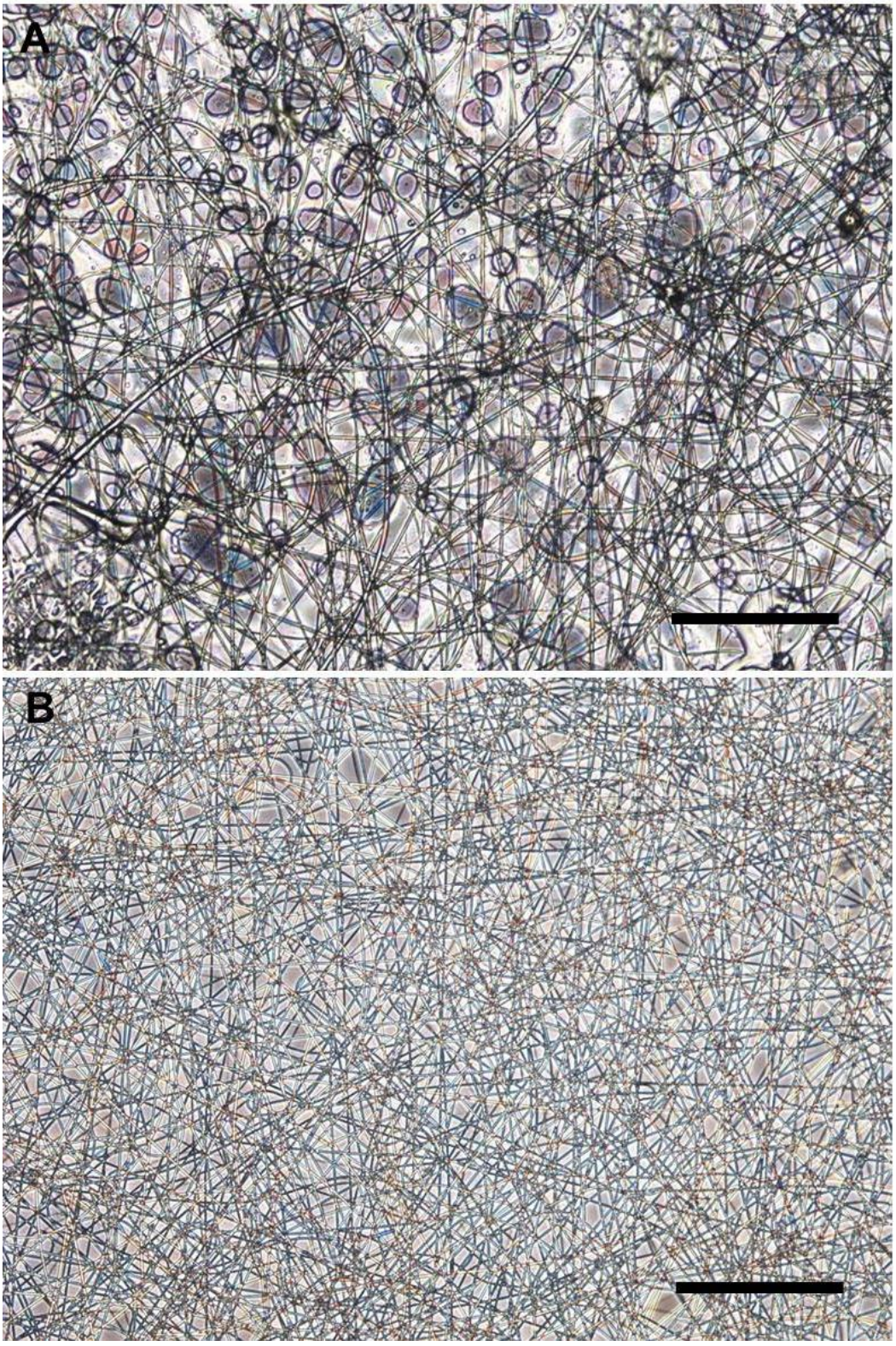

Figure 7.3 Incorporation of Span80 results in droplet deposition. PLGA nanofibres electrospun with (A) and without (B) Span80. Scale bar=100μm.

To conclude, PLGA-dH_2O and PLGA-PLL nanofibres were produced and analysed verifying the presence of PLL using fluorescence labelling. As the addition of dH_2O to PLGA polymer solution resulted in bead formation these samples were not used for cell culture studies, but PLGA only fibres were, as those fibres had a more uniform morphology. Samples produced with Span80 were also excluded from further experiments due to droplet deposition within the fibrous mats.

7.4 Effect of incorporated molecules on nanofibre diameter

In order to quantify the morphology of the nanofibre mats, the fibre diameter was measured to establish whether incorporation of the different molecules had an effect. The electrospinning settings were kept the same for each emulsion, i.e. applied voltage of 15kV, flow rate of 2ml/h, and needle-collector distance of 11cm. SEM images of electrospun nanofibres were taken and analysed using ImageJ (Fig 7.4). Four images per sample were analysed and three diameter measurements per fibre were recorded. The measurements were analysed using Microsoft Excel and the results are presented in Figure 7.5. Electrospinning PLGA resulted in the thinnest fibres with a mean diameter of 576±158nm, and the thickest fibres were produced with PLGA-PLL with a median diameter of 825±187nm. The nanofibres produced using the PLGA-PLL emulsion had a significantly larger fibre diameter than those produced using PLGA ($P<0.001$). The final concentration of PLL in the electrospinning solution was 0.053mg/ml. Theoretically, at a feeding rate of 2ml/h and with 1ml electrospun after 30min, 0.053mg of PLL were incorporated into each sample of 105mg of polymer, and 0.505µg of PLL per 1mg of produced PLGA scaffold. As no other parameter except the solute was changed, the fibre diameter increase can only be attributed to the presence of PLL. When electrospinning emulsions it was expected that thinner fibres would be obtained compared to non-emulsions, as the water phase reduces the viscosity of the solution which was not the case here.

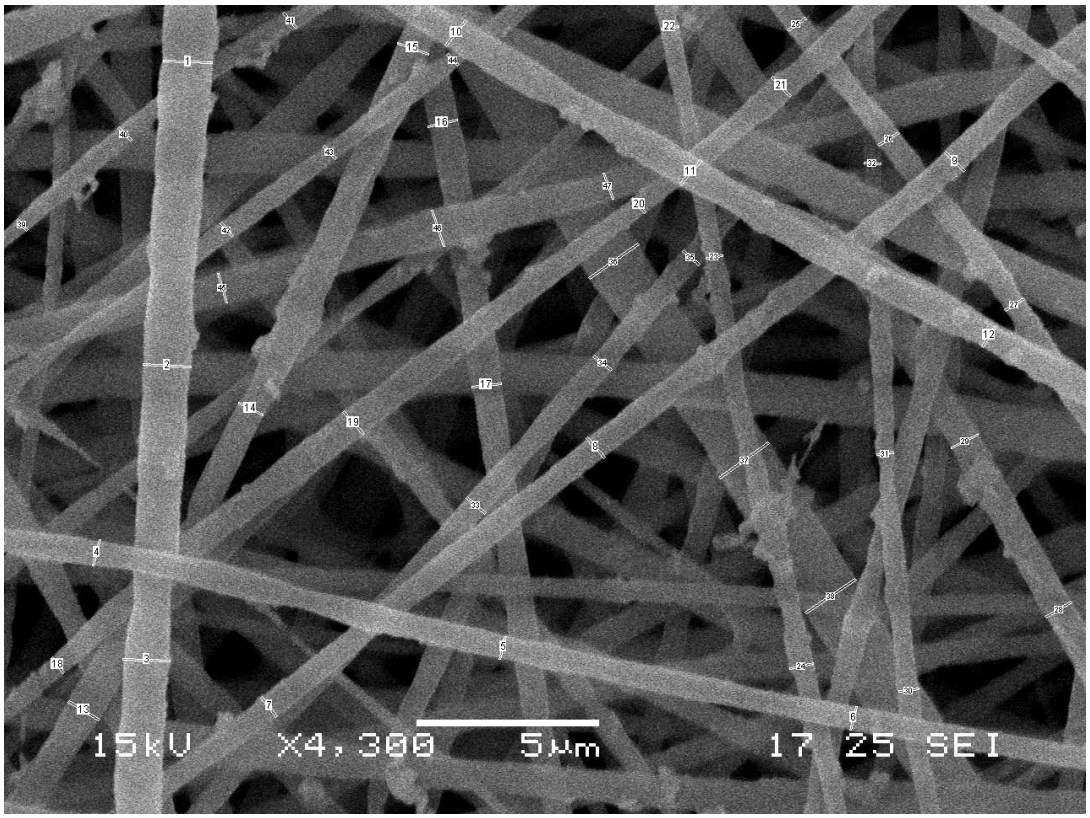

Figure 7.4 Analysis of nanofibre diameter. SEM images of PLGA and PLGA-PLL nanofibres were imported into ImageJ. The scale was set and at least three measurements per fibre (white-numbered lines) were recorded, with ten images being analysed per sample solution. The recorded data was processed using Microsoft Excel.

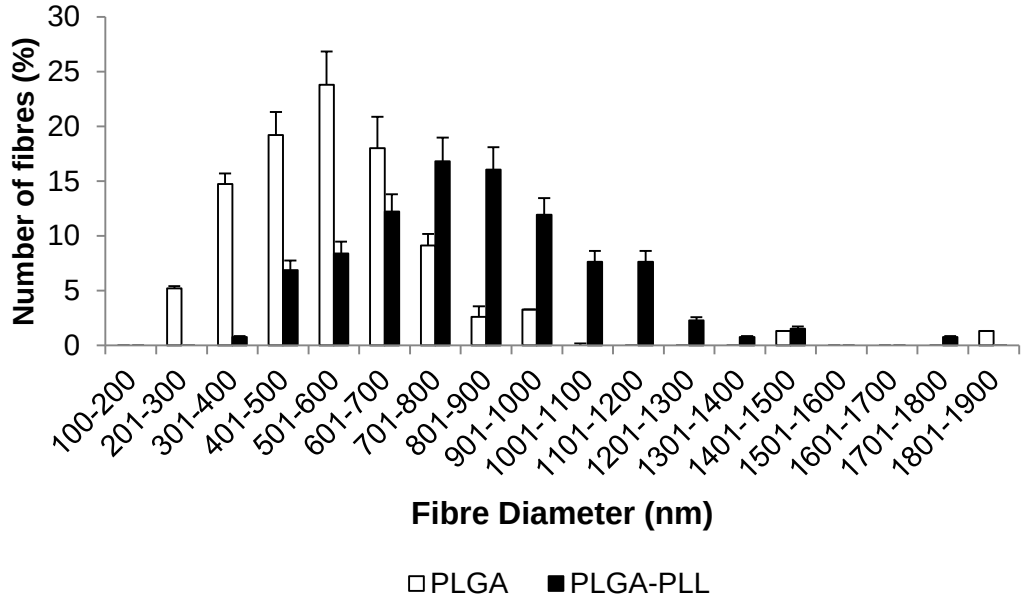

Figure 7.5 Fibre diameters of modified PLGA nanofibres. 10 random SEM images of the electrospun PLGA and PLGA-PLL fibrous mats were taken per sample with a minimum magnification of 4000x. Fibre diameter analysis was conducted using ImageJ, analysing a minimum of 30 fibres per image.

Sy and co-workers argue that in order to produce thinner fibres, the addition of a water phase is sufficient as viscosity dropped from 0.113PaS (20% w/w PLGA in chloroform) to 0.02PaS (2.5 vol % aqueous phase for the 10% (w/w) system) (Sy et al., 2009), which is a fourfold drop in viscosity for reducing the polymer concentration by factor two. In the current research, the fibre diameter did not decrease and it even increased with the addition of PLL by circa 250nm on average. PLL can also have an effect on fibre diameter and morphology changes (less beading), which can be explained by increased conductivity of the polymer solution (Kenawy et al., 2002).

To conclude, the addition of PLL to the electrospinning solution resulted in a 250nm diameter increase of the resulting electrospun nanofibres.

7.5 Hydrophilicity of electrospun PLGA nanofibre mats

In order to establish the effect of incorporated molecules on the hydrophilicity of the nanofibre mats, the water contact angles of PLGA and PLGA-PLL nanofibres were compared. A 5µl droplet of distilled water was deposited on the scaffolds's surface and an image was obtained (Fig. 7.6 A+B), followed by analysis using ImageJ. The contact angles measured were 120°±2° for PLGA and 117°±13° for PLGA-PLL nanofibres (Fig 7.6 C). Contact angles did not show any significant difference from each other indicating no effect of the incorporated substances on hydrophilicity of the nanofibrous mats ($P>0.05$).

The bigger error bar for PLGA-PLL can be attributed to the incorporation of PLL. Although the fluorescent image shows an even distribution of fluorescent fibres and consequently FITC-PLL (Fig. 7.1) only a small amount of PLL was labelled. It is possible that the non-labelled PLL formed aggregates throughout the fibres leading to a non-even distribution and leading to variances between the measurements.

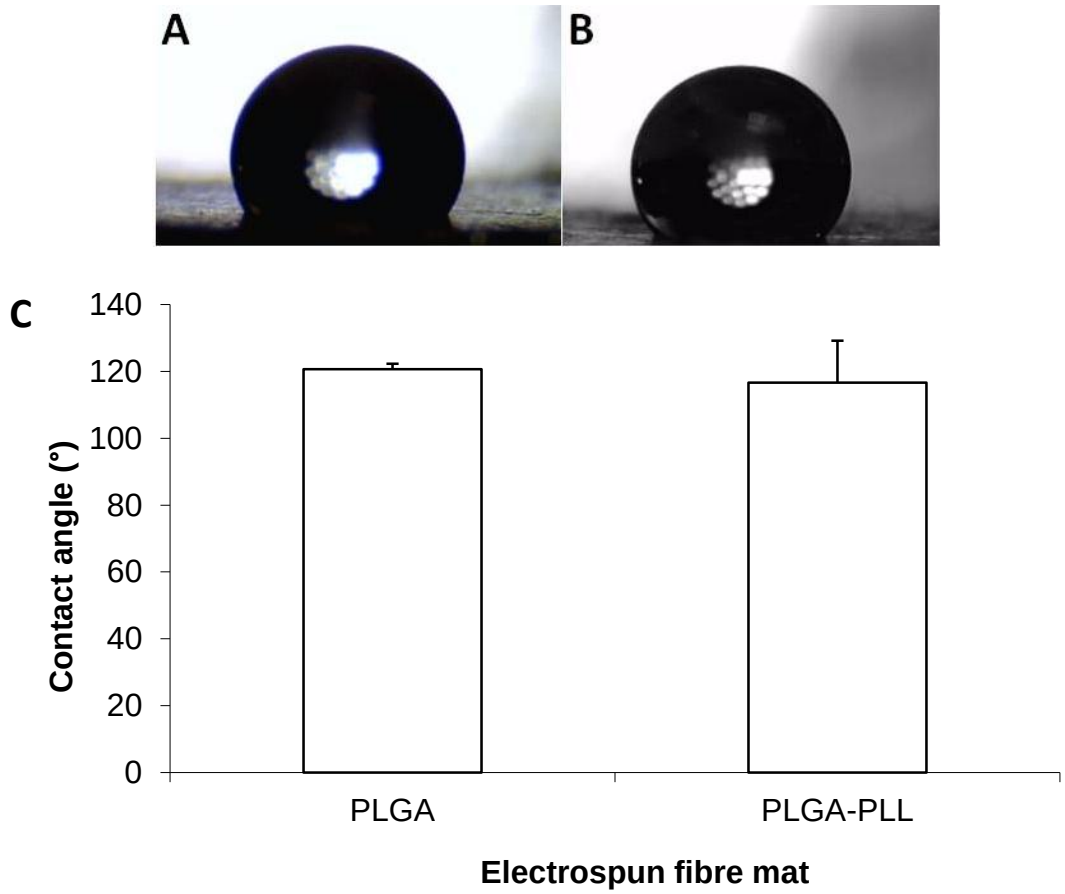

Figure 7.6 Water contact angle of electrospun PLGA nanofibre mats. Distilled water was deposited onto the surface of fibre mats consisting of PLGA (A) and PLGA-PLL (B). The contact angles measured for PLGA were 120°±2° and 117°±13° for PLGA-PLL fibres (C). Images were analysed using ImageJ software. Contact angle for the samples did not show any significant difference (Student's t-test, P>0.05) indicating no effect of the incorporated substances on hydrophilicity of the fibrous mats.

These results imply that the incorporated molecules had little effect on the hydrophilicity of the nanofibre mats. The lack of contact angle change can be explained by the fact that the bulk of incorporated molecules were encapsulated inside the fibre and none or a small amount of functional groups were present on the surface. It was attempted to quantify the amount of FITC-PLL in the nanofibres using infrared measurement and NMR but the results were inconclusive. One of the obstacles was the dilution of the sample for the procedures and filtration of non-diluted parts which may have resulted to removal of PLL from the samples. A solid-state NMR may be attempted making further dilutions of the polymer sample not necessary eradicating further potential degradation. Other methods to detect PLL include using high-performance liquid chromatography (HPLC) and ninhydrin

(triketohudrindene hydrate) colorimetric method which leads to oxidative deamination of alpha-amino groups resulting in a purple substrate that absorbs maximally at 570nm.

A report by Lamour and colleagues claimed that glass coated with PLL has a contact angle of 0°, thus PLL should improve the hydrophilicity of the polymer and decrease the contact angle (Lamour et al., 2009). This was not confirmed with the results achieved in this study. This was probably due to the small amount of PLL used, being not enough to result in contact angle decrease.

In the past, encapsulation of, for example, gelatin within PCL (Zhang et al., 2004) and BSA-PEG within PCL (Zhang et al., 2006) was only achieved by coaxial electrospinning (Zhang et al., 2004) and same solvent systems (polymer and the encapsulated molecule where dissolved in the same solvent), whereas recently, it has been reported that core-shell structures were created using emulsion electrospinning (Xu at al., 2006). Xu and co-workers have created core-shell structures by electrospinning a water-in-oil emulsion in which the aqueous phase consisted of a poly(ethylene oxide) (PEO) solution in water and the oil phase consisted of a poly(ethylene glycol)-poly(L-lactic acid) (PEG-PLA) diblock copolymer in chloroform solution. The PEO was encapsulated within the fibre with a clear boundary between the aqueous and oily phases. In order to investigate where the same was true for PLL, it would be indispensable to visualise PLL within the fibres. As PLGA is not transparent visualisation of fluorescent molecules within the fibre is difficult. There may be structural differences present within the fibres which can be investigated using SEM and transmission electron microscopy (TEM).

Taking everything into consideration, it should not be forgotten that fluorescent PLGA-PLL fibres were obtained (Fig. 7.1) indicating that PLL may be present throughout the fibre, within as well as on the surface.

7.6 Cell attachment to poly-L-lysine-containing PLGA nanofibres

After completing the characterisation of the nanofibre mats, work proceeded to cell attachment studies. For this, PC12 cells were seeded onto the polymer nanofibre

mats at a density of 50,000 cells/cm^2 and left to attach for 4 h, the standard time for cell attachment experiments throughout this work. Prior to seeding, cells were stained with Vybrant cell tracker and after attachment images were taken of cells on the polymer nanofibres using fluorescent microscopy. These images were analysed using the plug-in “cell counter” in ImageJ.

Cell attachment results are presented in figure 7.7. Cell attachment to PLGA and PLGA-PLL fibre mats were not significantly different from each other with 17±7% and 20±11% of seeded cells, respectively. When comparing results from previous chapters it becomes apparent that cell attachment did not increase when comparing PLGA flat sheet membranes to electrospun PLGA with 20±7% of seeded cells attaching to PLGA flat sheet membranes which is not significantly different to 17±7% ($P>0.05$).

PLL is known to enhance adsorption of serum or ECM proteins to the culture substrate, which results in increased cell attachment (McKeehan 1984). Cell adhesion to PLL is non-specific; it is the result of the negatively charged cell membrane which binds to the highly positive surface charge provided by PLL. It is possible that the amount of PLL present in the nanofibrous sample was not sufficient to increase cell attachment or that the majority of PLL was trapped within the nanofibres.

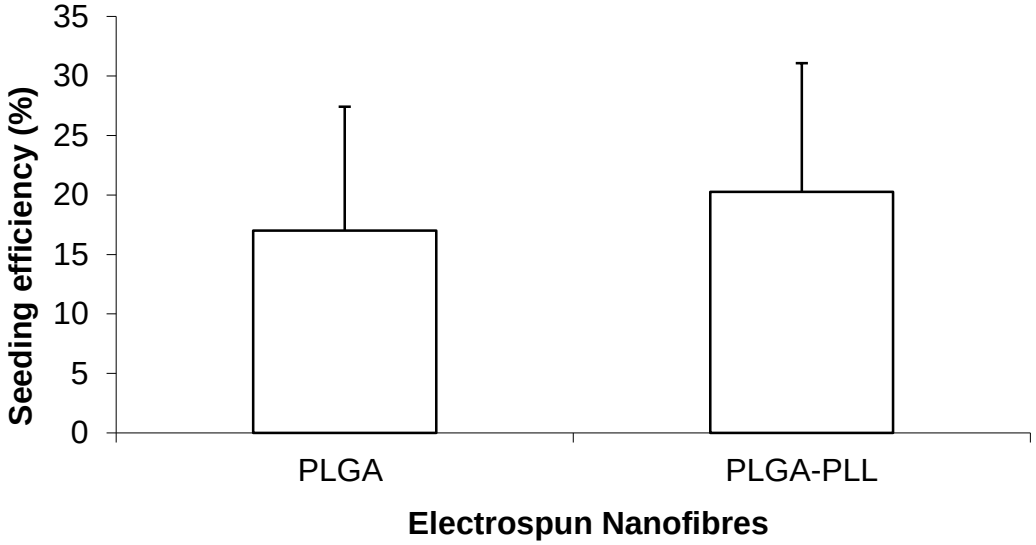

Figure 7.7 Cell seeding efficiency on electrospun PLGA and PLGA-PLL nanofibre mats. PC12 cells attach equally to PLGA and PGLA-PLL fibres. Data represent the mean ± SEM (n=4) and was analysed using the Student's t-test (P>0.05).

Although cell attachment to PLGA-PLL fibres was not significantly different to PLGA fibres, PC12 cell morphology differed. Cells attaching to PLGA-PLL fibres spread out more than those on PLGA fibres (Fig 7.8), resulting in higher contact surface. This effect may have been due to the PLL in the PLGA-PLL nanofibres which increases the strength of adhesion within a shorter period of time. One way to investigate this effect is to produce PLGA only nanofibres with the same diameter as the PLGA-PLL nanofibres used here and quantify cell spreading of single cells. It is also possible that PC12s might behave the same on PLGA nanofibres as on PLGA-PLL fibres when left to attach for longer than 4 hours.

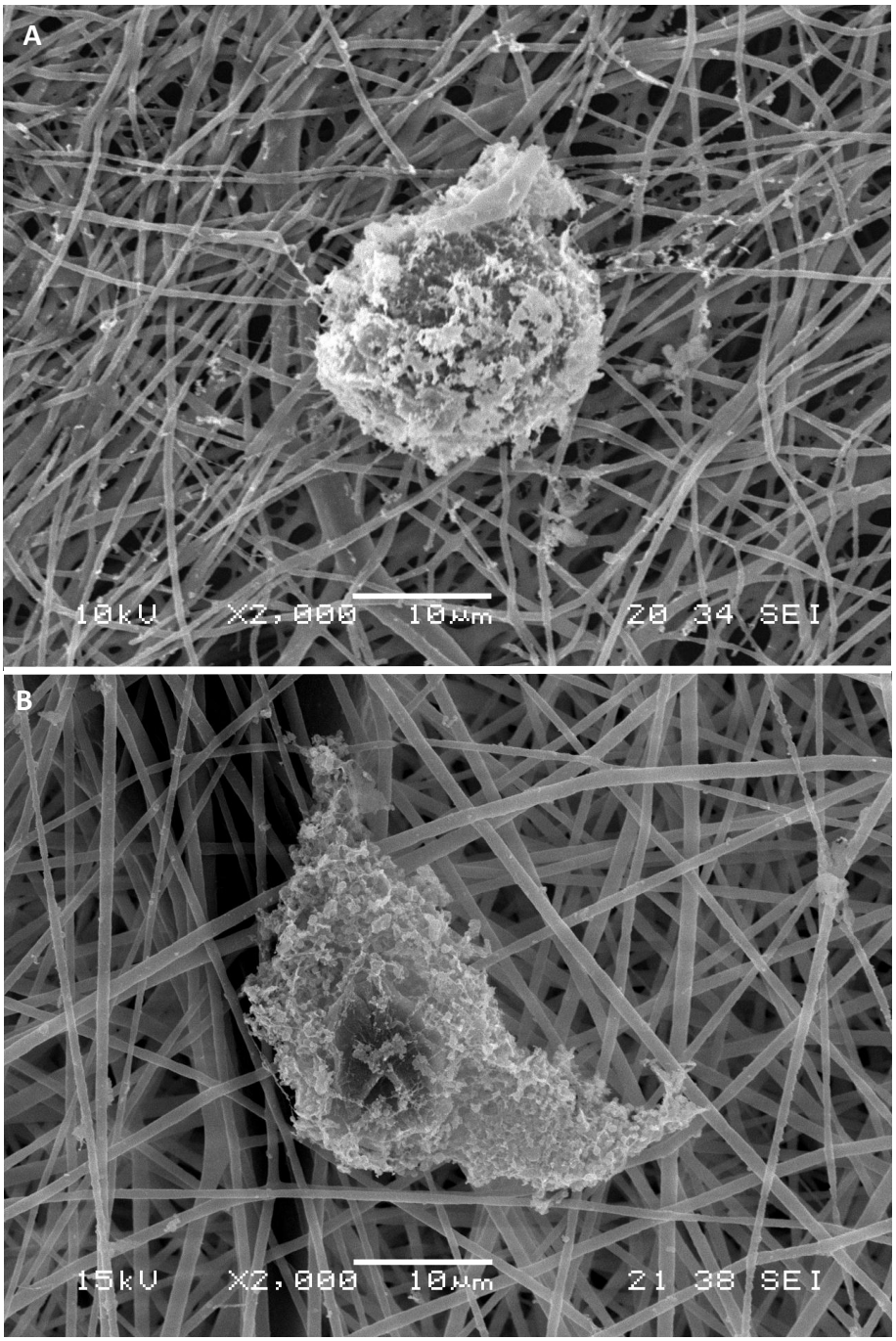

Figure 7.8 PC12 cells on electrospun PLGA and PLGA-PLL nanofibre mats. Representative images of PC12 cells seeded onto nanofibre mats and allowed to attach for 4 h. SEM images revealed that cells on PLGA fibres (A) remained round, whereas cells on PLGA-PLL spread out on the surface and had a higher surface contact (B).

7.7 Differentiation of PC12 cells on modified nanofibre mats

In order to examine differentiation of PC12 cells on modified nanofibre mats, cells were seeded onto the scaffolds and exposed to NGF, which was added to 1% FCS containing culture medium, and allowed to differentiate for seven days. Cells were

stained with calcein AM, ethidium homodimer and Hoechst in order to visualise and analyse the cells using fluorescence microscopy. Additionally, further samples were fixed and stained for SEM analysis.

Qualitative results revealed that although cells did differentiate on both PLGA and PLGA-PLL nanofibres, cells that differentiated on PLGA-PLL extend their neurites into the scaffold, whereas neurites of cells on PLGA remained on the surface of the nanofibre mat (Fig. 7.9). Cells are able to migrate through the porous structure of the scaffold by pushing the fibres to the side and expanding the pore, as the thin fibres offer little resistance thus not preventing cell migration (Li et al., 2002). Penetration of cells into the nanofibres was also observed by others, for example describing fibroblast on gelatin-PCL scaffolds penetrating the scaffold (Zhao et al., 2007). Here, cell bodies were on the surface of the fibrous mat whereas the neurites penetrated the scaffold (Fig 7.9B). Cell migration may have occurred over a longer period of incubation.

PC12 cell differentiation was analysed on random and aligned PLGA and PLGA-PLL nanofibres according to three parameters: number of neurites per cell (Fig 7.10 and 7.11), alignment of neurites along fibres (Fig 7.12 and 7.13) and length of neurites (Fig 7.14 and 7.15). For this, PC12 cells were seeded onto random and aligned PLGA and PLGA-PLL nanofibre mats, and differentiation was induced using NGF.

7.7.1 Number of neurites

The incorporated PLL did not have an effect on the number of neurites per cell (Fig 7.10 and 7.11), with an average number of neurites being 4.3±2.1 and 4.5±1.8 on random fibres and 1.5±0.5 and 1.7±0.3 on aligned fibres for PLGA and PLGA-PLL respectively.

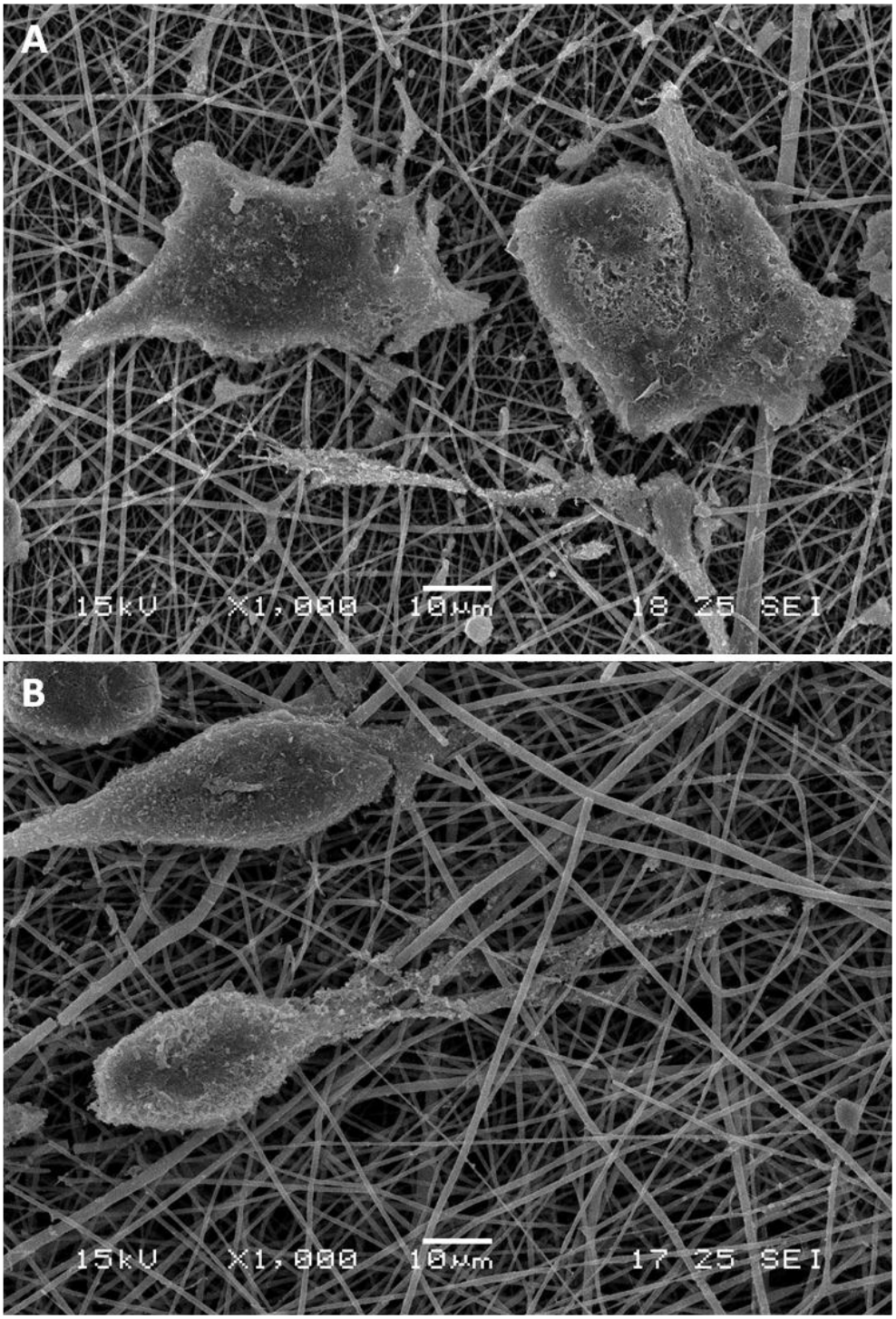

Figure 7.9 Differentiation of PC12 cells on electrospun PLGA and PLGA-PLL nanofibre mats. (A) PC12 cells on PLGA nanofibres. (B) Neurite extension on PLGA-PLL fibres. On PLGA-PLL neurites grow into the scaffold whereas on PLGA fibres neurites stay on the surface of the fibres.

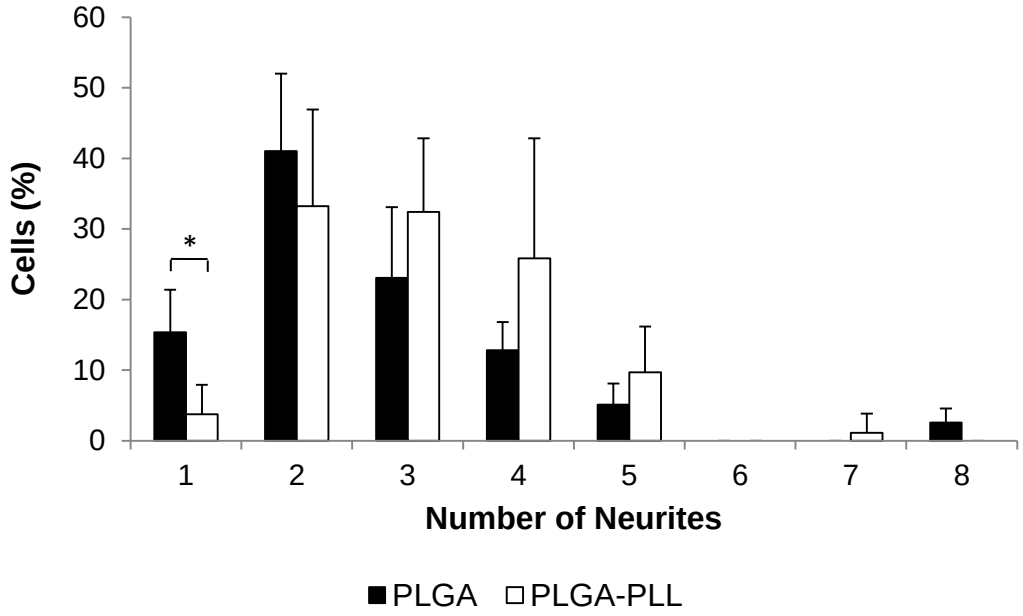

Figure 7.10 Number of neurites on random nanofibres. Number of neurites per cell on random electrospun PLGA and PLGA-PLL fibre mats after 7 days exposure to 40ng/ml NGF. *P<0.05. Data represent the mean ± SEM (n=3) and were analysed using Student's t-test.

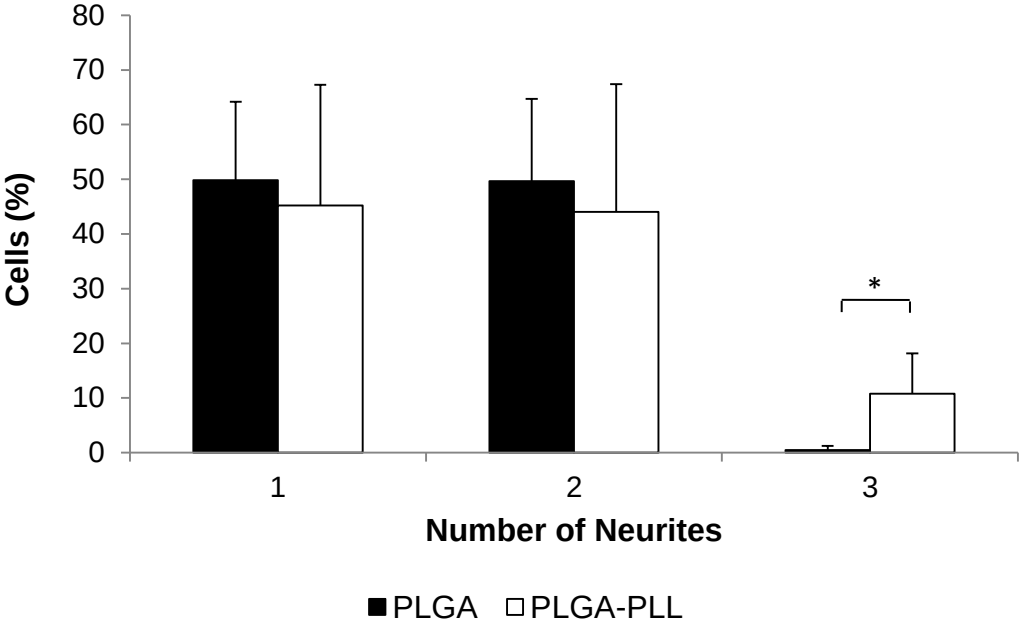

Figure 7.11 Number of neurites on aligned nanofibres. Number of neurites per cell on aligned electrospun PLGA and PLGA-PLL fibre mats after 7 days exposure to 40ng/ml NGF. *P<0.05. Data represent the mean ± SEM (n=3) and were analysed using Student's t-test.

Although no difference in number of neurites between PLGA and PLGA-PLL was established, the number of neurites on random PLGA and PLGA-PLL nanofibres was significantly higher compared aligned PLGA and PLGA-PLL nanofibres (P<0.05).

These results show that PLGA-PLL nanofibres affect neurite sprouting in the same way as PLGA fibres without any neurite sprouting inhibitory/promoting effects. Further statistical analysis revealed that the number of cells with one neurite on random PLGA-PLL nanofibres was significantly lower than on random PLGA nanofibres ($P<0.05$). Additionally, the number of cells with three neurites on aligned PLGA-PLL nanofibres was significantly higher than on aligned PLGA nanofibres ($P<0.05$). It seems that although the average of neurites per cell does not differ significantly, when looking at numbers in more detail it becomes apparent that small differences are present which can be attributed to PLL. It may be that cells seeded on PLGA-PLL nanofibres require less time to grow more than one neurite. Saying that, cells on PLGA nanofibres had the highest number of neurites per cell with eight neurites being the highest number counted in all experiments.

The error bars for all numbers obtained on PLGA-PLL are relatively large indicating high variances within the results. More data could lead to reduction of error bars.

These results indicate that PLL did not influence neurite outgrowth of PC12 cells on electrospun PLGA nanofibres. As PLL is not known to have effects on neurite sprouting these results were not unexpected.

7.7.2 Directional outgrowth of neurites

The alignment of PC12 cell neurites on random and aligned PLGA and PLGA-PLL nanofibres was recorded using ImageJ and analysed using Microsoft Excel. The angle values were established in 15 degree angle bins, with 0 degrees being completely parallel and 90 degrees being completely perpendicular.

The angle distribution of PC12 cell neurites on random fibres indicated no particular directional bias on neither random PLGA nor random PLGA-PLL nanofibre mats ($P>0.05$) (Fig. 7.12). The angle distribution of PC12 cell neurites on aligned fibres show a significant proportion of neurites, 79.2±2.3% on PLGA and 60.6±0.4% on PLGA-PLL, within the ±15 degrees along the 0-180° axis, indicating an alignment of neurites along electrospun fibres as 0° was set as the orientation of electrospun nanofibres (Fig. 7.13).

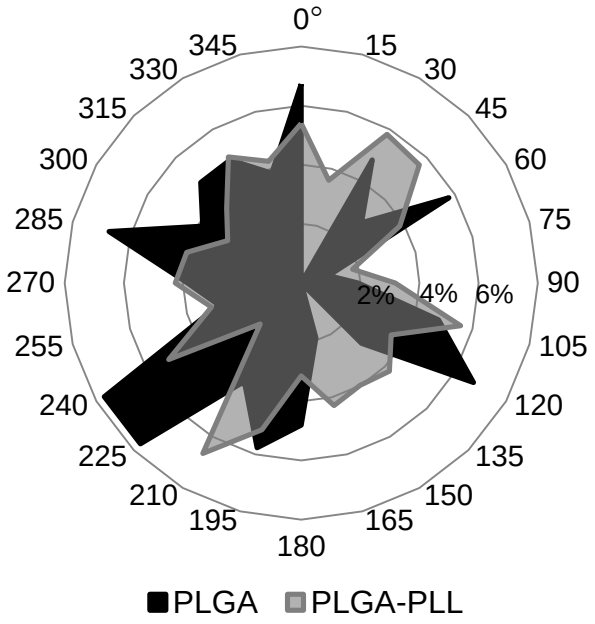

Figure 7.12 Alignment of neurites on random PLGA and PLGA-PLL nanofibres. Number of neurites (%) is presented and their directional outgrowth on random PLGA and PLGA-PLL nanofibres. The angle values were established in 15 degrees angle bins, with 0 and 180 degrees being completely parallel and 90 and 270 degrees being completely perpendicular. The angle distribution of PC12 cell neurites on random nanofibres indicated no particular directional bias. Data represent the mean (n=3) and were analysed using Student's t-test.

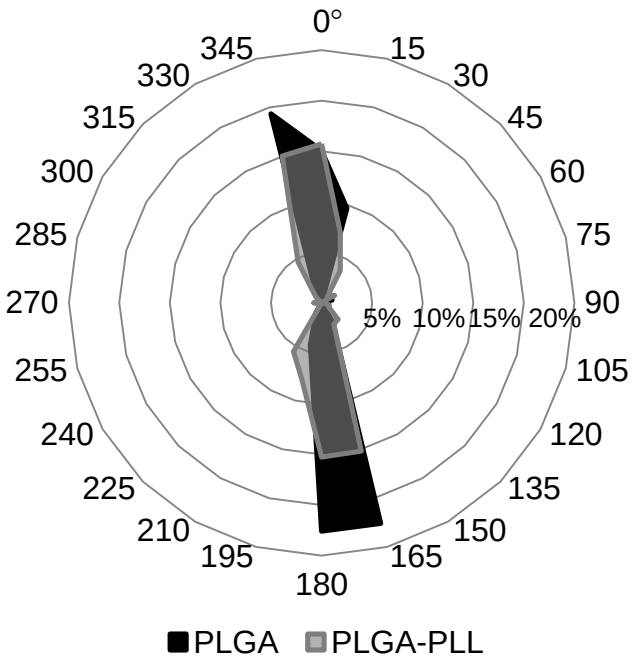

Figure 7.13 Alignment of neurites on aligned PLGA and PLGA-PLL nanofibres. Number of neurites (%) is presented and their directional outgrowth on aligned PLGA and PLGA-PLL nanofibres. The angle values were established in 15 degrees angle bins, with 0 and 180 degrees being completely parallel and 90 and 270 degrees being completely perpendicular. The angle distribution of PC12 cell neurites on aligned nanofibres indicated directional outgrowth. Data represent the mean (n=3) and were analysed using Student's t-test.

7.7.3 Analysis of neurite length

The next step was to analyse the length of neurites. On random nanofibres the neurites extended for 59±33µm on PLGA and for 113±11µm on PLGA-PLL nanofibres (Fig 7.14). On aligned nanofibres neurites reached mean lengths of 132±85µm on PLGA and 251±30µm on PLGA-PLL nanofibres, nearly a two fold increase in mean neurite length (Fig 7.15). The number of neurites with the length between 0 and 100µm is significantly higher on PLGA compared to PLGA-PLL ($P<0.01$), whereas the number of neurites between the length of 101 and 400µm is significantly higher on PLGA-PLL nanofibres ($P<0.01$).

The results indicate that the PLGA-PLL nanofibres positively influenced neurite sprouting from PC12 cells. The number of neurites on PLGA and PLGA-PLL fibres does not differ significantly from each other thus cannot explain the longer neurites. It may be possible that neurite outgrowth on PLGA-PLL is accelerated and neurites on PLGA will reach the same length, but require more time.

To date, there are no reports in the literature describing the effect of PLL on neurite outgrowth. But lysine is a component of the pentapeptide epitope isolucine-lysine-valine-alanine-valine (IKVAV), which is found in laminin and is known to promote neurite sprouting and neurite outgrowth (Silva et al., 2004). Laminin has also been conjugated with lysine to control attachment of hippocampal neurons (Kam et al., 2001). Unfortunately controls have shown that hippocampal neurons extended neurites on lysine-laminin but not on lysine patterned surfaces. On the other hand, hippocampal cells were seeded onto 2D glass surfaces with micro-scale patterns of PLL-conjugated laminin whereas PC12s were grown on a 3D surface, which might affect the differentiation process. Of course it has to be considered that the effect of PLL may be specific to PC12 cells and as there are not comparative reports published, it is difficult to compare the data.

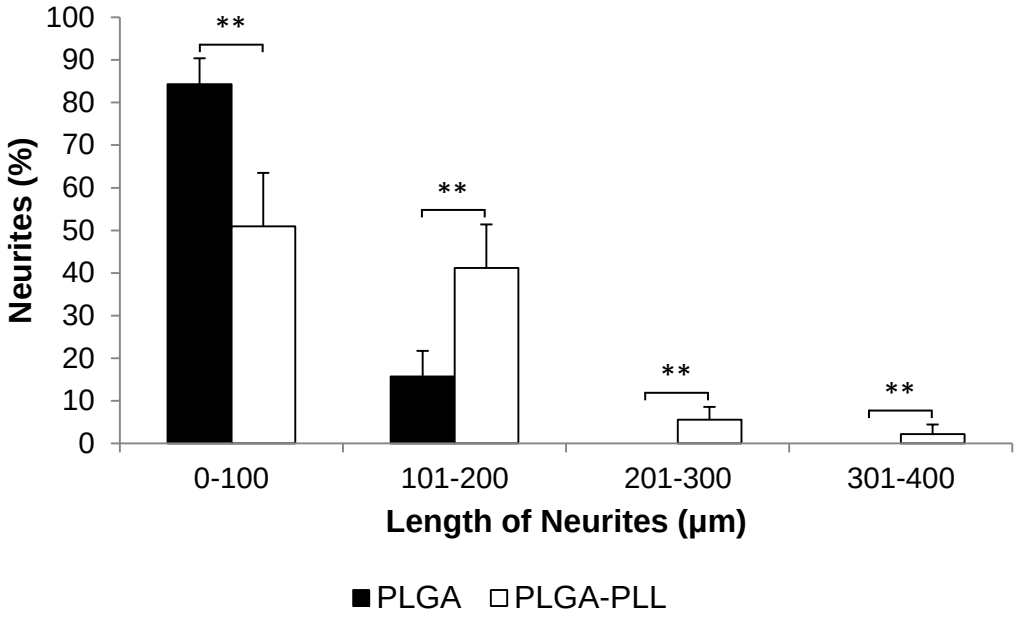

Figure 7.14 Neurite outgrowth is enhanced on random electrospun PLGA-PLL nanofibres. The length of neurites on random PLGA and PLGA-PLL nanofibres was measured after 7 days exposure to NGF. 10 random images were taken per sample. The average length of neurites on PLGA was 59±33µm and 113±11µm on PLGA-PLL fibres. Data represent the mean ± SEM (n=3) and were analysed using Student's t-test. **P<0.01.

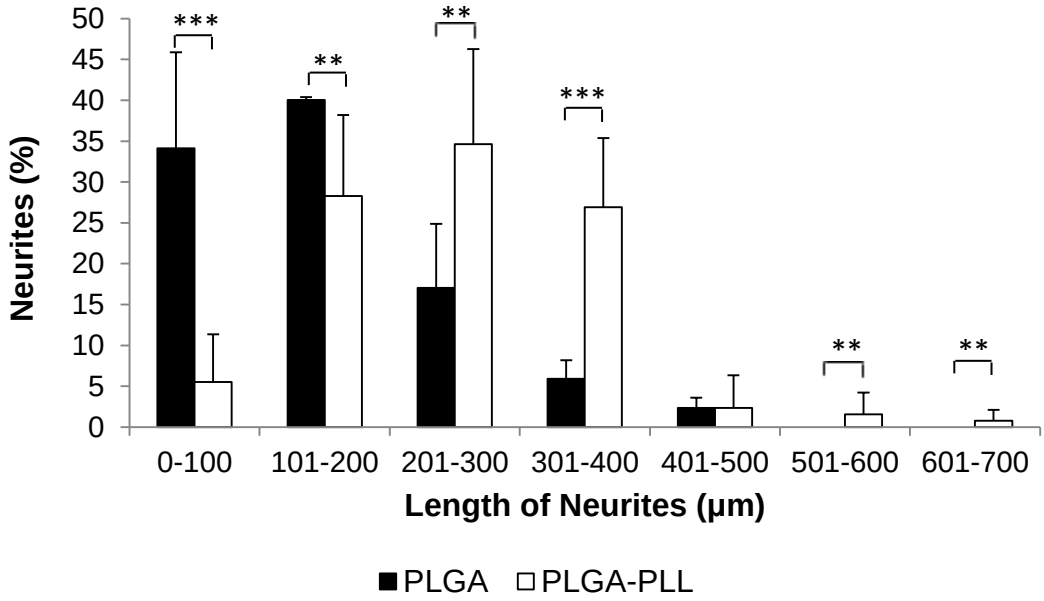

Figure 7.15 Neurite outgrowth is enhanced on aligned electrospun PLGA-PLL nanofibres. The length of neurites on aligned PLGA and PLGA-PLL nanofibres was measured after 7 days exposure to NGF. 10 random images were taken per well. The average length of neurites on aligned PLGA fibres is 132±85 µm and on PLGA-PLL nanofibres 251±30µm, clearly showing the positive effect the PLGA-PLL fibres have on neurite outgrowth. Data represent the mean ± SEM (n=3) and were analysed using Student's t-test. ** P<0.01, ***P<0.001.

It has been reported that positive surface charge has no effect on cell attachment of mouse neuroblastoma cells (Nb2a) but resulted in significantly higher levels of neurite outgrowth (Makohliso et al., 1993), indicating that cells other than PC12s are affected by PLL. In addition, Tombran-Tink and Johnson reported that poly-D-lysine (PDL) initiates neuronal differentiation of Y79 human retinoblastoma cells (Tombran-Tink and Johnson, 1989). PDL and PLL do not differ other than chirality, suggesting that PLL may have the same effect as PDL on Y79 cells. Lysine-alanine sequential polymer was shown to have a significant effect on process outgrowth of neural stem cells (Wang et al., 2006). Blending PLL into chitosan films resulted in higher cell attachment and higher degree of differentiation of PC12 cells compared to non-modified films (Mingyu et al., 2004). 65% of the seeded PC12 cells attached to the chitosan-PLL films compared to chitosan only films.

All these reports suggest that lysine may play a role in differentiation, but only in combination with laminin or other amino acids. This raises the question if other factors such as topography provide a means of differentiation.

7.8 Further considerations

The results presented in this chapter are promising for future therapies showing the potential of using electrospinning. Although this form of experiments was a good choice for *in vitro* studies, for *in vivo* experiments the scaffold has to fill the injury site thus has to be bigger resembling the void at the site of injury. For this a further factor for consideration can be the fixing of fibres in order to facilitate the processing such as submerging in media and for handling during implantation experiments.

In this study nanofibrous mats were cut to size and placed in tissue culture well plates retained by silicon rings. Although this is a good means for cell culture studies, for further experiments the scaffolds have to be securely fastened or fixed to a substrate or to itself via a non-toxic adhesive. Adhesive bandages (Corey et al., 2007), biocompatible “super glues” (Sun et al., 2007) and silicon glues (Yang et al., 2004) have been investigated. This role can be taken up by a polymer instead, which

means that the polymer only requires fastening during cell seeding. Also Corey and colleagues have shown that bandage, silicon and super glue are toxic to the neuronal types in serum free conditions (Corey et al., 2008). Ethanol can be used as fixative for PLGA. Although it leads to degradation of the scaffold, short exposure acts like glue and the degradation is limited. A preliminary test has confirmed the successful use of ethanol when fixing electrospun PLGA nanofibres on PLGA flat sheet membranes.

Electrospinning of emulsions is a fairly new technique with only a handful of publications to date, including electrospinning solutions where the water phase is added to the oil phase by droplets (Xu et al., 2006, Su et al., 2009) or the other way round (Angeles et al., 2008). For example, Xu and colleagues have electrospun poly(ethylene oxide) as the aqueous phase in chloroform solution containing the amphiphilic poly(ethylene glycol)-poly(lactic acid) diblock copolymer (Xu et al., 2006). On the other hand, Su and colleagues incorporated BSA into poly(l-lactide-cocaprolactone) nanofibres (Su et al., 2009). More importantly, it has been shown that emulsion electrospinning is an effective method to load drugs and functional substances into the nanofibre scaffolds (Xu et al., 2006, Xu et al., 2008, Liao et al., 2008).

Further investigations in close partnership with surgeons into handling methods of the produced scaffold are necessary in order to guarantee non-destructive handling of the scaffold.

7.9 Conclusion

In this chapter, it has been shown that incorporation of PLL is possible through emulsion electrospinning. This is the first study that reports the incorporation of PLL into electrospun PLGA nanofibres using electrospinning of emulsions. Additionally, the resulting PLGA-PLL fibres support cell attachment and differentiation of PC12s compared to PLGA only fibres. PLL is a poly peptide promoting adhesion of PC12 cells to various surfaces. It was shown that PLL in combination with a nanofibre surface significantly influences neurites outgrowth of PC12 cells resulting in neurites

up to 400µm in length. Importantly, emulsion electrospinning is a useful and easy method to modify biomaterials to produce biomimetic scaffolds with both biochemical and topographical cues.

8. GENERAL DISCUSSION

8.1 Introduction

Nerve injury, particularly to the central nervous system, can have traumatic consequences such as permanent disability due to loss of motor function. Many scaffold designs have been utilized in order to promote the growth of neurons across areas of nerve injury, bridging the gap created by trauma and offering a permissive environment for neuronal extension. PLGA has been widely used as a scaffold material for tissue engineering applications, as it is biodegradable, biocompatible and FDA approved. However, cell adhesion and growth can be hampered due to the lack of natural adhesion sites on the polymer. The aim of the project was to test PLGA for its ability to support cell adhesion, proliferation and differentiation of nerve cells. PLGA flat sheet membranes were the starting point providing physical support for cells while evaluating its cytocompatibility with PC12s. Furthermore, PLGA flat sheet membranes were modified in order to improve cell adhesion, using aminolysis, covalent attachment of adhesive peptides and ozonation. Additionally, it was demonstrated that aligned PLGA nanofibres are a suitable scaffold for nerve tissue engineering applications and their biological properties can be improved by incorporating poly-L-lysin (PLL) in the polymer matrix.

8.2 PLGA flat sheet membranes

Tissue engineering aims to develop and use biomaterials which are biocompatible with the tissue of interest. This means that these materials have characteristics which reflect the target tissue, including, cytocompatibility, genototixicity and inflammatory response. In order to increase cytocompatibility of biomaterials new techniques for surface modification post scaffold formation are being developed.

PLGA flat sheet membranes have previously been tested for bone cell lines and were now firstly evaluated with PC12 cells, a neuronal model cell line. It is clear from the data presented in chapter 4 that PLGA in the form of a flat sheet membrane is not sufficient for cell attachment of PC12 cells as attachment did not exceed 20±7% of seeded cells which is very low compared to numbers achieved on

TCP-PLL (69±12%) and with osteogenic and human bone derived cells where cell seeding efficiencies of 65-75% were achieved (Ellis and Chaudhuri, 2007, Ellis and Chaudhuri, 2008). The lack of attachment was not entirely unexpected as PC12 cells require coatings of TCP with for example PPL prior to seeding, a standard polystyrene surface for cell culture to which many cells attach without any additional coating.

Various surface modifications including aminolysis, peptide modification and ozonation, were tested on PLGA flat sheet membranes in order to increase cell attachment. Only the oligopeptide was used for peptide modification as the addition of ECM components to the scaffolds has some limitations including non-uniform adsorption and reproducibility (Park et al., 2007). Although, various short sequences derived from ECM components such as laminin and collagen have been shown to increase cell adhesion the exact cell-ECM interactions are still not fully understood. Further advance in this area might be achieved using ECM microarrays which will help to understand the cell-ECM and cell-material interactions (Flaim et al., 2005).

Cell attachment is an indirect indicator for successful surface modification, if it is assumed that successful surface modification automatically results in higher cell attachment. As higher cell attachment was not achieved it was assumed that surface modification was not successful, although this should be confirmed in future work. One of the weak points of chapter 4 is the lack of proof for successful surface modification other than cell attachment, quantification of surface roughness and wettability studies. It was not investigated how many amine and YIGSR-peptide groups were present on the surface of PLGA flat sheet membranes thus it is not possible to rule out a successful polymer modification without any effect on PC12 cell attachment behaviour, but the investigation of this possibility is discussed in Chapter 9.

Although the modifications were not successful in increasing cell attachment, they were a legitimate choice, as for example aminolysis was shown to increase

cytocompatibility of polycaprolactone for human endothelial cells (Zhu et al., 2002) and peptide modification of chitosan, by immobilisation of the YIGSR pentapeptide, increased cell attachment and neurite penetration of rat superior cervical ganglion neurons (Yu et al., 2007).

Despite low cell attachment results, PLGA flat sheet membranes can be used for other cell lines (e.g. bone) where this material is already widely used and higher cell attachment was achieved. Additionally, PLGA flat sheet membranes are robust to handling and do not tear easily, which offers an advantage for implantation procedures. That is why PLGA flat sheet membranes should not be ruled out as scaffolds for CNS applications but further investigated for combination with different scaffold structures, for example with electrospun nanofibres.

8.3 PLGA nanofibres

Although the results obtained from work with PLGA flat sheet membranes were disappointing, PLGA as a polymer has great advantages in terms of ease of process, biocompatibility and degradation rate and was further investigated in terms of producing different types of scaffolds. To date, electrospinning has been used to electrospin various polymers. The aim of electrospinning is to produce nanofibres which mimic the ECM environment, especialy collagen fibres which are 500-3000nm in diameter, thus increasing the cytocompatibility of biomaterials. 90% of the interstitial matrix of the ECM consists of collagen. Collagen molecules comprise of three polypeptide chains forming a triple helix of 300nm in length and 1.5nm in diameter. These collagen molecules spontaneously self-assemble into fibrillar collagens which then form larger fibrillar bundles (Kadler et al., 1996). On the negative site, research has shown that collagen IV is present in the glial scar and serves as binding site for growth-promoting factors as well as inhibitory molecules and the inhibition of collagen IV results in axonal regeneration and functional recovery in the spinal cord (Klapka and Muller, 2006). As electrospun nanofibres mimic the physical structure and not the amino acidic sequences of collagen they are unlikely to have inhibitory characteristics.

The data presented in chapter 5 has shown that electrospinning parameters can be adjusted to the polymer of interest, in this case PLGA, and random and aligned nanofibres can be produced by choosing different collectors. Various parameters such as the viscosity of the electrospinning solution, applied voltage and collector-to-needle distance were in correlation with the literature. Although the parameters discussed in chapter 5 were optimized for a 10% (w/w) PLGA in $CHCl_3$:MeOH (3:1) solution and the ambient parameters present in the laboratory at the point of execution, these parameters are only valid for the laboratory and the equipment used as laboratory equipment as well as ambient parameters vary in different laboratories. This is a problem when attempting to reproduce results. Most problematic was the investigation of the optimum solvent, as DMF and THF were reported to be the solvent of choice for PLGA (Li et al., 2006, Nisbet et al., 2007, Zhao et al., 2008, Bini et al., 2004, You at al., 2006) but did not result in uniform nanofibres without bead formation. This shows that electrospinning, although requiring a simple setup, is a sensitive technique, where parameters need adjustment in relation to each other and the environment. Nevertheless, it is a promising technique, especially for neural regeneration applications where aligned nanofibres affect cell attachment behaviour and orientation of neural and Schwann cells (Seidlits et al., 2008, Schnell et al., 2007) and as demonstrated in the work presented here increase neurite outgrowth of neuronal model cell line (chapter 6 and 7).

For further modification of the scaffold PLL has been incorporated into electrospun PLGA nanofibres using electrospinning of an emulsion. Theoretically, this form of scaffold modification is not restricted to the surface as PLL is added to the electrospinning solution prior to fibre formation. Although PLL is used to coat TCP prior to seeded of PC12 cells in order to increase cell attachment, attachment of PC12s did not increase on PLGA-PLL nanofibres (20±11%) compared to PLGA nanofibres (16±10%), PLGA flat sheet membranes (20±7%) and PLGA flat sheet membranes coated with PLL (23±14%).

The incorporation of PLL into electrospun PLGA nanofibres is a novel approach and has not been shown before. PLL incorporation resulted in larger fibre diameter, 825±187nm compared to 530±140nm for PLGA nanofibres. It is not clear from the current state of research which fibre diameter is optimum for spinal cord repair, thus it cannot be assumed that the increase of 295nm will have a negative effect on regeneration. If there is a negative effect this can be outweighed by the increase in neurite outgrowth achieved on PLGA-PLL nanofibres from 59±33µm to 113±11µm on random PLGA-PLL nanofibres and from 132±85µm to 251±30µm on aligned PLGA-PLL nanofibres. This effect achieved by PLL has not been previously reported.

Although electrospinning has potential there are still many challenges that have to be overcome. A major one is the fabrication of complex scaffolds. At the moment work focuses on nanofibrous mats. This mat-structure does not represent complex 3D tissue structures as cells are only seeded on the surface. The next step is to take the lessons learned on nanofibrous mats and apply them to highly complex 3D scaffolds which are representative of the host tissue. Factors such as mechanical strength of the scaffold, cell survival within the scaffold and nutrients supply to the cells within the scaffold need to be investigated in order to take electrospun scaffolds to the next level and produce structures such as tubes. There is clearly the need to move forward, but it is necessary to analyse effects of nano-architecture, functionalization and interfacial properties on cell behaviour first.

It is likely that electrospinning will be of interest for future research; especially further modifications of nanofibres to improve encapsulation of bioactive molecules. After the work presented here was finished various papers appeared presenting data about encapsulated molecules, such as proteinase K in poly(ethylene glycol)-poly(L-lactide), and more relevant to nerve regeneration, poly(L-lactide-co-caprolactone) fibrous mats with encapsulated NGF (Xu et al., 2010, Li et al., 2010b, Li et al., 2010a). In this manner other substances can be encapsulated into the electrospun fibres and applied to other tissues as well as to the nervous system. Furthermore, patents were filed for electrospun PLGA

nanofibres as drug delivery (Griswold et al., 2011) and cell delivery vehicles (Arinzeh et al., 2010).

8.4 CELL CULTURE STUDIES

Cell adhesion is the most important factor in tissue regeneration as interactions of cells with their surroundings can determine the cell fate. For example, it has been shown that cells need a minimum surface area in order to survive (Chen and Hunt, 2007) and the nature of the surface area may control the formation of contacts with the surroundings (Chen et al., 2003).

On an artificial surface such as biomaterials the process of attachment proceeds in four steps (LeBaron and Athanasiou, 2000): (1) initial cell attachment, (2) cell spreading, (3) organization of actin cytoskeleton and (4) formation of focal adhesions. The initial cell attachment creates physical contact between cells and surface preventing cell detachment when exposed to minor shear stresses. This is followed by flattening or spreading of the cell on the surface area. Spreading is followed by actin reorganisation which results in formation of microfilament cytoskeleton bundles. Finally, integrins link the cells to the components of the extracellular matrix (ECM).

It is well known that cell-cell and cell-EMC interactions are vital for tissue regeneration (Chen et al., 2004), Yu et al., 2008). Various molecules such as collagen and laminin have been shown to promote neuronal regeneration, adhesion, proliferation and differentiation in the CNS (Venstrom and Reichardt, 1993). In order to enhance the interactions between cells and materials leading to improved material integration, materials can be modified with short recognition sequences that mimic the ECM resulting in stronger adhesion of cells (for examples peptides or proteins). Various modification have been developed and can be applied to various material targeting more than one tissue including surface deposition, blending, electrostatic attachment and covalent attachment (Rao and Winter, 2009).

In the work presented here covalent attachment of the YIGSR-peptide to PLGA flat sheet membranes and blending of PLL within electrospun PLGA nanofibres were conducted resulting in interesting outcomes. Blending was chosen as it was a quick and simple method. Whereas covalent attachment was chosen as it results in much stronger and more stable compositions because of stronger forces between biomaterial and YIGSR-peptides.

In order to evaluate the suitability of a scaffold, cells were seeded onto the surface and left to attach, proliferate and/or differentiate. PC12 cells have been tested on a variety of materials to study the materials' suitability (Tomaselli et al., 1987), (Dai et al., 1994), (Ranieri et al., 1994), (Zielinski and Aebischer, 1994),(Ranieri et al., 1995),(Lhoest et al., 1996),(Holmes et al., 2000),(Waddell et al., 2003),(Neal et al., 2009),(Runge et al., 2010). Cell counts, increased cell numbers and the increased length of neurites, all in the presence of nerve growth factor (NGF) are accepted as indicators of positive PC12 cell response to presented scaffolds. Still, PC12 cells are a model cell line, and in this case will never be implanted into the human body.

Other cells that can be used to evaluate the scaffold are cells of the central nervous system such as Schwann cells, olfactory ensheathing cells and stem/progenitor cells. None of these cells have been tested on PLGA flat sheet membranes. To some extent, these cells have been tested on electrospun fibres showing similar behaviour as PC12 cells. For example, DRGs have been seeded onto aligned electrospun polydioxanone fibres (Chow et al., 2007), poly-epsilon-caprolactone/collagen fibres (Schnell et al., 2007) and PLLA (Wang et al., 2009) and displayed directional neurite outgrowth along fibre alignment on all materials. This was also true for glial cells such as astrocytes, which additionally supported neurite outgrowth of DRG neurites when co-cultured (Chow et al., 2007). Neural stem cells (NSCs) were seeded on aligned PLLA (Yang et al., 2005), random PLLA (Yang et al., 2004) and PCL fibres (Nisbet et al., 2008) showing the effect of the scaffold on directional neurite outgrowth. This evidence demonstrates that although PC12 cells are only used as a model, other neuronal and glial cell types were shown to behave

similarly, making the results presented here, a good indication of how CNS cells will behave, verifying PC12s as a model.

Foetal calf serum (FCS) is a complex mix of albumins, growth factors, growth inhibitors and ECM molecules such as fibronectin and is probably the most important and most commonly used component in cell culture medium. FCS has various advantages such as it helps to protect against mechanical damage in stirred cultures; it increases the buffering capacity of cell cultures; and it is able to bind and neutralise toxins. However, serum is subject to bath-batch variation and can lead to contamination. The work presented here has revealed another characteristic of FCS in relation to PC12 cell culture: the addition of FCS hampers cell attachment of PC12 cells significantly. This novel effect has not been reported previously making comparison to published data not possible but is likely to be of interest for future investigations.

Cell culture studies using PC12 cells have succeeded in showing the potential of the newly created PLGA-PLL nanofibrous scaffold. Further experiments *in vitro* using neural stem cells, Schwann cells or oligodendrocyte precursor cells and *in vivo* in rats are necessary to show the applicability of this scaffold.

9. CONCLUSIONS AND FUTURE WORK

9.1 Introduction

The work of this thesis had the aim to investigate the suitability of PLGA as scaffold for neural tissue engineering. PLGA flat sheet membranes and electrospun nanofibres were assessed. PLGA flat sheet membranes were investigated in terms of cell attachment and surface modification methods, including aminolysis, peptide immobilisation and ozonation. Cell attachment, proliferation and differentiation of cells were investigated on electrospun nanofibres. This chapter is the conclusion to the results chapters 4 - 7.

The overall aim of CNS tissue engineering is to support the regeneration of tissue that would otherwise not heal. The regeneration inhibiting environment of the CNS has proven to be a challenging task. PLGA flat sheet membranes and electrospun fibre mats have been investigated for their suitability for 3D tissue engineering. Electrospun fibres are of particular interest for nerve tissue, the benefits being:

- The electrospun fibres mimic the extra cellular matrix, increasing the cytocompatibility of PLGA.
- The fibres provide a large surface area which can be modified with immobilised molecules of interest.
- The scaffold is highly porous allowing migration of cells into the scaffold without necrosis or lack of nutrients creating a natural 3D tissue matrix.
- By controlling the alignment of the fibres the differentiation of PC12 cells can be controlled.

The scaffold presented in this work has the potential to direct neurite outgrowth of PC12 cells and can be used as an implant for spinal cord injuries, with potentially helping axons to bridge the damaged area and to reconnect with the distal part reintroducing signal transduction from the brain to various body parts.

9.2 Conclusions

9.2.1 Interactions of PC12 cells with PLGA flat sheet membrane (Chapter 4)

The PLGA flat sheet membrane was chosen as a scaffold to evaluate the polymers suitability for attachment of PC12 cells. This was based on the ease of production of the scaffold and previous work showing its suitability for other cell lines. Additionally, PLGA is approved by the FDA and has been used in applications for the human body making it a safe material to work with and more easily transferable from the laboratory to human applications due to its approvement.

- PLGA flat sheet membrane did not support attachment of PC12 cells as only a significantly lower cell number of 16±7% attached to PLGA compared to 73±13% of initially seeded cells on TCP+PLL.
- Further surface modification including amynolysis, peptide immobilisation and ozone treatment failed to increase the wettability of the flat sheet membrane as the contact angle (average of 73.42°±3.80°) did not decrease.
- Modified surfaces did not show significantly higher cell attachment compared to non-modified surfaces.
- Removal of FCS from the media results in a nearly six fold increase in PC12 cell attachment. 60±15% of seeded PC12 cells attached to PLGA films when using medium without FCS and only 11±5% of cell attached when using medium supplemented with 10% FCS.

The PLGA flat sheet membranes failed to provide an adequate surface to support attachment of PC12 cells and consequently failed to provide physical support for PC12s. Cell attachment was low and the attached cells were easily detached during washing steps, thus differentiation experiments were not conducted. These results demonstrate that although PLGA is a widely used polymer for tissue engineering applications, flat sheet membranes are not suitable for PC12 cell studies. Nevertheless PC12 cells attached to the polymer and were further used for a different type of scaffold, electrospun nanofibres, which were investigated for neuronal tissue engineering. FCS was removed during initial attachment

experiments. Electrospinning processing parameters were investigated (chapter 5) and cell culture studies were conducted (chapter 6).

9.2.2 Electrospinning (Chapter 5)

An electrospinning process was established. Although PLGA flat sheet membranes were not successful in supporting cell attachment various publications have indicated the potential of electrospinning nanofibres in providing the correct surface structure for cells to recognize and attach. Thus work with PLGA was further pursued. Parameters affecting electrospinning of PLGA were investigated, including polymer concentration, solution viscosity, feeding rate, applied voltage and collector-to-needle distance.

- Various solvents including dimethylfomamide (DMF), tetrahydrofuran (THF), DMF and THF at volumentric ratios of 3:1 and 1:1, 1-methyl-2-pyrrolidinone (NMP), Isopropanol, dichloromethane (DCM), chloroform ($CHCl_3$) and methanol (MeOH) at ratio 3:1 were tested as solvent of choice for electrospinning PLGA.
- The $CHCl_3$:MeOH (3:1) mixture was chosen as the solvent of choice as its use resulted in continuous homologous fibres (no bead formation) with the highest amount of polymer collected in relation to polymer solution used. Processing difficulties, such as needle clogging, were also minimised.
- Optimum polymer concentration was established at 10% (w/w). Polymer concentrations lower than 10% (w/w) resulted in bead formation, whereas higher concentrations resulted in processing difficulties (i.e. needle clogging).
- For the electrospinning set up used in this project the optimum viscosity of the polymer solution was established as being 0.07Pa.S. Higher and lower viscosities did not result in continuous fibres, but in droplet formation or non-efficient evaporation of the solvent leading to merging of already collected fibres.

- Aligned PLGA nanofibres were fabricated by carefully manipulating electrospinning parameters, including solution feeding rate (2ml/h) and collector type (spinneret or aligned electrodes).
- Aligned fibres were produced by replacing the aluminium foil collector with two aligned aluminium rods with an optimal air gap of 1 cm.

The aim was to produce random and aligned PLGA nanofibres. This was achieved by carefully manipulating the settings of the electrospinning set up. The aim of producing electrospun PLGA nanofibres was to mimic the ECM. In connection to this work it was interesting to investigate how the electrospun fibre mats would influence cell attachment of PC12 cells. The most suitable fibres, with an average fibre diameter of 530±140nm, were obtained using a 10% w/w PLGA polymer solution in $CHCl_3$/MeOH (3:1) with an optimum viscosity of 0.07Pa.S which was electrospun using a needle with 0.4mm inner diameter and 15kV applied voltage onto a collector placed at a distance of 11cm.

9.2.3 Interactions of PC12 cells with electrospun PLGA fibres (Chapter 6)

PC12 cells were seeded on random and aligned electrospun PLGA fibres their attachment, proliferation and differentiation were analysed. It was demonstrated that aligned PLGA nanofibres were able to direct neurite outgrowth thus providing topographical guidance for neurites of PC12 cells.

- PC12 cells were shown to attach and proliferate (within 48 h after seeding) on electrospun PLGA scaffolds.
- Differentiation of PC12 cells was highly influenced by the orientation of electrospun fibres.
- The number of neurite bearing cells was significantly higher on aligned (68±6%) than random PLGA (55±5%) nanofibres and TCP coated with PLL (16±8%).
- Number of neurites per cell was reduced on aligned fibres (1-3 neurites per cell) compared to random fibres (1-8 neurites per cell).

- Neurite outgrowth was directed along electrospun PLGA nanofibres with a high proportion of neurites growing within 30 degrees of parallel, whereas on random fibres no particular directional bias was observed.
- Neurites were three times longer on aligned fibres (mean length of neurites 184±119µm) compared to random fibres (mean length of neurites 59±33µm).

This work suggests that aligned PLGA electrospun fibre scaffold strongly influences neurite organisation, and can potentially be used as a guidance conduit for spinal cord repair strategies, fulfilling one of the major aims of this thesis.

9.2.4 Incorporation of bioactive molecules into PLGA nanofibres (Chapter 7)

Electrospun fibres can be modified by means of incorporation of various molecules, which are released as the scaffold degrades. A novel scaffold was created by incorporation poly-L-lysine (PLL) into random and aligned PLGA nanofibres by emulsion electrospinning. Attachment and differentiation of PC12 cells on the novel scaffold were analysed.

- For electrospinning of emulsions the flow rate of the polymer solution was reduced (form 3ml/h to 2ml/h) in order to achieve high uniformity of resulting fibres.
- Fibre diameter of electrospun PLGA was influenced by incorporated PLL resulting in larger fibres with a diameter of 825± 187nm for PLL-PLGA fibres, which were significantly different from 530±140nm PLGA only fibres.
- PLL was successfully incorporated into electrospun PLGA fibres. The presence of PLL in PLGA fibres was visualised by electrospinning FITC-PLL and analysing the resulting fibres using fluorescence microscopy.
- PLL-PLGA fibres supported cell differentiation as they increased the length of neurites by factor 1.5 compared to PLGA fibres. Attachment and directional neurite outgrowth was not compromised by incorporated PLL.

This is the first report demonstrating the incorporation of PLL into electrospun PLGA nanofibres using emulsion electrospinning and demonstrating its effect on the attachment and differentiation of PC12 cells. The PLGA-PLL nanofibrous scaffold is a novel and potentially promising new scaffold for nerve regeneration. The results have demonstrated that PLGA is a suitable scaffold for nerve regeneration and can be formed into various forms. Incorporation of bioactive molecules can be performed using emulsion electrospinning a simple, efficient and reliable method which can be used for countless substances bearing great potential for drug delivery vehicle design.

9.3 Future work

As research into spinal cord repair continues to progress, it is for future research and clinical trials to establish which polymer combines the best possible characteristics for supporting and promoting regeneration in the central nervous system. The suitability of flat sheet membranes and electrospun PLGA nanofibres has been investigated for applications in nerve tissue repair. Chapter 7 has demonstrated that by adding a small amount of PLL the neurite outgrowth of PC12 cells increased significantly. This opens the door to investigation of many other substances. This scaffold is a further step towards a “smart” scaffold, combining topographical and chemical queues thus increasing the biocompatibility of PLGA. To take the results presented in this thesis towards useful a clinical product will take intensive analysis *in vivo* and *in vitro* and by considering the interactions between the two (Fig 9.1).

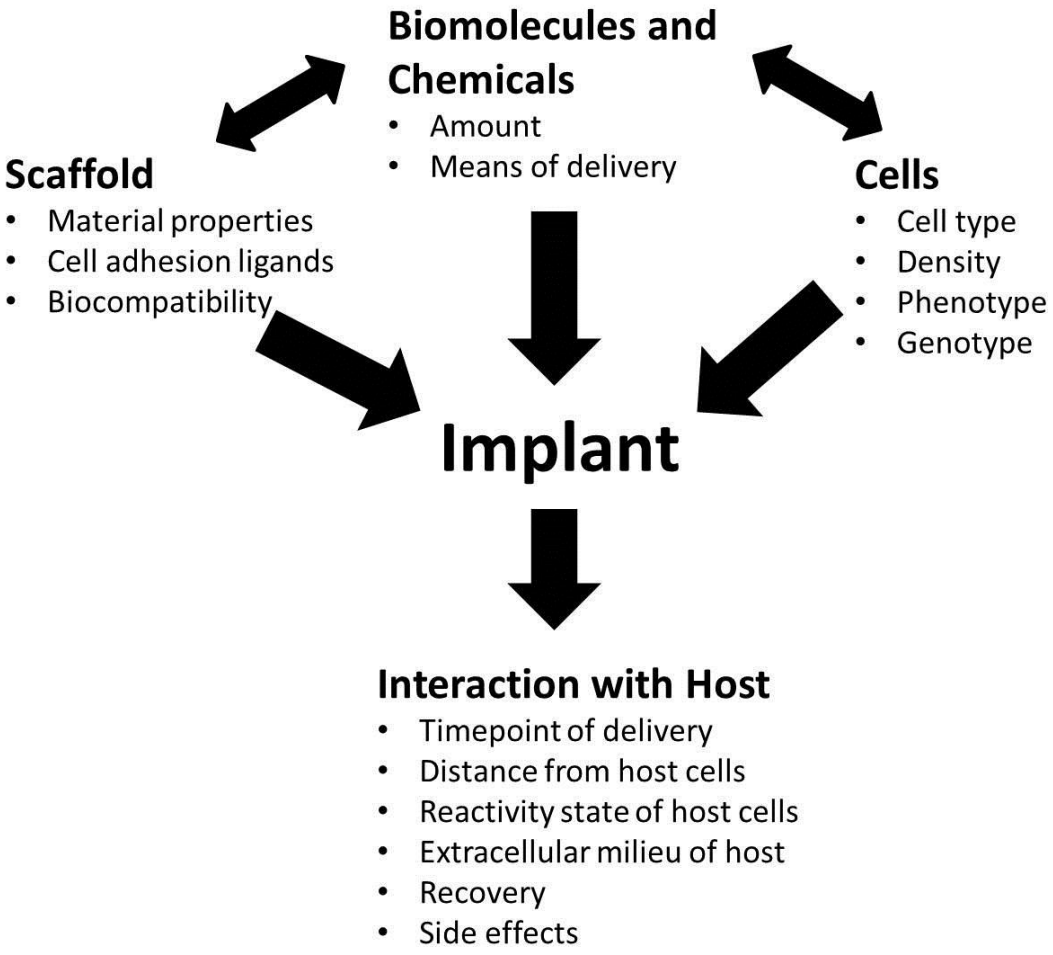

Figure 9.1 Future work model towards clinical application of electrospun PLGA nanofibres

9.3.1 Short term studies

Optimisation of the electrospinning process

Electrospinning is now a widely used method and many cell types have been seeded onto electrospun fibre mats. The majority of the research is limited to analysing cellular attachment only, sometimes producing contradicting results. The exact benefit of using electrospun fibres has to be evaluated with more in depth assessment of cellular functions, for example growth cone development of neural cells. Nevertheless, studies available to date already illustrate the potential benefit of electrospun fibres for tissue engineering applications.

One of the key challenges is the deposition of electrospun fibres, controlled down to nanometre scale, in order to achieve better mimicking of the ECM and

consequently more control over cell behaviour. For this, various collectors can be tested. But most importantly, an apparatus needs to be designed which facilitates the control of environmental parameters, such as humidity and temperature and which reduces disturbances of the jet by other chargeable surroundings. An enclosed non-conductive box can be built with incorporated inlets for cables (voltage, grounding) and syringe. Preferably, it should be possible to control the temperature to exclude temperature dependent jet behaviour changes due to viscosity change of the polymer solution. This can lead to an automated process having the advantage of increasing the effectiveness of electrospinning. This would give the opportunity to screen more polymers and make electrospinning a less laborious and time consuming process.

Although all key parameters of the electrospinning process are identified, more research is necessary for full understanding of the process which will make it more predictable and reproducible. This will lead to accelerated electrospinning set up development and electrospun scaffolds will find more applications in the sector of drug delivery and tissue engineering. The step into clinical trials is necessary in order to validate the potential of *in vitro* studies *in vivo*.

Modelling

Mathematical modelling of electrospinning may help to predict the resulting fibres. Effects of forces such as surface charge, point-charges, ring charges and Coulomb forces can be investigated to predict jet behaviour and fibre morphology, taking into account the polymer, polymer concentration and solution viscosity.

Characteristics of the scaffold may also be investigated using mathematical modelling. The mechanical properties have been investigated and the mechanical strength of electrospun polyurethane was predicted using a modelling strategy depending on fibre diameter and degree of fibre alignment (Stylianopoulos et al., 2008). Parameters such as degradation rate, fibre density, diameter of individual fibres as well as of the whole implant may be assessed in order to predict the effectiveness of the scaffold after implantation. The optimum parameters for cell

survival such as oxygen density in relation to fibre density can be calculated and help to optimise the scaffold.

Molecular studies

As described in chapter 7, other substances of interest such as growth factors and antibiotics can also be incorporated into the scaffold and promote regeneration. For growth factors, such as NGF and other neurotrophic factors, several parameters can be investigated including the encapsulation efficiency, release profile (ELISA) and biological activity (cellular studies). The purpose of these substances is e.g. to suppress inhibitory signals in the area of injury, or to increase neurite outgrowth. To guide axons over a biodegradable bridge an electrospun scaffold with a release gradient may further increase axon outgrowth (Fig 9.2).

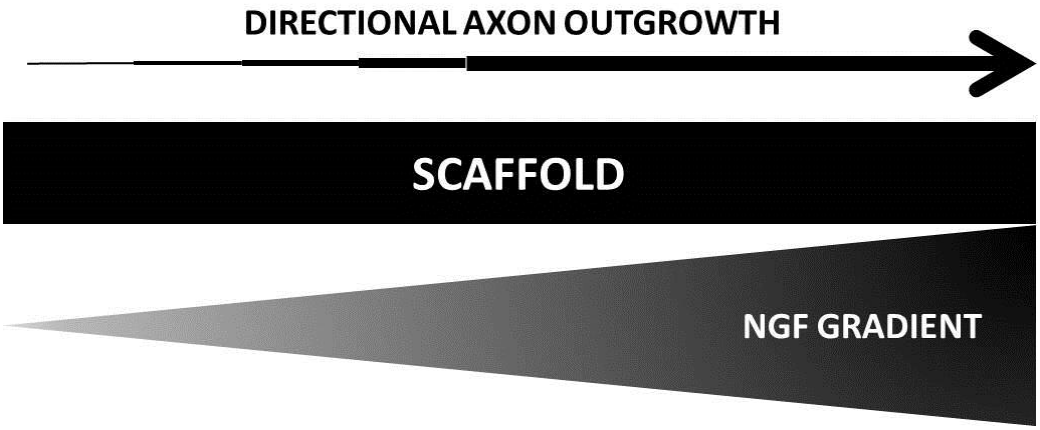

Figure 9.2 Scaffold with an incorporated NGF gradient. This scaffold might increase axonal outgrowth even further than already achieved.

Microspheres have received a great deal of attention as means of drug delivery, incorporating e.g. insulin, dexamethasone and growth factors (Bae et al., 2009, Willerth and Sakiyama-Elbert, 2007, Khafagy et al., 2007). NGF was shown to be released in a controlled manner from biodegradable poly(phosphoester), resulting in morphological regeneration of peripheral nerves (Xu et al., 2003). A new approach may be the combination of microspheres with other types of scaffolds,

such as flat sheet membranes or electrospun fibres, creating alternating layers of cell supporting scaffold with biomolecules releasing scaffold.

Scaffold modification

As PLGA is a very hydrophobic polymer, and addition of PLL did not change its characteristic, introduction of hydrophilic polymer such as PVA may increase its hydrophilicity. PLGA-PVA polyblends can be electrospun and assessed according to this work. Blends of synthetic and natural polymers can be produced and electrospun to produce new polybend scaffolds. These scaffolds have the advantage of combining the properties of several single polymers and stabilizing the solutions containing natural polymers which are not amenable to electrospinning due to molecular weight or solubility issues.

Surface modification can be performed to introduce ligands that influence differentiation of cells. For example, neural stem cell differentiation can be controlled by altering ligand density and mechanical properties (Saha et al., 2008). Although the synthetic scaffolds offer more designing, more concerns into potential immunogenicity as well as the toxicity of degrading fragments, cross linking and activating agents used manufacturing them remain to be eradicated (Williams et al., 2005).

9.3.2 Medium and long term studies

Animal studies

In order to establish whether the newly developed scaffold consisting of PLGA with incorporated PLL has a positive effect on nerve regeneration *in vivo* animal studies may be conducted. For this the scaffold has to be tested in animal models, with induced spinal cord injuries, such as contusion and complete injuries in mice and rats. These studies can help to establish the safety of the scaffold as well as its positive or negative effect on axon regrowth and axon behaviour during entering and exiting the scaffolds.

Processing

During the experiments conducted in this project, sterilisation was a challenge needing a solution. PLGA is biodegradable and biocompatible, but its handling, including preparation of the scaffold takes place in a non-sterile environment and sterilization is an inevitable step prior to cell culture work. Sterilisation is necessary to avoid infections after cell seeding and implantation. In the laboratory, sterilization of the produced scaffolds was achieved via exposure to antibiotic/antimicotic solutions for at least 24h. This method raises the question of resistance. And it is not clear what affect this implants that have been exposed to antibiotics/animicotics on the host tissue.

The speed of production is also important as the implant has to be available within several hours after the patient sustained the injury. As the material is biodegradable, the scaffolds have a shorter lifespan than non-biodegradable materials, due to which storing precautions have to be considered, such as storing implants in -80°C freezers. Ones the scaffolds are produced and sterilized, they have to be sealed in sterile packaging that prevents any infections. The parameters effecting packaging and storage need to be investigated for SCI procedures and therapies.

A further point for interest is the creation of a scaffold that can be easily handled without breaking or deformation before and during the surgical procedure of implantation. All injuries vary from patient to patient. Thus, it is necessary to create a scaffold that can be produced quickly and in different shapes. For this manufacturing of scaffolds for a number of injury types is inevitable. The implantation of a tubular implant may be counterproductive as most injuries occur without complete transection. To fit a tubular implant into the site of injury may require further damage to the spinal cord with a complete transection or a midline myelotomy (surgical severing of the midline transverse fibres of the spinal cord). More research into fabrication of various implants and implantation procedures, which are more suitable for different types of injury (partial transections, contusions, cavitation and lacerations), has to be addressed in collaboration with

surgeons. For example, in case of cavitation an implant is required which is smaller than the native spinal cord, with a microstructure suited for the location of the injury.

Timepoint of implantation

The optimal timepoint of implantation for chronic and acute spinal cord injuries is not known and has to be investigated.

It is important to note that even with complete axon extension over the scaffolds the degree of regeneration cannot be predicted and the current understanding needs to be further improved. The type of functional recovery needs to be investigated and whether the remyelination of axons needs additional promotion with further interventions.

References

AJEMIAN, A., NESS, R. & DAVID, S. 1994. Tenascin in the injured rat optic nerve and in non-neuronal cells in vitro: potential role in neural repair. *J Comp Neurol,* 340**,** 233-42.

ALABED, Y. Z., GRADOS-MUNRO, E., FERRARO, G. B., HSIEH, S. H. K. & FOURNIER, A. E. 2006. Neuronal responses to myelin are mediated by rho kinase. *Journal of Neurochemistry,* 96**,** 1616-1625.

ALEXANDER, J. K., FUSS, B. & COLELLO, R. J. 2006. Electric field-induced astrocyte alignment directs neurite outgrowth. *Neuron Glia Biol,* 2**,** 93-103.

ANGELES, M., CHENG, H. L. & VELANKAR, S. S. 2008. Emulsion electrospinning: composite fibers from drop breakup during electrospinning. *Polymers for Advanced Technologies,* 19**,** 728-733.

ARINZEH, T., JAFFE, M., SHANMUGASUNDARAM, S., 16th Sept 2010, United Stated patent application publication. SUBSTRATE RECOGNITION BY DIFFERENTIABLE HUMAN MESENCHYMAL STEM CELLS. Pub.No.: US 2010/0233807 A1.

AUBERT-POUESSEL, A., BIBBY, D. C., VENIER-JULIENNE, M. C., HINDRE, F. & BENOIT, J. P. 2002. A novel in vitro delivery system for assessing the biological integrity of protein upon release from PLGA microspheres. *Pharmaceutical Research,* 19**,** 1046-1051.

BAE, S. E., SON, J. S., PARK, K. & HAN, D. K. 2009. Fabrication of covered porous PLGA microspheres using hydrogen peroxide for controlled drug delivery and regenerative medicine. *Journal of Controlled Release,* 133**,** 37-43.

BHATTARAI, N., EDMONDSON, D., VEISEH, O., MATSEN, F. A. & ZHANG, M. 2005. Electrospun chitosan-based nanofibers and their cellular compatibility. *Biomaterials,* 26**,** 6176-84.

BINI, T. B., GAO, S. J., TAN, T. C., WANG, S., LIM, A., HAI, L. B. & RAMAKRISHNA, S. 2004. Electrospun poly(L-lactide-co-glycolide) biodegradable polymer nanofibre tubes for peripheral nerve regeneration. *Nanotechnology,* 15**,** 1459-1464.

BINI, T. B., GAO, S. J., WANG, S. & RAMAKRISHNA, S. 2006. Poly(l-lactide-co-glycolide) biodegradable microfibers and electrospun nanofibers for nerve tissue engineering: an in vitro study. *Journal of Materials Science,* 41**,** 6453-6459.

BLACKWOOD, K. A., MCKEAN, R., CANTON, I., FREEMAN, C. O., FRANKLIN, K. L., COLE, D., BROOK, I., FARTHING, P., RIMMER, S., HAYCOCK, J. W., RYAN, A. J. & MACNEIL, S. 2008. Development of biodegradable electrospun scaffolds for dermal replacement. *Biomaterials,* 29**,** 3091-104.

BLEWITT, M. J. & WILLITS, R. K. 2007. The effect of soluble peptide sequences on neurite extension on 2D collagen substrates and within 3D collagen gels. *Ann Biomed Eng,* 35**,** 2159-67.

BOLSOVER, S., FABES, J. & ANDERSON, P. N. 2008. Axonal guidance molecules and the failure of axonal regeneration in the adult mammalian spinal cord. *Restor Neurol Neurosci,* 26**,** 117-30.

BOVOLENTA, P. & FERNAUD-ESPINOSA, I. 2000. Nervous system proteoglycans as modulators of neurite outgrowth. *Prog Neurobiol,* 61**,** 113-32.

BRADBURY, E. J. & MCMAHON, S. B. 2006. Spinal cord repair strategies: why do they work? *Nat Rev Neurosci,* 7**,** 644-53.

BRADBURY, E. J., MOON, L. D., POPAT, R. J., KING, V. R., BENNETT, G. S., PATEL, P. N., FAWCETT, J. W. & MCMAHON, S. B. 2002. Chondroitinase ABC promotes functional recovery after spinal cord injury. *Nature,* 416**,** 636-40.

BRUNETTI, V., MAIORANO, G., RIZZELLO, L., SORCE, B., SABELLA, S., CINGOLANI, R. & POMPA, P. P. 2010. Neurons sense nanoscale roughness with nanometer sensitivity. *Proceedings of the National Academy of Sciences of the United States of America,* 107**,** 6264-6269.

BUNGE, M. B. 2001. Bridging areas of injury in the spinal cord. *Neuroscientist,* 7**,** 325-39.

CANNING, D. R., MCKEON, R. J., DEWITT, D. A., PERRY, G., WUJEK, J. R., FREDERICKSON, R. C. & SILVER, J. 1993. beta-Amyloid of Alzheimer's disease induces reactive gliosis that inhibits axonal outgrowth. *Exp Neurol,* 124**,** 289-98.

CAO, H., LIU, T. & CHEW, S. Y. 2009. The application of nanofibrous scaffolds in neural tissue engineering. *Adv Drug Deliv Rev,* 61**,** 1055-64.

CAO, X. & SCHOICHET, M. S. 1999. Delivering neuroactive molecules from biodegradable microspheres for application in central nervous system disorders. *Biomaterials,* 20**,** 329-39.

CAO, Y., CROLL, T. I., COOPER-WHITE, J. J., O'CONNOR, A. J. & STEVENS, G. W. 2004. Production and surface modification of polylactide-based polymeric scaffolds for soft-tissue engineering. *Methods Mol Biol,* 238**,** 87-112.

CARROLL, C. P. & JOO, Y. L. 2006. Electrospinning of viscoelastic Boger fluids: Modeling and experiments. *Physics of Fluids,* 18**,** -.

CEBALLOS, D., NAVARRO, X., DUBEY, N., WENDELSCHAFER-CRABB, G., KENNEDY, W. R. & TRANQUILLO, R. T. 1999. Magnetically aligned collagen gel filling a collagen nerve guide improves peripheral nerve regeneration. *Exp Neurol,* 158**,** 290-300.

CHEN, C. S., ALONSO, J. L., OSTUNI, E., WHITESIDES, G. M. & INGBER, D. E. 2003. Cell shape provides global control of focal adhesion assembly. *Biochem Biophys Res Commun,* 307**,** 355-61.

CHEN, C. S., TAN, J. & TIEN, J. 2004. Mechanotransduction at cell-matrix and cell-cell contacts. *Annu Rev Biomed Eng,* 6**,** 275-302.

CHEN, R. & HUNT, J. A. 2007. Biomimetic materials processing for tissue-engineering processes. *Journal of Materials Chemistry,* 17**,** 3974-3979.

CHEN, Z. J., NEGRA, M., LEVINE, A., UGHRIN, Y. & LEVINE, J. M. 2002. Oligodendrocyte precursor cells: reactive cells that inhibit axon growth and regeneration. *J Neurocytol,* 31**,** 481-95.

CHEW, S. Y., MI, R., HOKE, A. & LEONG, K. W. 2008. The effect of the alignment of electrospun fibrous scaffolds on Schwann cell maturation. *Biomaterials,* 29**,** 653-61.

CHOW, W. N., SIMPSON, D. G., BIGBEE, J. W. & COLELLO, R. J. 2007. Evaluating neuronal and glial growth on electrospun polarized matrices: bridging the gap in percussive spinal cord injuries. *Neuron Glia Biology,* 3**,** 119-126.

CONNOLLY, J. L., GREENE, L. A., VISCARELLO, R. R. & RILEY, W. D. 1979. Rapid, sequential changes in surface morphology of PC12 pheochromocytoma cells in response to nerve growth factor. *J Cell Biol,* 82**,** 820-7.

COOKE, M. J., PHILLIPS, S. R., SHAH, D. S. H., ATHEY, D., LAKEY, J. H. & PRZYBORSKI, S. A. 2008. Enhanced cell attachment using a novel cell culture surface presenting functional domains from extracellular matrix proteins. *Cytotechnology,* 56**,** 71-79.

COREY, J. M., GERTZ, C. C., WANG, B. S., BIRRELL, L. K., JOHNSON, S. L., MARTIN, D. C. & FELDMAN, E. L. 2008. The design of electrospun PLLA nanofiber scaffolds compatible with serum-free growth of primary motor and sensory neurons. *Acta Biomater*.

COREY, J. M., GERTZ, C. C., WANG, B. S., BIRRELL, L. K., JOHNSON, S. L., MYCEK, K. B., CHEN, Q., MARTIN, D. C. & FELDMAN, E. L. 2007. Aligned, electrospun nanofibers for nervous system regeneration. *Journal of the Peripheral Nervous System,* 12**,** 22-22.

CROLL, T. I., O'CONNOR, A. J., STEVENS, G. W. & COOPER-WHITE, J. J. 2004. Controllable surface modification of poly(lactic-co-glycolic acid) (PLGA) by hydrolysis or aminolysis I: Physical, chemical, and theoretical aspects. *Biomacromolecules,* 5**,** 463-473.

CROWE, M. J., BRESNAHAN, J. C., SHUMAN, S. L., MASTERS, J. N. & BEATTIE, M. S. 1997. Apoptosis and delayed degeneration after spinal cord injury in rats and monkeys. *Nat Med,* 3**,** 73-6.

DAI, W. G., BELT, J. & SALTZMAN, W. M. 1994. Cell-Binding Peptides Conjugated to Poly(Ethylene Glycol) Promote Neural Cell-Aggregation. *Bio-Technology,* 12**,** 797-801.

DALTON, P. D., FLYNN, L. & SHOICHET, M. S. 2002. Manufacture of poly(2-hydroxyethyl methacrylate-co-methyl methacrylate) hydrogel tubes for use as nerve guidance channels. *Biomaterials,* 23**,** 3843-51.

DE LAPORTE, L., YAN, A. L. & SHEA, L. D. 2009. Local gene delivery from ECM-coated poly(lactide-co-glycolide) multiple channel bridges after spinal cord injury. *Biomaterials,* 30**,** 2361-8.

DEBELLARD, M. E., TANG, S., MUKHOPADHYAY, G., SHEN, Y. J. & FILBIN, M. T. 1996. Myelin-associated glycoprotein inhibits axonal regeneration from a variety of neurons via interaction with a sialoglycoprotein. *Molecular and Cellular Neuroscience,* 7**,** 89-101.

DHOOT, N. O., TOBIAS, C. A., FISCHER, I. & WHEATLEY, M. A. 2004. Peptide-modified alginate surfaces as a growth permissive substrate for neurite outgrowth. *J Biomed Mater Res A,* 71**,** 191-200.

DI LULLO, G. A., SWEENEY, S. M., KORKKO, J., ALA-KOKKO, L. & SAN ANTONIO, J. D. 2002. Mapping the ligand-binding sites and disease-associated mutations on the most abundant protein in the human, type I collagen. *J Biol Chem,* 277**,** 4223-31.

DJORDJEVIC, I., BRITCHER, L. G. & KUMAR, S. 2008. Morphological and surface compositional changes in poly(lactide-co-glycolide) tissue engineering scaffolds upon radio frequency glow discharge plasma treatment. *Applied Surface Science,* 254**,** 1929-1935.

DOMENICONI, M. & FILBIN, M. T. 2005. Overcoming inhibitors in myelin to promote axonal regeneration. *Journal of the Neurological Sciences,* 233**,** 43-47.

DONG, Y., YONG, T., LIAO, S., CHAN, C. K. & RAMAKRISHNA, S. 2008. Long-term viability of coronary artery smooth muscle cells on poly(L-lactide-co-epsilon-caprolactone) nanofibrous scaffold indicates its potential for blood vessel tissue engineering. *J R Soc Interface,* 5**,** 1109-18.

DOSHI, J. & RENEKER, D. H. 1995. Electrospinning Process and Applications of Electrospun Fibers. *Journal of Electrostatics,* 35**,** 151-160.

DRUBIN, D. G., FEINSTEIN, S. C., SHOOTER, E. M. & KIRSCHNER, M. W. 1985. Nerve growth factor-induced neurite outgrowth in PC12 cells involves the coordinate induction of microtubule assembly and assembly-promoting factors. *J Cell Biol,* 101**,** 1799-807.

DUAN, B., YUAN, X. Y., ZHU, Y., ZHANG, Y. Y., LI, X. L., ZHANG, Y. & YAO, K. D. 2006. A nanofibrous composite membrane of PLGA-chitosan/PVA prepared by electrospinning. *European Polymer Journal,* 42**,** 2013-2022.

DUBEY, N., LETOURNEAU, P. C. & TRANQUILLO, R. T. 1999. Guided neurite elongation and schwann cell invasion into magnetically aligned collagen in simulated peripheral nerve regeneration. *Exp Neurol,* 158**,** 338-50.

DUBEY, N., LETOURNEAU, P. C. & TRANQUILLO, R. T. 2001. Neuronal contact guidance in magnetically aligned fibrin gels: effect of variation in gel mechano-structural properties. *Biomaterials,* 22**,** 1065-75.

EIDELBERG, E., STRAEHLEY, D., ERSPAMER, R. & WATKINS, C. J. 1977. Relationship between Residual Hindlimb-Assisted Locomotion and Surviving Axons after Incomplete Spinal-Cord Injuries. *Experimental Neurology,* 56**,** 312-322.

EL-GHANNAM, A., DUCHEYNE, P. & SHAPIRO, I. M. 1995. Bioactive material template for in vitro synthesis of bone. *J Biomed Mater Res,* 29**,** 359-70.

ELLIS, M. J. & CHAUDHURI, J. B. 2007. Poly(lactic-co-glycolic acid) hollow fibre membranes for use as a tissue engineering scaffold. *Biotechnology and Bioengineering,* 96**,** 177-187.

ELLIS, M. J. & CHAUDHURI, J. B. 2008. Human bone derived cell culture on PLGA flat sheet membranes of different lactide : glycolide ratio. *Biotechnology and Bioengineering,* 101**,** 369-377.

FAN, H., HU, Y., ZHANG, C., LI, X., LV, R., QIN, L. & ZHU, R. 2006. Cartilage regeneration using mesenchymal stem cells and a PLGA-gelatin/chondroitin/hyaluronate hybrid scaffold. *Biomaterials,* 27**,** 4573-80.

FAN, Y. W., CUI, F. Z., CHEN, L. N., ZHAI, Y., XU, Q. Y. & LEE, I. S. 2002a. Adhesion of neural cells on silicon wafer with nano-topographic surface. *Applied Surface Science,* 187**,** 313-318.

FAN, Y. W., CUI, F. Z., HOU, S. P., XU, Q. Y., CHEN, L. N. & LEE, I. S. 2002b. Culture of neural cells on silicon wafers with nano-scale surface topograph. *Journal of Neuroscience Methods,* 120**,** 17-23.

FAWCETT, J. W. & ASHER, R. A. 1999. The glial scar and central nervous system repair. *Brain Res Bull,* 49**,** 377-91.

FEHLINGS, M. G. & TATOR, C. H. 1999. An evidence-based review of decompressive surgery in acute spinal cord injury: rationale, indications, and timing based on experimental and clinical studies. *J Neurosurg,* 91**,** 1-11.

FLEMMING, R. G., MURPHY, C. J., ABRAMS, G. A., GOODMAN, S. L. & NEALEY, P. F. 1999. Effects of synthetic micro- and nano-structured surfaces on cell behavior. *Biomaterials,* 20**,** 573-588.

FOLEY, J. D., GRUNWALD, E. W., NEALEY, P. F. & MURPHY, C. J. 2005. Cooperative modulation of neuritogenesis by PC12 cells by topography and nerve growth factor. *Biomaterials,* 26**,** 3639-44.

FONG, H., CHUN, I. & RENEKER, D. H. 1999. Beaded nanofibers formed during electrospinning. *Polymer,* 40**,** 4585-4592.

FRIDRIKH, S. V., YU, J. H., BRENNER, M. P. & RUTLEDGE, G. C. 2003. Controlling the fiber diameter during electrospinning. *Phys Rev Lett,* 90**,** 144502.

FRIEDMAN, J. A., WINDEBANK, A. J., MOORE, M. J., SPINNER, R. J., CURRIER, B. L. & YASZEMSKI, M. J. 2002. Biodegradable polymer grafts for surgical repair of the injured spinal cord. *Neurosurgery,* 51**,** 742-51; discussion 751-2.

FUJIMOTO, K., TAKEBAYASHI, Y., INOUE, H. & IKADA, Y. 1993. Ozone-Induced Graft-Polymerization onto Polymer Surface. *Journal of Polymer Science Part a-Polymer Chemistry,* 31**,** 1035-1043.

FUJITA, K., LAZAROVICI, P. & GUROFF, G. 1989. Regulation of the differentiation of PC12 pheochromocytoma cells. *Environ Health Perspect,* 80**,** 127-42.

GATTI, R., BELLETTI, S., ORLANDINI, G., BUSSOLATI, O., DALL'ASTA, V. & GAZZOLA, G. C. 1998. Comparison of annexin V and calcein-AM as early vital markers of apoptosis in adherent cells by confocal laser microscopy. *J Histochem Cytochem,* 46**,** 895-900.

George, J.H.S., Shaffer, M.M., 2006. Tissue Engineering [online]. London: Imperial College London. Available from: http://www.centropede.com/UKSB2006/ePoster/background.html [Accessed 19 October 2010].

GERARDO-NAVA, J., FUHRMANN, T., KLINKHAMMER, K., SEILER, N., MEY, J., KLEE, D., MOLLER, M., DALTON, P. D. & BROOK, G. A. 2009. Human neural cell interactions with orientated electrospun nanofibers in vitro. *Nanomedicine,* 4**,** 11-30.

GHASEMI-MOBARAKEH, L., PRABHAKARAN, M. P., MORSHED, M., NASR-ESFAHANI, M. H. & RAMAKRISHNA, S. 2008. Electrospun poly(epsilon-caprolactone)/gelatin nanofibrous scaffolds for nerve tissue engineering. *Biomaterials,* 29**,** 4532-4539.

Gondim, F. De A., Thomas, F.P., 2009. Spinal Cord, Topographical and Functional Anatomy [online]. Available from: http://emedicine.medscape.com/article/1148570-overview [19 October 2010].

GRILL, R., MURAI, K., BLESCH, A., GAGE, F. H. & TUSZYNSKI, M. H. 1997. Cellular delivery of neurotrophin-3 promotes corticospinal axonal growth and partial functional recovery after spinal cord injury. *J Neurosci,* 17**,** 5560-72.

GRIMPE, B. & SILVER, J. 2002. The extracellular matrix in axon regeneration. *Prog Brain Res,* 137**,** 333-49.

GRISWOLD, K.A., PRESTIGIAMO, C.J., 17th Feb 2011, United States patent application publication, SYSTEM AND METHOD FOR ELECTROSPUN DRUG LOADED BIODEGRADABLE CHEMOTHERAPY. Pub.No.: US 2011/0038936 A1.GUNN, J. & ZHANG, M. Q. 2010. Polyblend nanofibers for biomedical applications: perspectives and challenges. *Trends in Biotechnology,* 28**,** 189-197.

GUNN, J. W., TURNER, S. D. & MANN, B. K. 2005. Adhesive and mechanical properties of hydrogels influence neurite extension. *J Biomed Mater Res A,* 72**,** 91-7.

GUPTA, D., VENUGOPAL, J., MITRA, S., GIRI DEV, V. R. & RAMAKRISHNA, S. 2009. Nanostructured biocomposite substrates by electrospinning and electrospraying for the mineralization of osteoblasts. *Biomaterials*.

HADLOCK, T., ELISSEEFF, J., LANGER, R., VACANTI, J. & CHENEY, M. 1998. A tissue-engineered conduit for peripheral nerve repair. *Arch Otolaryngol Head Neck Surg,* 124**,** 1081-6.

HALL, E. D. & SPRINGER, J. E. 2004. Neuroprotection and acute spinal cord injury: a reappraisal. *NeuroRx,* 1**,** 80-100.

HAN, D. W., SUB LEE, M., PARK, B. J., KIM, J. K. & PARK, J. C. 2005. Enhanced neurite outgrowth of rat neural cortical cells on surface-modified films of poly(lactic-co-glycolic acid). *Biotechnol Lett,* 27**,** 53-8.

HAQ, F., KEITH, C. & ZHANG, G. 2006. Neurite development in PC12 cells on flexible micro-textured substrates under cyclic stretch. *Biotechnol Prog,* 22**,** 133-40.

HARTGERINK, J. D., BENIASH, E. & STUPP, S. I. 2001. Self-assembly and mineralization of peptide-amphiphile nanofibers. *Science,* 294**,** 1684-1688.

HAYMAN, E. G., PIERSCHBACHER, M. D., SUZUKI, S. & RUOSLAHTI, E. 1985. Vitronectin--a major cell attachment-promoting protein in fetal bovine serum. *Exp Cell Res,* 160**,** 245-58.

HE, L., ZHANG, Y., ZENG, C., NGIAM, M., LIAO, S., QUAN, D., ZENG, Y., LU, J. & RAMAKRISHNA, S. 2009. Manufacture of PLGA multiple-channel conduits with precise hierarchical pore architectures and in vitro/vivo evaluation for spinal cord injury. *Tissue Eng Part C Methods,* 15**,** 243-55.

HEYDARKHAN-HAGVALL, S., SCHENKE-LAYLAND, K., DHANASOPON, A. P., ROFAIL, F., SMITH, H., WU, B. M., SHEMIN, R., BEYGUI, R. E. & MACLELLAN, W. R. 2008. Three-dimensional electrospun ECM-based hybrid scaffolds for cardiovascular tissue engineering. *Biomaterials,* 29**,** 2907-14.

HIMES, B. T., LIU, Y., SOLOWSKA, J. M., SNYDER, E. Y., FISCHER, I. & TESSLER, A. 2001. Transplants of cells genetically modified to express neurotrophin-3 rescue axotomized Clarke's nucleus neurons after spinal cord hemisection in adult rats. *Journal of Neuroscience Research,* 65**,** 549-564.

HIRSCHBERG, D. L. & SCHWARTZ, M. 1995. Macrophage Recruitment to Acutely Injured Central-Nervous-System Is Inhibited by a Resident Factor - a Basis for an Immune Brain Barrier. *Journal of Neuroimmunology,* 61**,** 89-96.

HO, M. H., LEE, J. J., FAN, S. C., WANG, D. M., HOU, L. T., HSIEH, H. J. & LAI, J. Y. 2007. Efficient modification on PLLA by ozone treatment for biomedical applications. *Macromolecular Bioscience,* 7**,** 467-474.

HOLMES, T. C., DE LACALLE, S., SU, X., LIU, G., RICH, A. & ZHANG, S. 2000. Extensive neurite outgrowth and active synapse formation on self-assembling peptide scaffolds. *Proc Natl Acad Sci U S A,* 97**,** 6728-33.

HOUCHIN-RAY, T., SWIFT, L. A., JANG, J. H. & SHEA, L. D. 2007. Patterned PLG substrates for localized DNA delivery and directed neurite extension. *Biomaterials,* 28**,** 2603-11.

HOUCHIN, M. L., NEUENSWANDER, S. A. & TOPP, E. M. 2007. Effect of excipients on PLGA film degradation and the stability of an incorporated peptide. *Journal of Controlled Release,* 117**,** 413-420.

HUDSON, T. W., EVANS, G. R. & SCHMIDT, C. E. 1999. Engineering strategies for peripheral nerve repair. *Clin Plast Surg,* 26**,** 617-28, ix.

JOSE, M. V., THOMAS, V., JOHNSON, K. T., DEAN, D. R. & NYAIRO, E. 2009. Aligned PLGA/HA nanofibrous nanocomposite scaffolds for bone tissue engineering. *Acta Biomater,* 5**,** 305-15.

KAM, L., SHAIN, W., TURNER, J. N. & BIZIOS, R. 2001. Axonal outgrowth of hippocampal neurons on micro-scale networks of polylysine-conjugated laminin. *Biomaterials,* 22**,** 1049-1054.

KANO, T., KATAYAMA, Y., FUKUDA, S., SHIMOJI, K., WILLIS, W. D. & WILLIS, W. D. 2006. Physiology of the Spinal Cord. *Evoked Spinal Cord Potentials.* Springer Japan.

KATTI, D. S., ROBINSON, K. W., KO, F. K. & LAURENCIN, C. T. 2004. Bioresorbable nanofiber-based systems for wound healing and drug delivery: Optimization of fabrication parameters. *Journal of Biomedical Materials Research Part B-Applied Biomaterials,* 70B**,** 286-296.

KAUSHIVA, A., TURZHITSKY, V. M., DARMOC, M., BACKMAN, V. & AMEER, G. A. 2007. A biodegradable vascularizing membrane: a feasibility study. *Acta Biomater,* 3**,** 631-42.

KENAWY, E. R., BOWLIN, G. L., MANSFIELD, K., LAYMAN, J., SANDERS, E., SIMPSON, D. G. & WNEK, G. E. 2002. Release of tetracycline hydrochloride from electrospun polymers. *Abstracts of Papers of the American Chemical Society,* 223**,** C115-C115.

KHAFAGY, E. S., MORISHITA, M., ONUKI, Y. & TAKAYAMA, K. 2007. Current challenges in non-invasive insulin delivery systems: A comparative review. *Advanced Drug Delivery Reviews,* 59**,** 1521-1546.

KHAN, S. P., AUNER, G. G. & NEWAZ, G. M. 2005. Influence of nanoscale surface roughness on neural cell attachment on silicon. *Nanomedicine,* 1**,** 125-9.

KIDOAKI, S., KWON, I. K. & MATSUDA, T. 2005. Mesoscopic spatial designs of nano- and microfiber meshes for tissue-engineering matrix and scaffold based on newly devised multilayering and mixing electrospinning techniques. *Biomaterials,* 26**,** 37-46.

KIM, C. H., BAE, J. H., SON, S., KIM, J. H., LEE, J. G. & YOON, J. H. 2006a. Use of PLGA scaffold for mucociliary epithelium transfer in airway reconstruction: a preliminary study. *Acta Oto-Laryngologica,* 126**,** 594-599.

KIM, I. A., PARK, S. A., KIM, Y. J., KIM, S. H., SHIN, H. J., LEE, Y. J., KANG, S. G. & SHIN, J. W. 2006b. Effects of mechanical stimuli and microfiber-based substrate on neurite outgrowth and guidance. *Journal of Bioscience and Bioengineering,* 101**,** 120-126.

KIM, T. G. & PARK, T. G. 2006. Biomimicking extracellular matrix: Cell adhesive RGD peptide modified electrospun poly(D,L-lactic-Co-glycolic acid) nanofiber mesh. *Tissue Engineering,* 12**,** 221-233.

KISHAN, S., VIVES, M. J. & REITER, M. F. 2005. Timing of surgery following spinal cord injury. *J Spinal Cord Med,* 28**,** 11-9.

KLEINFELD, D., KAHLER, K. H. & HOCKBERGER, P. E. 1988. Controlled outgrowth of dissociated neurons on patterned substrates. *J Neurosci,* 8**,** 4098-120.

KO, Y. G., KIM, Y. H., PARK, K. D., LEE, H. J., LEE, W. K., PARK, H. D., KIM, S. H., LEE, G. S. & AHN, D. J. 2001. Immobilization of poly(ethylene glycol) or its sulfonate onto polymer surfaces by ozone oxidation. *Biomaterials,* 22**,** 2115-2123.

KORKMAZ, M., GUVENC, B. H., BILIR, A., KARAL-YILMAZ, O., KUMBASAR, A., CAFERLER, J. & BAYSAL, K. 2003. Isolation and culture of adult and fetal rabbit bladder smooth muscle cells and their interaction with biopolymers. *J Pediatr Surg,* 38**,** 21-4.

KOSE, G. T., KENAR, H., HASIRCI, N. & HASIRCI, V. 2003. Macroporous poly(3-hydroxybutyrate-co-3-hydroxyvalerate) matrices for bone tissue engineering. *Biomaterials,* 24**,** 1949-1958.

KOTTIS, V., THIBAULT, P., MIKOL, D., XIAO, Z. C., ZHANG, R., DERGHAM, P. & BRAUN, P. E. 2002. Oligodendrocyte-myelin glycoprotein (OMgp) is an inhibitor of neurite outgrowth. *Journal of Neurochemistry,* 82**,** 1566-1569.

LAMOUR, G., JOURNIAC, N., SOUES, S., BONNEAU, S., NASSOY, P. & HAMRAOUI, A. 2009. Influence of surface energy distribution on neuritogenesis. *Colloids Surf B Biointerfaces,* 72**,** 208-18.

LEACH, J. B., BROWN, X. Q., JACOT, J. G., DIMILLA, P. A. & WONG, J. Y. 2007. Neurite outgrowth and branching of PC12 cells on very soft substrates sharply decreases below a threshold of substrate rigidity. *J Neural Eng,* 4**,** 26-34.

LEBARON, R. G. & ATHANASIOU, K. A. 2000. Extracellular matrix cell adhesion peptides: functional applications in orthopedic materials. *Tissue Eng,* 6**,** 85-103.

LEE, J. Y., BASHUR, C. A., GOLDSTEIN, A. S. & SCHMIDT, C. E. 2009. Polypyrrole-coated electrospun PLGA nanofibers for neural tissue applications. *Biomaterials,* 30**,** 4325-4335.

LEVINE, J. M., REYNOLDS, R. & FAWCETT, J. W. 2001. The oligodendrocyte precursor cell in health and disease. *Trends Neurosci,* 24**,** 39-47.

LHOEST, J. B., DETRAIT, E., DEWEZ, J. L., DEAGUILAR, P. V. & BERTRAND, P. 1996. A new plasma-based method to promote cell adhesion on micrometric tracks on polystyrene substrates. *Journal of Biomaterials Science-Polymer Edition,* 7**,** 1039-1054.

LI, D., OUYANG, G., MCCANN, J. T. & XIA, Y. 2005. Collecting electrospun nanofibers with patterned electrodes. *Nano Lett,* 5**,** 913-6.

LI, D. & XIA, Y. N. 2004. Electrospinning of nanofibers: Reinventing the wheel? *Advanced Materials,* 16**,** 1151-1170.

LI, W. J., LAURENCIN, C. T., CATERSON, E. J., TUAN, R. S. & KO, F. K. 2002. Electrospun nanofibrous structure: a novel scaffold for tissue engineering. *J Biomed Mater Res,* 60**,** 613-21.

LIANG, D., HSIAO, B. S. & CHU, B. 2007. Functional electrospun nanofibrous scaffolds for biomedical applications. *Advanced Drug Delivery Reviews,* 59**,** 1392-1412.

LIAO, Y. L., ZHANG, L. F., GAO, Y., ZHU, Z. T. & FONG, H. 2008. Preparation, characterization, and encapsulation/release studies of a composite nanofiber mat electrospun from an emulsion containing poly(lactic-co-glycolic acid). *Polymer,* 49**,** 5294-5299.

LIESI, P. 1985. Do neurons in the vertebrate CNS migrate on laminin? *Embo J,* 4**,** 1163-70.

LIU, X. H., SMITH, L., WEI, G. B., WON, Y. J. & MA, P. X. 2005. Surface Engineering of Nano-Fibrous Poly(L-Lactic Acid) Scaffolds via Self-Assembly Technique for Bone Tissue Engineering. *Journal of Biomedical Nanotechnology,* 1**,** 54-60.

Liverman, C. T., Altevogt B.M., Joy J. E., Johnson R.T., 2005. Spinal Cord Injury: Progress, Promise, and Priorities [online]. THE NATIONAL ACADEMIES PRESS, Washington, D.C. Available from: http://books.nap.edu/openbook.php?record_id=11253&utm_source=WID%8615323159201010197442 8&utm_medium=Widgetv3&utm_content=11253&utm_campaign=Widget&utm_term=homeview [Accessed 19 October 2010].

LOCHTER, A., TAYLOR, J., BRAUNEWELL, K. H., HOLM, J. & SCHACHNER, M. 1995. Control of Neuronal Morphology in-Vitro - Interplay between Adhesive Substrate Forces and Molecular Instruction. *Journal of Neuroscience Research,* 42**,** 145-158.

LU, L., PETER, S. J., LYMAN, M. D., LAI, H. L., LEITE, S. M., TAMADA, J. A., UYAMA, S., VACANTI, J. P., LANGER, R. & MIKOS, A. G. 2000. In vitro and in vivo degradation of porous poly(DL-lactic-co-glycolic acid) foams. *Biomaterials,* 21**,** 1837-45.

LU, P., JONES, L. L. & TUSZYNSKI, M. H. 2005. BDNF-expressing marrow stromal cells support extensive axonal growth at sites of spinal cord injury. *Exp Neurol,* 191**,** 344-60.

MAHONEY, M. J., CHEN, R. R., TAN, J. & SALTZMAN, W. M. 2005. The influence of microchannels on neurite growth and architecture. *Biomaterials,* 26**,** 771-8.

MAKOHLISO, S. A., VALENTINI, R. F. & AEBISCHER, P. 1993. Magnitude and polarity of a fluoroethylene propylene electret substrate charge influences neurite outgrowth in vitro. *J Biomed Mater Res,* 27**,** 1075-85.

MARTINS, A., REIS, R. L. & NEVES, N. M. 2008. Electrospinning: processing technique for tissue engineering scaffolding. *International Materials Reviews,* 53**,** 257-274.

MASSIA, S. P., HOLECKO, M. M. & EHTESHAMI, G. R. 2004. In vitro assessment of bioactive coatings for neural implant applications. *Journal of Biomedical Materials Research Part A,* 68A**,** 177-186.

MASSIA, S. P., RAO, S. S. & HUBBELL, J. A. 1993. Covalently immobilized laminin peptide Tyr-Ile-Gly-Ser-Arg (YIGSR) supports cell spreading and co-

localization of the 67-kilodalton laminin receptor with alpha-actinin and vinculin. *Journal of Biological Chemistry,* 268**,** 8053-8059.

MATSUMOTO, K., OHNISHI, K., KIYOTANI, T., SEKINE, T., UEDA, H., NAKAMURA, T., ENDO, K. & SHIMIZU, Y. 2000. Peripheral nerve regeneration across an 80-mm gap bridged by a polyglycolic acid (PGA)-collagen tube filled with laminin-coated collagen fibers: a histological and electrophysiological evaluation of regenerated nerves. *Brain Res,* 868**,** 315-28.

MAYER, J., KARAMUK, E., AKAIKE, T. & WINTERMANTEL, E. 2000. Matrices for tissue engineering-scaffold structure for a bioartificial liver support system. *J Control Release,* 64**,** 81-90.

MCDONALD, J. W. & SADOWSKY, C. 2002. Spinal-cord injury. *Lancet,* 359**,** 417-25.

McKeehan, W.L., 1984. Methods for Preparation of Media, Supplements, and
Substrata for Serum-free Animal Cell Culture, A.R. Liss, NY p.209.

MCKEON, R. J., SCHREIBER, R. C., RUDGE, J. S. & SILVER, J. 1991. Reduction of neurite outgrowth in a model of glial scarring following CNS injury is correlated with the expression of inhibitory molecules on reactive astrocytes. *J Neurosci,* 11**,** 3398-411.

MCKERRACHER, L. 2001. Spinal cord repair: strategies to promote axon regeneration. *Neurobiol Dis,* 8**,** 11-8.

MCKERRACHER, L., DAVID, S., JACKSON, D. L., KOTTIS, V., DUNN, R. J. & BRAUN, P. E. 1994. Identification of myelin-associated glycoprotein as a major myelin-derived inhibitor of neurite growth. *Neuron,* 13**,** 805-11.

MCKINLEY, W. O., JACKSON, A. B., CARDENAS, D. D. & DEVIVO, M. J. 1999. Long-term medical complications after traumatic spinal cord injury: a regional model systems analysis. *Arch Phys Med Rehabil,* 80**,** 1402-10.

MENEI, P., MONTERO-MENEI, C., WHITTEMORE, S. R., BUNGE, R. P. & BUNGE, M. B. 1998. Schwann cells genetically modified to secrete human BDNF promote enhanced axonal regrowth across transected adult rat spinal cord. *European Journal of Neuroscience,* 10**,** 607-621.

MENET, V., GIMENEZ Y RIBOTTA, M., CHAUVET, N., DRIAN, M. J., LANNOY, J., COLUCCI-GUYON, E. & PRIVAT, A. 2001. Inactivation of the glial fibrillary acidic protein gene, but not that of vimentin, improves neuronal survival and neurite growth by modifying adhesion molecule expression. *J Neurosci,* 21**,** 6147-58.

MENG, W., KIM, S. Y., YUAN, J., KIM, J. C., KWON, O. H., KAWAZOE, N., CHEN, G. P., ITO, Y. & KANG, I. K. 2007. Electrospun PHBV/collagen composite nanofibrous scaffolds for tissue engineering. *Journal of Biomaterials Science-Polymer Edition,* 18**,** 81-94.

MICELI, M. V., NEWSOME, D. A. & TATE, D. J., JR. 1997. Vitronectin is responsible for serum-stimulated uptake of rod outer segments by cultured retinal pigment epithelial cells. *Invest Ophthalmol Vis Sci,* 38**,** 1588-97.

MINGYU, C., KAI, G., JIAMOU, L., YANDAO, G., NANMING, Z. & XIUFANG, Z. 2004. Surface modification and characterization of chitosan film blended with poly-L-lysine. *J Biomater Appl,* 19**,** 59-75.

MIRZA, S. K., KRENGEL, W. F., 3RD, CHAPMAN, J. R., ANDERSON, P. A., BAILEY, J. C., GRADY, M. S. & YUAN, H. A. 1999. Early versus delayed surgery for acute cervical spinal cord injury. *Clin Orthop Relat Res*, 104-14.

MOCHIZUKI, M., YAMAGATA, N., PHILP, D., HOZUMI, K., WATANABE, T., KIKKAWA, Y., KADOYA, Y., KLEINMAN, H. K. & NOMIZU, M. 2007. Integrin-dependent cell behavior on ECM peptide-conjugated chitosan membranes. *Biopolymers,* 88, 122-130.

MOROZOV, V. N., MOROZOVA, T. Y. & KALLENBACH, N. R. 1998. Atomic force microscopy of structures produced by electrospraying polymer solutions. *International Journal of Mass Spectrometry,* 178, 143-159.

MUKHOPADHYAY, G., DOHERTY, P., WALSH, F. S., CROCKER, P. R. & FILBIN, M. T. 1994. A Novel Role for Myelin-Associated Glycoprotein as an Inhibitor of Axonal Regeneration. *Neuron,* 13, 757-767.

NEAL, R. A., MCCLUGAGE, S. G., LINK, M. C., SEFCIK, L. S., OGLE, R. C. & BOTCHWEY, E. A. 2009. Laminin Nanofiber Meshes That Mimic Morphological Properties and Bioactivity of Basement Membranes. *Tissue Engineering Part C-Methods,* 15, 11-21.

NICOLI ALDINI, N., FINI, M., ROCCA, M., GIAVARESI, G. & GIARDINO, R. 2000. Guided regeneration with resorbable conduits in experimental peripheral nerve injuries. *Int Orthop,* 24, 121-5.

NIE, H. M., KHEW, S. T., LEE, L. Y., POH, K. L., TONG, Y. W. & WANG, C. H. 2009. Lysine-based peptide-functionalized PLGA foams for controlled DNA delivery. *Journal of Controlled Release,* 138, 64-70.

NISBET, D. R., PATTANAWONG, S., RITCHIE, N. E., SHEN, W., FINKELSTEIN, D. I., HORNE, M. K. & FORSYTHE, J. S. 2007. Interaction of embryonic cortical neurons on nanofibrous scaffolds for neural tissue engineering. *J Neural Eng,* 4, 35-41.

NOJEHDEHIAN, H., MOZTARZADEH, F., BAHARVAND, H., MEHRJERDI, N. Z., NAZARIAN, H. & TAHRIRI, M. Effect of poly-L-lysine coating on retinoic acid-loaded PLGA microspheres in the differentiation of carcinoma stem cells into neural cells. *Int J Artif Organs,* 33, 721-30.

NOMURA, H., TATOR, C. H. & SHOICHET, M. S. 2006. Bioengineered strategies for spinal cord repair. *J Neurotrauma,* 23, 496-507.

O'SHEA, K. S., LIU, L. H. & DIXIT, V. M. 1991. Thrombospondin and a 140 kd fragment promote adhesion and neurite outgrowth from embryonic central and peripheral neurons and from PC12 cells. *Neuron,* 7, 231-7.

OERTLE, T., VAN DER HAAR, M. E., BANDTLOW, C. E., ROBEVA, A., BURFEIND, P., BUSS, A., HUBER, A. B., SIMONEN, M., SCHNELL, L., BROSAMLE, C., KAUPMANN, K., VALLON, R. & SCHWAB, M. E. 2003. Nogo-A inhibits neurite outgrowth and cell spreading with three discrete regions. *Journal of Neuroscience,* 23, 5393-5406.

OUDEGA, M., GAUTIER, S. E., CHAPON, P., FRAGOSO, M., BATES, M. L., PAREL, J. M. & BUNGE, M. B. 2001. Axonal regeneration into Schwann cell grafts within resorbable poly(alpha-hydroxyacid) guidance channels in the adult rat spinal cord. *Biomaterials,* 22, 1125-36.

PANSERI, S., CUNHA, C., LOWERY, J., DEL CARRO, U., TARABALLI, F., AMADIO, S., VESCOVI, A. & GELAIN, F. 2008. Electrospun micro- and nanofiber tubes for functional nervous regeneration in sciatic nerve transections. *Bmc Biotechnology,* 8**,** -.

PARK, A., WU, B. & GRIFFITH, L. G. 1998. Integration of surface modification and 3D fabrication techniques to prepare patterned poly(L-lactide) substrates allowing regionally selective cell adhesion. *J Biomater Sci Polym Ed,* 9**,** 89-110.

PARK, K. S., KIM, S. M., KIM, M. S., LEE, I., RHEE, J. M., LEE, H. B. & KHANG, G. 2008. Effect of cell-adhesive-molecule-coated poly(lactide-co-glycolide) film on the cellular Behaviors of olfactory ensheathing cells and Schwann cells. *Journal of Applied Polymer Science,* 107**,** 1243-1251.

PASTERKAMP, R. J., RUITENBERG, M. J. & VERHAAGEN, J. 1999. Semaphorins and their receptors in olfactory axon guidance. *Cell Mol Biol (Noisy-le-grand),* 45**,** 763-79.

PATEL, S., KURPINSKI, K., QUIGLEY, R., GAO, H., HSIAO, B. S., POO, M. M. & LI, S. 2007. Bioactive nanofibers: synergistic effects of nanotopography and chemical signaling on cell guidance. *Nano Lett,* 7**,** 2122-8.

PIOTROWICZ, A. & SHOICHET, M. S. 2006. Nerve guidance channels as drug delivery vehicles. *Biomaterials,* 27**,** 2018-27.

QI, H. X., HU, P., XU, J. & WANG, A. J. 2006. Encapsulation of drug reservoirs in fibers by emulsion electrospinning: Morphology characterization and preliminary release assessment. *Biomacromolecules,* 7**,** 2327-2330.

QUENCER, R. M. & BUNGE, R. P. 1996. The injured spinal cord: imaging, histopathologic clinical correlates, and basic science approaches to enhancing neural function after spinal cord injury. *Spine,* 21**,** 2064-6.

RANIERI, J. P., BELLAMKONDA, R., BEKOS, E. J., GARDELLA, J. A., JR., MATHIEU, H. J., RUIZ, L. & AEBISCHER, P. 1994. Spatial control of neuronal cell attachment and differentiation on covalently patterned laminin oligopeptide substrates. *Int J Dev Neurosci,* 12**,** 725-35.

RANIERI, J. P., BELLAMKONDA, R., BEKOS, E. J., VARGO, T. G., GARDELLA, J. A., JR. & AEBISCHER, P. 1995. Neuronal cell attachment to fluorinated ethylene propylene films with covalently immobilized laminin oligopeptides YIGSR and IKVAV. II. *J Biomed Mater Res,* 29**,** 779-85.

RAO, S. S. & WINTER, J. O. 2009. Adhesion molecule-modified biomaterials for neural tissue engineering. *Front Neuroeng,* 2**,** 6.

RHO, K. S., JEONG, L., LEE, G., SEO, B. M., PARK, Y. J., HONG, S. D., ROH, S., CHO, J. J., PARK, W. H. & MIN, B. M. 2006. Electrospinning of collagen nanofibers: Effects on the behavior of normal human keratinocytes and early-stage wound healing. *Biomaterials,* 27**,** 1452-1461.

RIES, M. D. 2003. Complications in primary total hip arthroplasty: avoidance and management: wear. *Instr Course Lect,* 52**,** 257-65.

RUNGE, M. B., DADSETAN, M., BALTRUSAITIS, J., KNIGHT, A. M., RUESINK, T., LAZCANO, E. A., LU, L. C., WINDEBANK, A. J. & YASZEMSKI, M. J. 2010. The development of electrically conductive polycaprolactone fumarate-

polypyrrole composite materials for nerve regeneration. *Biomaterials,* 31**,** 5916-5926.

SAHA, K., KEUNG, A. J., IRWIN, E. F., LI, Y., LITTLE, L., SCHAFFER, D. V. & HEALY, K. E. 2008. Substrate Modulus Directs Neural Stem Cell Behavior. *Biophysical Journal,* 95**,** 4426-4438.

SANTIAGO, L. Y., NOWAK, R. W., PETER RUBIN, J. & MARRA, K. G. 2006. Peptide-surface modification of poly(caprolactone) with laminin-derived sequences for adipose-derived stem cell applications. *Biomaterials,* 27**,** 2962-9.

SCHENSE, J. C., BLOCH, J., AEBISCHER, P. & HUBBELL, J. A. 2000. Enzymatic incorporation of bioactive peptides into fibrin matrices enhances neurite extension. *Nat Biotechnol,* 18**,** 415-9.

SCHMIDT, C. E. & LEACH, J. B. 2003. Neural tissue engineering: strategies for repair and regeneration. *Annu Rev Biomed Eng,* 5**,** 293-347.

SCHMIDT, C. E., SHASTRI, V. R., VACANTI, J. P. & LANGER, R. 1997. Stimulation of neurite outgrowth using an electrically conducting polymer. *Proc Natl Acad Sci U S A,* 94**,** 8948-53.

SCHNELL, E., KLINKHAMMER, K., BALZER, S., BROOK, G., KLEE, D., DALTON, P. & MEY, J. 2007. Guidance of glial cell. migration and axonal growth on electrospun nanofibers of poly-epsilon-caprolactone and a collagen/poly-epsilon-caprolactone blend. *Biomaterials,* 28**,** 3012-3025.

SCHWAB, M. E. 2004. Nogo and axon regeneration. *Curr Opin Neurobiol,* 14**,** 118-24.

SCHWAB, M. E. & BARTHOLDI, D. 1996. Degeneration and regeneration of axons in the lesioned spinal cord. *Physiological Reviews,* 76**,** 319-370.

SEKHON, L. H. S. & FEHLINGS, M. G. 2001. Epidemiology, demographics, and pathophysiology of acute spinal cord injury. *Spine,* 26**,** S2-S12.

SHARON, J. L. & PULEO, D. A. 2008. The use of N-terminal immobilization of PTH(1-34) on PLGA to enhance bioactivity. *Biomaterials,* 29**,** 3137-3142.

SHIN, Y. M., HOHMAN, M. M., BRENNER, M. P. & RUTLEDGE, G. C. 2001. Electrospinning: A whipping fluid jet generates submicron polymer fibers. *Applied Physics Letters,* 78**,** 1149-1151.

Shorgen, R.L., Bagley, E.B., 1999. Natural polymers as advanced materials: some research needs and directions. *In*: Imam, S.H., Greene, R.V., Zaidi, B.R., *Biopolymers: Utilizing Nature's Advanced Materials*. Washington, DC: American Chemical Society, pp 2-11.

SILVA, G. A., CZEISLER, C., NIECE, K. L., BENIASH, E., HARRINGTON, D. A., KESSLER, J. A. & STUPP, S. I. 2004. Selective differentiation of neural progenitor cells by high-epitope density nanofibers. *Science,* 303**,** 1352-5.

SJOLUND, B. H. 2002. Pain and rehabilitation after spinal cord injury: the case of sensory spasticity? *Brain Res Brain Res Rev,* 40**,** 250-6.

SOLDANI, G., VARELLI, G., MINNOCCI, A. & DARIO, P. 1998. Manufacturing and microscopical characterisation of polyurethane nerve guidance channel featuring a highly smooth internal surface. *Biomaterials,* 19**,** 1919-24.

STOKOLS, S. & TUSZYNSKI, M. H. 2006. Freeze-dried agarose scaffolds with uniaxial channels stimulate and guide linear axonal growth following spinal cord injury. *Biomaterials,* 27**,** 443-51.

STYLIANOPOULOS, T., BASHUR, C. A., GOLDSTEIN, A. S., GUELCHER, S. A. & BAROCAS, V. H. 2008. Computational predictions of the tensile properties of electrospun fibre meshes: effect of fibre diameter and fibre orientation. *J Mech Behav Biomed Mater,* 1**,** 326-35.

SU, Y., LI, X. Q., LIU, S. P., MO, X. M. & RAMAKRISHNA, S. 2009. Controlled release of dual drugs from emulsion electrospun nanofibrous mats. *Colloids and Surfaces B-Biointerfaces,* 73**,** 376-381.

SUN, T., NORTON, D., MCKEAN, R. J., HAYCOCK, J. W., RYAN, A. J. & MACNEIL, S. 2007. Development of a 3D cell culture system for investigating cell interactions with electrospun fibers. *Biotechnology and Bioengineering,* 97**,** 1318-1328.

SUNDBACK, C., HADLOCK, T., CHENEY, M. & VACANTI, J. 2003. Manufacture of porous polymer nerve conduits by a novel low-pressure injection molding process. *Biomaterials,* 24**,** 819-30.

SY, J. C., KLEMM, A. S. & SHASTRI, V. P. 2009. Emulsion as a Means of Controlling Electrospinning of Polymers. *Advanced Materials,* 21**,** 1814-+.

Symon, K.R., 1971. Mechanics. 3rd ed.

TAI, H. C. & BUETTNER, H. M. 1998. Neurite outgrowth and growth cone morphology on micropatterned surfaces. *Biotechnol Prog,* 14**,** 364-70.

TAN, J. & SALTZMAN, W. M. 2002. Topographical control of human neutrophil motility on micropatterned materials with various surface chemistry. *Biomaterials,* 23**,** 3215-25.

TATARD, V. M., VENIER-JULIENNE, M. C., SAULNIER, P., PRECHTER, E., BENOIT, J. P., MENEI, P. & MONTERO-MENEI, C. N. 2005. Pharmacologically active microcarriers: a tool for cell therapy. *Biomaterials,* 26**,** 3727-3737.

TATOR, C. H. 1998. Biology of neurological recovery and functional restoration after spinal cord injury. *Neurosurgery,* 42**,** 696-707; discussion 707-8.

TENG, Y. D., LAVIK, E. B., QU, X., PARK, K. I., OUREDNIK, J., ZURAKOWSKI, D., LANGER, R. & SNYDER, E. Y. 2002. Functional recovery following traumatic spinal cord injury mediated by a unique polymer scaffold seeded with neural stem cells. *Proc Natl Acad Sci U S A,* 99**,** 3024-9.

The National SCI Statistical Center, 2009. *Spinal Cord Injury Facts and Figures at a Glance* [online]. Birmingham, AL. Available from: https://www.nscisc.uab.edu/public_content/pdf/Facts%20and%20Figures%20at%20a%20Glance%202010.pdf [Accessed 19 October20 10].

Thermo Fischer Scientific Inc, 2011, Chemistry of Crosslinking [online]. Rockford, IL USA. Availablefrom: http://www.piercenet.com/Proteomics/browse.cfm?fldID=CE4D6C5C-5946-4814-9904-C46E01232683

THOMPSON, D. M. & BUETTNER, H. M. 2004. Oriented Schwann cell monolayers for directed neurite outgrowth. *Annals of Biomedical Engineering,* 32**,** 1120-1130.

THOMSON, C. E., HUNTER, A. M., GRIFFITHS, I. R., EDGAR, J. M. & MCCULLOCH, M. C. 2006. Murine spinal cord explants: A model for evaluating axonal growth and myelination in vitro. *Journal of Neuroscience Research,* 84**,** 1703-1715.

TIMPL, R., ROHDE, H., ROBEY, P. G., RENNARD, S. I., FOIDART, J. M. & MARTIN, G. R. 1979. Laminin--a glycoprotein from basement membranes. *J Biol Chem,* 254**,** 9933-7.

TOMASELLI, K. J., DAMSKY, C. H. & REICHARDT, L. F. 1987. Interactions of a Neuronal Cell-Line (Pc12) with Laminin, Collagen-Iv, and Fibronectin - Identification of Integrin-Related Glycoproteins Involved in Attachment and Process Outgrowth. *Journal of Cell Biology,* 105**,** 2347-2358.

TOMBRAN-TINK, J. & JOHNSON, L. V. 1989. Neuronal differentiation of retinoblastoma cells induced by medium conditioned by human RPE cells. *Investigative Ophthalmology & Visual Science,* 30**,** 1700-1707.

TONG, H. W. & WANG, M. 2007. Electrospinning of aligned biodegradable polymer fibers and composite fibers for tissue engineering applications. *J Nanosci Nanotechnol,* 7**,** 3834-40.

TYSSELING-MATTIACE, V. M., SAHNI, V., NIECE, K. L., BIRCH, D., CZEISLER, C., FEHLINGS, M. G., STUPP, S. I. & KESSLER, J. A. 2008. Self-assembling nanofibers inhibit glial scar formation and promote axon elongation after spinal cord injury. *J Neurosci,* 28**,** 3814-23.

VALENTINI, R. F., VARGO, T. G., GARDELLA, J. A. & AEBISCHER, P. 1993. Patterned Neuronal Attachment and Outgrowth on Surface-Modified, Electrically Charged Fluoropolymer Substrates. *Journal of Biomaterials Science-Polymer Edition,* 5**,** 13-36.

VALMIKINATHAN, C. M., TIAN, J., WANG, J. & YU, X. 2008. Novel nanofibrous spiral scaffolds for neural tissue engineering. *J Neural Eng,* 5**,** 422-32.

VANDERHAEGHEN, P. & CHENG, H. J. 2010. Guidance molecules in axon pruning and cell death. *Cold Spring Harb Perspect Biol,* 2**,** a001859.

VELARDO, M. J., BURGER, C., WILLIAMS, P. R., BAKER, H. V., LOPEZ, M. C., MARECI, T. H., WHITE, T. E., MUZYCZKA, N. & REIER, P. J. 2004. Patterns of gene expression reveal a temporally orchestrated wound healing response in the injured spinal cord. *J Neurosci,* 24**,** 8562-76.

VENSTROM, K. A. & REICHARDT, L. F. 1993. Extracellular matrix. 2: Role of extracellular matrix molecules and their receptors in the nervous system. *Faseb J,* 7**,** 996-1003.

WADDELL, R. L., MARRA, K. G., COLLINS, K. L., LEUNG, J. T. & DOCTOR, J. S. 2003. Using PC12 cells to evaluate poly(caprolactone) and collagenous microcarriers for applications in nerve guide fabrication. *Biotechnol Prog,* 19**,** 1767-74.

WALD, H. L., SARAKINOS, G., LYMAN, M. D., MIKOS, A. G., VACANTI, J. P. & LANGER, R. 1993. Cell seeding in porous transplantation devices. *Biomaterials,* 14**,** 270-8.

WANNATONG, L., SIRIVAT, A., SUPAPHOL, P. 2004 Effects of solvents on electrospun polymeric fibers: preliminary study on polystyrene. *Polymer International,* 53, 1851-1859.

WANG, J. H., HUNG, C. H. & YOUNG, T. H. 2006. Proliferation and differentiation of neural stem cells on lysine-alanine sequential polymer substrates. *Biomaterials,* 27**,** 3441-50.

WEI, Z. & GU, Z. 2001. A study of one-bath alkali–amine hydrolysis and silk-fibroin finishing of polyester microfiber crepe fabric. *Journal of Applied Polymer Science,* 81**,** 1467-1473.

WILLERTH, S. M. & SAKIYAMA-ELBERT, S. E. 2007. Approaches to neural tissue engineering using scaffolds for drug delivery. *Adv Drug Deliv Rev,* 59**,** 325-38.

WILLIAMS, C. G., MALIK, A. N., KIM, T. K., MANSON, P. N. & ELISSEEFF, J. H. 2005. Variable cytocompatibility of six cell lines with photoinitiators used for polymerizing hydrogels and cell encapsulation. *Biomaterials,* 26**,** 1211-1218.

WOERLY, S., DOAN, V. D., EVANS-MARTIN, F., PARAMORE, C. G. & PEDUZZI, J. D. 2001. Spinal cord reconstruction using NeuroGel implants and functional recovery after chronic injury. *J Neurosci Res,* 66**,** 1187-97.

WOLSWIJK, G. & NOBLE, M. 1989. Identification of an adult-specific glial progenitor cell. *Development,* 105**,** 387-400.

WONG, S. T., HENLEY, J. R., KANNING, K. C., HUANG, K. H., BOTHWELL, M. & POO, M. 2002. A p75(NTR) and Nogo receptor complex mediates repulsive signaling by myelin-associated glycoprotein. *Nature Neuroscience,* 5**,** 1302-1308.

XU, X., YEE, W. C., HWANG, P. Y., YU, H., WAN, A. C., GAO, S., BOON, K. L., MAO, H. Q., LEONG, K. W. & WANG, S. 2003. Peripheral nerve regeneration with sustained release of poly(phosphoester) microencapsulated nerve growth factor within nerve guide conduits. *Biomaterials,* 24**,** 2405-12.

XU, X. L., CHEN, X. S., MA, P. A., WANG, X. R. & JING, X. B. 2008. The release behavior of doxorubicin hydrochloride from medicated fibers prepared by emulsion-electrospinning. *European Journal of Pharmaceutics and Biopharmaceutics,* 70**,** 165-170.

XU, X. L., ZHUANG, X. L., CHEN, X. S., WANG, X. R., YANG, L. X. & JING, X. B. 2006. Preparation of core-sheath composite nanofibers by emulsion electrospinning. *Macromolecular Rapid Communications,* 27**,** 1637-1642.

XU, X. M., CHEN, A., GUENARD, V., KLEITMAN, N. & BUNGE, M. B. 1997. Bridging Schwann cell transplants promote axonal regeneration from both the rostral and caudal stumps of transected adult rat spinal cord. *J Neurocytol,* 26**,** 1-16.

YANG, F., MURUGAN, R., WANG, S. & RAMAKRISHNA, S. 2005. Electrospinning of nano/micro scale poly(L-lactic acid) aligned fibers and their potential in neural tissue engineering. *Biomaterials,* 26**,** 2603-2610.

YANG, F., XU, C. Y., KOTAKI, M., WANG, S. & RAMAKRISHNA, S. 2004. Characterization of neural stem cells on electrospun poly(L-lactic acid) nanofibrous scaffold. *J Biomater Sci Polym Ed,* 15**,** 1483-97.

YANG, X. B., ROACH, H. I., CLARKE, N. M., HOWDLE, S. M., QUIRK, R., SHAKESHEFF, K. M. & OREFFO, R. O. 2001. Human osteoprogenitor growth and differentiation on synthetic biodegradable structures after surface modification. *Bone,* 29**,** 523-31.

YANG, Y., LI, X., CUI, W., ZHOU, S., TAN, R. & WANG, C. 2008. Structural stability and release profiles of proteins from core-shell poly (DL-lactide) ultrafine fibers prepared by emulsion electrospinning. *Journal of Biomedical Materials Research Part A,* 86A**,** 374-385.

YIU, G. & HE, Z. G. 2006. Glial inhibition of CNS axon regeneration. *Nature Reviews Neuroscience,* 7**,** 617-627.

YOU, Y., LEE, S. J., MIN, B. M. & PARK, W. H. 2006. Effect of solution properties on nanofibrous structure of electrospun poly(lactic-co-glycolic acid). *Journal of Applied Polymer Science,* 99**,** 1214-1221.

YOUNG, R. C., WIBERG, M. & TERENGHI, G. 2002. Poly-3-hydroxybutyrate (PHB): a resorbable conduit for long-gap repair in peripheral nerves. *Br J Plast Surg,* 55**,** 235-40.

YU, L. M., KAZAZIAN, K. & SHOICHET, M. S. 2007. Peptide surface modification of methacrylamide chitosan for neural tissue engineering applications. *J Biomed Mater Res A,* 82**,** 243-55.

ZHANG, Y. Z., WANG, X., FENG, Y., LI, J., LIM, C. T. & RAMAKRISHNA, S. 2006. Coaxial electrospinning of (fluorescein isothiocyanate-conjugated bovine serum albumin)-encapsulated poly(epsilon-caprolactone) nanofibers for sustained release. *Biomacromolecules,* 7**,** 1049-57.

ZHAO, L., HE, C. G., GAO, Y. J., CEN, L., CUI, L. & CAO, Y. L. 2008. Preparation and cytocompatibility of PLGA scaffolds with controllable fiber morphology and diameter using electrospinning method. *Journal of Biomedical Materials Research Part B-Applied Biomaterials,* 87B**,** 26-34.

ZHAO, P., JIANG, H., PAN, H., ZHU, K. & CHEN, W. 2007. Biodegradable fibrous scaffolds composed of gelatin coated poly(epsilon-caprolactone) prepared by coaxial electrospinning. *J Biomed Mater Res A,* 83**,** 372-82.

ZHOU, F. C. 1990. Four patterns of laminin-immunoreactive structure in developing rat brain. *Brain Res Dev Brain Res,* 55**,** 191-201.

ZHOU, S. B., DENG, X. M., LI, X. H., JIA, W. X. & LIU, L. 2004. Synthesis and characterization of biodegradable low molecular weight aliphatic polyesters and their use in protein-delivery systems. *Journal of Applied Polymer Science,* 91**,** 1848-1856.

ZHU, Y., GAO, C., LIU, X. & SHEN, J. 2002. Surface Modification of Polycaprolactone Membrane via Aminolysis and Biomacromolecule Immobilization for Promoting Cytocompatibility of Human Endothelial Cells. *Biomacromolecules,* 3**,** 1312-1319.

ZIELINSKI, B. A. & AEBISCHER, P. 1994. Chitosan as a Matrix for Mammalian-Cell Encapsulation. *Biomaterials,* 15**,** 1049-1056.

ZONG, X., BIEN, H., CHUNG, C. Y., YIN, L., FANG, D., HSIAO, B. S., CHU, B. & ENTCHEVA, E. 2005. Electrospun fine-textured scaffolds for heart tissue constructs. *Biomaterials,* 26**,** 5330-8.

ZONG, X., RAN, S., KIM, K. S., FANG, D., HSIAO, B. S. & CHU, B. 2003. Structure and morphology changes during in vitro degradation of electrospun poly(glycolide-co-lactide) nanofiber membrane. *Biomacromolecules,* 4**,** 416-23.

APPENDIX

A1. Materials

All materials are divided into three groups; cell culture, cell culture analysis; and scaffold fabrication and analysis. In the tables below all materials and chemicals are listed according to the method used. All solvents were high performance liquid chromatography (HPLC) grade of American Chemical Society analytical grade reagents.

Table 10.1 Alphabetical list of materials used for fabrication and analysis of flat sheet membranes and electrospun fibre mats

Name of Material/Chemical	Supplier	Catalogue number
13mm glass cover slips	Fisher Scientic UK Ltd., Bishop Meadow Road, Loughborough, Leicestershire, LE11 5RG	MNJ-500-010G
N-methyl-2-pyrrolidinon (NMP)	Fisher	12763-0025
Albumin from bovine serum	Sigma-Aldrich Company Ltd., Dorset England	A9418
Chloroform	Fisher	C/4960/17
Dichloromethane	Fisher	D/1852/17
Ethanol	Fisher	E/0650DF/17
Gene frames	Fisher	GEN-100-010Y
Hamilton syringe 1000 series	Sigma-Aldrich	21000-U
Methanol	Fisher	M/4056/17
N-Hydroxysuccinimide	Sigma-Aldrich	13,067-2
Ozone generator	**Triogen Ltd.,** Unit 14 Langlands Place East Kilbride G75 0YF	TOG C2B
PLGA resomer RG 756 S, 75:25, Mw = 76,000-116,000	Boehringer Ingelheim Limited, Ellesfield Avenue, Bracknell, Berkshire, RG12 8YS	66633

Name of Material/Chemical	Supplier	Catalogue number
Poly-L-lysine-FITC	Sigma-Aldrich	P3069
Power supply	Spellman, Broomers Park, Broomers Hill Lane Pulborough, West Sussex, RH20 2RY	CZE1000R
Syringe Pump	Cole-Parmer Instrument Company Ltd., Unit 3, River Brent Business Park, Trumpers Way, Hanwell, London W7 2QA	EW-74900-10
Collectors	Assembled out of paper, cable, steel	
Lab support stand and clamp		
Aluminium foil	Bought in supermarket	
Cling film	Bought in supermarket	

Table 10.2 Materials used for maintenance of cell culture and for experiments where cells were involved

Name of Material	Supplier	Catalogue number
Antibiotic antimicotic solution (100x)	Sigma-Aldrich Company Ltd., Dorset, England	A5955
Isopropanol	Fisher	
Nerve growth factor	Sigma-Aldrich	N6009
Nunc Cryotube vials, 1.8ml	Fisher	368632
PC12 cells	LGC Standards, Queens Road, Teddington, Middlesex TW11 0LY	CRL-1721
Phosphate buffered saline	Sigma-Aldrich	BR0014G
Poly-L-lysine, solid form	Sigma-Aldrich	81339
Poly-L-lysine, solution	Sigma-Aldrich	P4707
RPMI1640	Sigma-Aldrich	R8758

Name of Material	Supplier	Catalogue number
Sodium Pyruvate	Sigma-Aldrich	P2256
Tissue culture flasks (72 cm^2)	Fisher	3046503 - 5000
Trypsin/EDTA 10x solution	Sigma-Aldrich	T4674

Table 10.3 Materials used for analysis of experiments with cells

Name of Material	Supplier	Catalogue number
Bradford Protein Assay	Bio-Rad Laboratories Ltd., Bio-Rad House, Maxted Road, Hemel Hempstead, Hertfordshire HP2 7DX	500-0006
Calcein acetoxymethyl (AM)	Invitrogen molecular probes	C3099
Ethidium homodimer	Sigma-Aldrich	E1903
Formalin solution, 10%	Sigma-Aldrich	HT501128
Human β-NGF ELISA development kit	PeproTech House, 29 Margravine Road, London, W6 8LL, UK	900-K60
Quant-iT PicoGreen dsDNA Assay kit	Invitrogen molecular probes, 3 Fountain Drive, Inchinnan Business Park, Paisley, PA4 9RF	P7589
Tween20	Sigma-Aldrich	P1379

A2. Alternative electrospinning set up

Other factors, like airflow and surrounding objects have a high disturbance factor and deflect the polymer jet. As the electrospinning process relies on the potential difference between the solution and the collector, the introduction of an additional electric field can be used to control the charged electrospinning jet. This electric field can be applied via an additional power supply which is connected to a metal

ring with appropriate radius which is placed between the needle and the collector. The same voltage is applied to the metal ring as is to the needle tip.

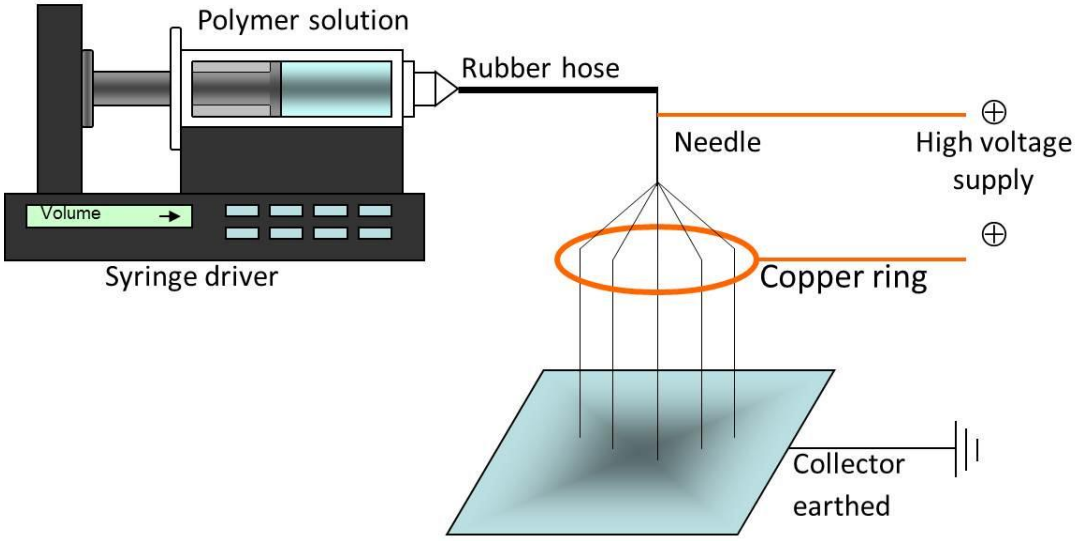

Figure 10.1 Alternative electrospinning set up.

*